U.PORTO

DOUTORAMENTO EM CIÊNCIAS BIOMÉDICAS

Dissection of molecular mechanisms involved in the last stages of cytokinesis

Inês da Costa Santos

D

2023

Inês da Costa Santos
Dissection of molecular mechanisms involved in the last stages of cytokinesis

D.ICBAS 2023

Dissection of molecular mechanisms involved in the last stages of cytokinesis
Inês da Costa Santos

INSTITUTO DE CIÊNCIAS BIOMÉDICAS ABEL SALAZAR

INÊS DA COSTA SANTOS

DISSECTION OF MOLECULAR MECHANISMS INVOLVED IN THE LAST STAGES OF CYTOKINESIS

Tese de Candidatura ao grau de Doutor em Ciências Biomédicas;

Programa Doutoral da Universidade do Porto (Instituto de Ciências Biomédicas de Abel Salazar)

Orientador –Doutora Ana Xavier de Carvalho
Categoria –Investigador Principal
Afiliação –Instituto de Investigação e Inovação em Saúde (i3S)/Instituto de Biologia Molecular e Celular (IBMC), Universidadedo Porto

Co-orientador –Doutora Ana Marta Silva
Categoria –Investigador Júnior
Afiliação –Instituto de Investigação e Inovação em Saúde (i3S)/Instituto de Biologia Molecular e Celular (IBMC), Universidade do Porto

The experimental work present in this thesis was developed at:

i3S – Instituto de Investigação e Inovação em Saúde
IBMC – Instituto de Biologia Molecular e Celular
Universidade do Porto
Cytoskeletal Dynamics Group
Rua Alfredo Allen, 208
4200-135 Porto, Portugal
www.i3s.up.pt

FUNDING

Funding to develop this work was provided by the European Research Council under the European Union's Horizon 2020 Research and Innovation Programme (640553 – ACTOMYO). Inês da Costa Santos was supported by an FCT PhD Scholarship (SFRH/BD/138446/2018). Support from tuition fees was also provided by the academic institution ICBAS – Instituto de Ciências Biomédicas Abel Salazar da Universidade do Porto.

DECLARAÇÃO DE HONRA

Declaro que a presente tese é de minha autoria e não foi utilizada previamente noutro curso ou unidade curricular, desta ou de outra instituição. As referências a outros autores (afirmações, ideias, pensamentos) respeitam escrupulosamente as regras da atribuição, e encontram-se devidamente indicadas no texto e nas referências bibliográficas, de acordo com as normas de referenciação. Tenho consciência de que a prática de plágio e auto-plágio constitui um ilícito académico

Porto, Maio de 2023

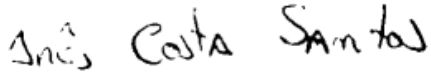

“Necessário, somente o necessário“

AGRADECIMENTOS/ACKNOWLEDGEMENTS

Por mais solitária que a jornada do doutoramento possa ser, este é um caminho que não se faz só. Um doutoramento observa desde logo um conjunto de formalidades às quais impera a colaboração de várias pessoas e instituições. Assim sendo gostaria de endereçar um agradecimento a todos os intervenientes formais do processo:

Á minha orientadora, **Ana Carvalho**, por aceder a embarcar nesta jornada como minha orientadora, providenciando-me meios para a execução do trabalho laboratorial necessário á elaboração desta tese.

Á minha coorientadora, **Ana Marta Silva**, por me ter introduzido na microscopia confocal, na análise e tratamento de imagens e por me ter auxiliado nas demais tarefas.

Á **Fundação para a Ciência e Tecnologia** (FCT) pela atribuição da Bolsa individual de doutoramento (SFRH/BD/138446/2018), ao **ICBAS** , em especial à Professora Paula, e ao **i3S/IBMC** pelo apoio institucional bem como às demais entidades que permitiram que tivesse financiamento para a concretização de todos os trabalhos.

A todos os restantes intervenientes que me acompanharam durante esta jornada e que foram a minha verdadeira força motora, verdeiros extensores dos meus braços e das minhas pernas quando a força e a motivação me faltaram:

A todos os membros que passaram e que atualmente integram o **GC lab** (grupos Cytoskeletal Dynamics e Cell Division Mechanisms), obrigada pelas gargalhadas e pelas discussões científicas. Em especial, à **Inês Loureiro** pelo suporte, à **Marisa** pelas discussões científicas, por me ter ensinado e ajudado com o yeast-two-hybrid, à **Tânia** pela boa energia, à **Rita** por me incentivar e motivar, ao **Bernardo** por ser tão paciente e boa onda, ao **Hugo, à Cátia, à Vanessa** e à **Adriana** pelos bons momentos.

À **Dra. Sofia**, **Dr. Ângelo**, e à **Tita**. Muito obrigada.

Às minhas amigas de longa data, **Diana**, **Ana Patrícia**, **Telma** e **Ângela**, obrigada por me relembrarem o verdadeiro significado da amizade, os vossos filhos crescem, mas nós não.

Às minhas amigas de Vila Real, **Diana**, **Ana Luísa**, **Teresa**, **Cristiana**, **Maria Inês**, e **Joana** obrigada pela partilha da vossa jornada comigo e pelo suporte.

Aos meus recém amigos do Corte e Costura, **Joana Marques**, **Joana Cardoso**, **Catarina**, **David** e **Sara**, por me ampararem, levando-me a cometer as maiores loucuras. Têm mais fé mim (e falta de noção também) do que eu própria.

Às piriguetes, **Rute**, **Leonor**, **Mafalda**, **Carolina**, **Filipa**, **Liliana** e **Elisabete** obrigada pelas gargalhadas infindáveis. Os jantares de Natal nunca mais serão os mesmos. Em especial á **Madame** (Leonor), por ser minha conselheira e por tirar o pior que

há em mim, e à **Lili**, por ser o meu ombro amigo, por ouvir os meus disparates com uma paciência estoica, és uma *professional mother* do caraças!

Ao **Daniel Barbosa**, o meu verdadeiro mentor e amigo, por nunca ter desistido de mim, por me mostrar o que é o verdadeiro altruísmo e honestidade, por me ajudar a colocar os pés assentes na Terra, por ter sido o meu amparo e os meus braços quando as forças me faltaram, por toda ajuda prestada mesmo antes de ter dito fosse o que fosse. Um obrigada nunca será suficiente para expressar toda a minha gratidão.

Ás minhas colegas de doutoramento: **Joana Leite, Joana Saramago** e **Filipa Sobral**, o que dizer? As discussões científicas, as gargalhadas, os choros, as frustrações, e os projetos maquiavélicos inacabados que partilhamos foram sem dúvida uma fonte de suporte e são a verdadeira materialização de uma das palavras mais ouvidas durante o meu doutoramento "RELATIVIZAR". Do doutoramento retiramos o reconhecimento máximo de humanidade e dos valores interpessoais.

Às muchachas, **Bete** e **Filipa**, por me lembrarem que as melhores histórias podem surgir nos momentos mais inusitados, por terem uma confiança cega em mim depois de tudo a que as sujeitei. Nunca mais um pós-defesa foi o mesmo. Sem vocês, isto teria sido muito mais difícil.

Ao meu grande pilar, á minha base, ao meu porto de abrigo, ao meu centro gravítico, ao meu ponto forte e também o meu ponto fraco, a toda a minha família, obrigada! À minha **Avó Laida**, por me ensinares a sub-rogar as adversidades ao sentido de humor, por me ensinares que as tristezas não pagam dívidas e que as feras indomáveis existem, obrigada. Em especial aos meus pais, **Ângelo** e **Rosa** por terem sempre sido pais atentos e preocupados, não há tarefa mais ingrata e mais difícil no mundo do que ser pai e mãe. Sem vocês nada do que consegui e do que sou hoje seria possível. Esta também é uma vitória vossa. Aos meus irmãos, **Tomás** e **Joana** por todo o apoio, por ouvirem todas as minhas reclamações, vocês também foram parte deste doutoramento. À minha afilhada **Maria Clara** e ao meu pseudo-afilhado **Afonso**, obrigada por me mostrarem o quanto é bom ser criança novamente. Convosco o meu dia acalma, e a vida volta a ganhar cor. Ao meu fiel e amoroso companheiro, **Teddy**, que nunca me abandona, obrigada.

Aos que já cá não estão fisicamente: **Nanda** (por me ensinares que é possível amar tanto ou mais aqueles que não são do nosso sangue mas que nos pertencem irremediavelmente ao coração), **Avô Abel** (por me mostrares que somos donos do nosso próprio destino e que podemos fazer das adversidades verdadeiros trampolins para alcançar mais do que ambicionamos), **Avó Esmeraldina** (por me mostrares a sabedoria, a eloquência e a doçura do silêncio, e que nunca é tarde para mudar as hostilidades e aproveitar com amor o que de mais precioso temos) e **Avô Elísio** (o meu avô inolvidável, de paixão fácil pela simplicidade da vida, da natureza, da arte, dos valores, da terra e da

família;, os teus 14 netos eram as flores mais bonitas do teu jardim e tu és o nosso sobreiro mais tenaz, atento e imortal) agora estão sempre comigo. Que sorte a minha!

Por fim, ao **Chico**, ao meu companheiro ao longo desta jornada, obrigada pelo suporte, pelo respeito, pela amizade, pelo carinho, pelo amor, pela compreensão e por festejares as minhas vitórias como se fossem as tuas. Se houve alguém negligenciado durante este processo, em prol deste doutoramento, foste tu. Não existem palavras para qualificar a tua paciência e dedicação neste processo. Obrigada por confiares em mim e me devolveres a confiança quando esta esmoreceu.

LISTA DE PUBLICAÇÕES/ LIST OF PUBLICATIONS

Esta tese de Doutoramento consiste numa compilação de resultados originais. Alguns dos resultados aqui expostos encontram-se já aceites para publicação numa revista internacional indexada. A autora declara que teve participação ativa na conceção, execução, análise, interpretação, discussão e redação do trabalho aqui apresentado.

Faz parte integrante desta tese o seguinte artigo aceite para publicação:

This Doctoral thesis consists in a compilation of original data. Part of the results present here are already accepted for publication in international peer-reviewed journal. The author declares that she had an active role in the conception, execution, analysis, interpretation, discussion and writing of the work here presented.

The following paper accepted for publication is included in this thesis:

- **Santos, I. C.*,** Silva, A. M.*, Gassman, R. and Carvalho, A. X. (2023). Anillin and the microtubule bundler PRC1 maintain myosin in the contractile ring to ensure completion of cytokinesis. *Development*. *Accepted for publication.*

SUMMARY

Cytokinesis is the last step of cell division when one cell physically divides into two cells. Cytokinesis is driven by an equatorial contractile ring and signals from antiparallel microtubule bundles (the central spindle) that form between the two masses of segregating chromosomes. During the last stages of constriction, the contractile ring encounters the central spindle microtubules and compacts them. Compacted microtubules fill the narrow bridge between the two daughter cells and the contractile ring transitions into a midbody ring once constriction stops. The contractile ring to midbody ring transition is likely accomplished by structural and molecular changes that set the stage for abscission. The midbody orchestrates the final step of cytokinesis by recruiting abscission effectors.

To deepen our understanding of the last stages of cytokinesis when crosstalk between the contractile ring and the central spindle likely takes place, we characterized the contractile ring behavior during the second half of ring constriction and evaluated the impact of disrupting central spindle microtubules. To reach these aims we used a temperature-sensitive mutant and RNAi depletion of SPD-1 (the *C. elegans* homolog of the microtubule bundler PRC1), biochemistry, and confocal live microscopy in *C. elegans* 1-cell and 4-cell embryos. We observed that some contractile ring (myosin, anillin, and septin) and central spindle (CYK-4, the homolog of the centralspindlin complex protein MgcRacGAP) proteins increased their level during the last stages of cytokinesis. Additionally, anillin turnover decreased during the second half of ring constriction when SPD-1 was depleted. Using a yeast two-hybrid assay we were able to identify some potential SPD-1 interactors that include contractile ring, central spindle, and abscission proteins. Interestingly, we show that penetrant SPD-1 inactivation, but not RNAi-mediated depletion of SPD-1, results in frequent failure to complete the last stages of furrow ingression in the 1-cell embryo and all cells of the 4-cell embryo. Detailed characterization of the SPD-1 inhibition phenotype revealed that SPD-1-mediated microtubule bundling is required to maintain the tight back-to-back configuration of the cleavage furrow and that in the absence of midzone microtubule bundles anillin (ANI-1) becomes essential to maintain myosin in the contractile ring, specifically during the later stages of cytokinesis. Our results thus reveal a novel mechanism involving the joint action of anillin in the contractile ring and SPD-1 in the central spindle, which operates during the later stages of furrow ingression to ensure the continued functioning of the contractile ring until cytokinesis is complete.

Besides this, we observed differences in the unperturbed central spindle functioning between the P0 (1-cell embryo) and the EMS cell (in 4-cell embryos), which indicates that different mechanisms for central spindle organization may operate in the two contexts.

Keywords: Cytokinesis, Contractile ring, Midbody ring, Central spindle, midzone microtubule bundling, PRC1, SPD-1, Anillin.

RESUMO

A citocinese é a última etapa da divisão celular em que uma célula se divide fisicamente em duas células. A citocinese é impulsionada por um anel contrátil que se forma na zona equatorial e sinais provenientes de feixes de microtúbulos antiparalelos (o fuso central) que se formam entre as duas massas de cromossomas segregantes. Durante as últimas etapas de constrição, o anel contrátil encontra os microtúbulos do fuso central e compacta-os. Os microtúbulos compactados preenchem o espaço existente entre as duas células filhas e o anel contrátil transforma-se num anel do "midbody" assim que a constrição para. A transição do anel contrátil para o anel do "midbody" é provavelmente acompanhada por mudanças estruturais e moleculares que preparam o cenário para a abscisão. O "midbody" coordena a etapa final da citocinese recrutando efetores da abscisão.

Para aprofundar o nosso conhecimento acerca das últimas etapas da citocinese, quando provavelmente ocorre uma comunicação cruzada entre o anel contrátil e o fuso central, caracterizamos o comportamento do anel contrátil e avaliamos o impacto da desestabilização dos microtúbulos do fuso central durante a segunda metade da constrição do anel. Para alcançar esses objetivos, usamos um mutante sensível à temperatura e depletamos por RNA de interferência (*RNAi*) o SPD-1 (o homólogo do agregador de microtúbulos PRC1), bioquímica e microscopia confocal ao de embriões de *C. elegans* de 1-célula e 4-células vivos. Observamos que algumas proteínas do anel contrátil (miosina, anilina e septina) e do fuso central (CYK-4, o homólogo da proteína do complexo da "centralspindlin" MgcRacGAP) aumentaram de níveis durante as últimas etapas da constrição. Além disso, o "turnover" da anilina diminuiu durante a segunda metade da constrição do anel quando o SPD-1 foi depletado. Usando um ensaio "yeast-two-hybrid", foi possível identificar alguns potenciais interatores do SPD-1 que incluem proteínas do anel contrátil, do fuso central e de abscisão. Curiosamente, mostramos que a inativação penetrante do SPD-1, mas não a depleção por *RNAi* do SPD-1, resulta em falha frequente nas últimas etapas de constrição no embrião de 1-célula e em todas as células do embrião de 4-células. A caracterização detalhada do fenótipo de inibição do SPD-1 revelou que o agrupamento de microtúbulos mediado por SPD-1 é necessário para manter a configuração apertada do anel e que, na ausência de interligação dos microtúbulos do fuso central, a anilina (ANI-1) torna-se essencial para manter a miosina no anel contrátil especificamente durante as fases finais da constrição. Os resultados revelam um novo mecanismo que envolve a ação conjunta da anilina presente no anel contrátil e do SPD-1 presente no fuso central, que opera durante as últimas fases de constrição para garantir o funcionamento contínuo do anel contrátil até que a citocinese esteja completa.

Para além disto, observamos diferenças no funcionamento do fuso central entre a célula PO (do embrião de 1-célula) e a célula EMS (do embrião de 4-células) que indicam a existência de mecanismos de organização do fuso central diferentes que operam nestes dois contextos.

Palavras-Chave: Citocinese, Anel contrátil, Anel do “midbody”, Fuso central, Interligação dos microtúbulos centrais, PRC1, SPD-1, Anilina.

CONTENTS

LIST OF FIGURES

LIST OF TABLES

LIST OF SYMBOLS AND ABBREVIATIONS

ºC – Degree Celsius

% – Percentage

α– Alpha

β – Beta

Δ – Delta

ABD- Actin Binding Domain

ADP – Adenosine Diphosphate

AHR- Anillin-Homology Region

AO- Anaphase Onset

ATP – Adenosine Triphosphate

C. elegans – *Caenorhabditis elegans*

cDNA – Complementary deoxyribonucleic acid

Cdk- Cyclin-Dependent Kinase

CGC – Caenorhabditis Genetics Center

CI – Confidence Interval

CPC- Chromosomal Passenger Complex

D. melanogaster – *Drosophila melanogaster*

DNA – Deoxyribonucleic acid

dsRNA – Double-stranded RNAs

E. coli – *Escherichia coli*

ELC – Myosin essential light chain

ESCRT – Endosomal sorting complexes required for transport

F-actin – Filamentous actin

FIP- Feo interacting protein

FRAP – Fluorescence recovery after photobleaching

G-actin – Globular actin

GAP- GTPase-Activating Proteins

GDP- Guanosine Diphosphate

GEF – Guanine nucleotide exchange factor

GFP – Green fluorescent protein

GTP – Guanosine-5'-triphosphate

GTPase – Guanosine triphosphatase

IPTG – Isopropyl β-D-1-tiogalactopiranosida

L, mL, µL – Liter, milliliter, microliter

LB – Luria/Lysogenic broth

LED – Light emitting diode

MAPS- Microtubule-associated proteins

MDCK- Madin-Darby canine kidney

mg, µg, ng – Milligram, microgram, nanogram

MHC – Myosin heavy chain

MRLC- Myosin Regulatory Light Chain

mRNA – Messenger ribonucleic acid

mW – Milliwatt

NEBD- Nuclear Envelope Breakdown

NGM – Nematode growth media

nm, µm, mm – Nanometer; micrometer, millimeter

PCR – Polymerase chain reaction

PH – Pleckstrin homology domain

RISC – RNA-induced silencing complex RLC –regulatory light chain

RNA – Ribonucleic acid

RNAi – RNA interference

(RT)-PCR – Reverse-Transcription-PCR

s – seconds

S. cerevisiae – *Saccharomyces cerevisiae*

S. pombe – Schizosaccharomyces pombe

siRNA – small interference RNA

TS- Temperature Sensitive

µM, mM, M – Micromolar, millimolar, molar

UTR – Untranslated region

WT – Wild-type

X. laevis – *Xenopus laevis*

CHAPTER I

INTRODUCTION

Introduction

1. Mitosis

Mitosis is a key stage of the cell cycle, common to all living organisms, and comprehends the equal distribution of genetic material and organelles between the two daughter cells, which is followed by cell physical division. It can be typically divided into five phases: 1) prophase, 2) prometaphase, 3) metaphase, 4) anaphase, and 5) telophase (Figure 1).

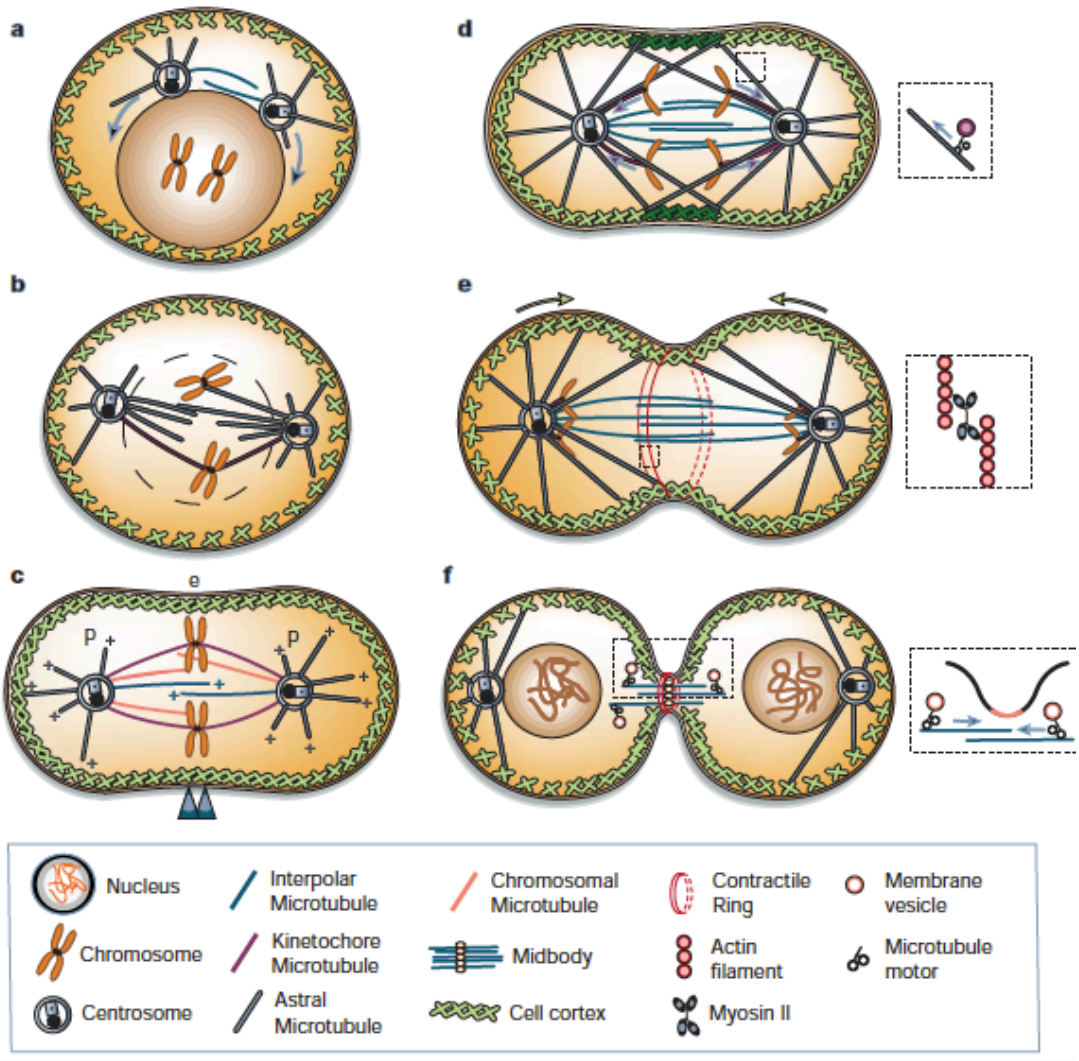

Figure 1- Scheme illustrating progression through mitosis.

(a) Prophase -chromosomes start condensing and centrosomes move around the nucleus. (b) Prometaphase - Nuclear envelope breakdown happens to allow those microtubules to have access to chromosomes and to orient them towards the spindle equator. (c) Metaphase – Chromosomes align at the division equator with sister chromatids (arrowheads) facing opposing poles (p). (d) Anaphase A - chromatids move towards opposite cell poles and the spindle delivers signals to the cortex (inset) that will determine

the position of the contractile ring. (e) Anaphase B - Pole-to-pole distance increases and the division plane is determined by the assembly of an actomyosin contractile ring at the cell equator. Myosin-II slides actin filaments to drive constriction (inset). (f) Telophase – Nuclear envelope reassembles around the decondensed chromosomes, and the contractile ring constricts driving cell division. Microtubules placed at the cell midzone may serve as tracks for motor-mediated transport of vesicles and signaling molecules to the midbody to support abscission (inset) (Scholey, Brust-Mascher, and Mogilner 2003; figure used under permission).

During prophase, replicated chromatin condenses, progressively shortening its length and increasing its thickness, giving rise to chromosomes, each containing two chromatids. It was thought that it resulted in DNA transcription silencing, however, it is known that cells present low levels of transcription that increase as mitosis progress (Palozola, Liu, et al. 2017; Palozola, Donahue, et al. 2017). Also, during prophase, kinetochores are assembled on centromeric DNA. This multi-protein structure works as a platform to link chromosomes to microtubules of the mitotic spindle (Musacchio and Desai 2017). Fully mature centrosomes nucleate microtubules that will be required for chromatid separation and migration toward opposing poles of the cell at anaphase (Petry 2016). For many organisms, nuclear envelope breakdown (NEBD) marks the end of prophase.

In prometaphase, microtubules continue to nucleate from centrosomes and every chromosome becomes associated with microtubules of the mitotic spindle. All chromosomes properly attached to the mitotic spindle migrate towards the spindle equator, in a process called “chromosome congression”. Once all chromosomes are perfectly aligned at the cell center, the cell is said to be in metaphase. The metaphase spindle is composed of kinetochores microtubules, astral microtubules that radiate from each spindle pole towards the cell periphery, and microtubules that overlap and that extended from each centrosome and links the two halves of the bipolar spindle (Wadsworth 2021).

Anaphase starts when sister chromatids, each correctly attached to microtubules coming from one of the poles, are pulled into the corresponding cell pole via microtubule depolymerization. At this time point, a microtubule array is formed between the two segregating masses of chromatids, called the central spindle (section 4). Anaphase can be divided into anaphase A (Figure 1D) when the segregating masses of chromatids start to be pulled apart, and anaphase B, when the pole-to-pole distance increases and the division site is specified at the cell equator (Figure 1e) (Scholey, Brust-Mascher, and Mogilner 2003).

After chromatid separation, telophase takes place and chromosomes start to decondense. Telophase includes cytokinesis, which consists of the physical separation of the two daughter cells.

2. Cytokinesis

Cytokinesis is the final stage of cell division during which two daughter cells with the same genetic information, become physically separated (Green, Paluch, and Oegema 2012; Thieleke-Matos et al. 2017; Leite et al. 2019). This process was described more than 100 years ago by Fleming in 1882 and Within in 1887 and has been studied in many different biological models such as plants, budding and fission yeast, slime mold, marine invertebrates, nematodes, fruit flies, and vertebrate cells (Guertin, Trautmann, and McCollum 2002). Cytokinesis starts after anaphase onset and is accomplished by the assembly of an actomyosin ring at the cell equator, beneath the plasma membrane. Constriction of the contractile ring brings behind it the plasma membrane, creating a cleavage furrow that keeps ingressing toward the center of the cell. Full cleavage furrow ingression is followed by membrane scission. Thus, cytokinesis can be subdivided into three essential steps: 1) contractile ring assembly, 2) contractile ring constriction, and 3) membrane abscission (Figure 2).

Failure in cytokinesis leads to the formation of polyploid cells, contributing to genomic instability, and can ultimately lead to cancer (Eggert, Mitchison, and Field 2006). Since cancer is one of the most devastating pathologies of the 21st century, it is of great importance to study the mechanisms behind cytokinesis.

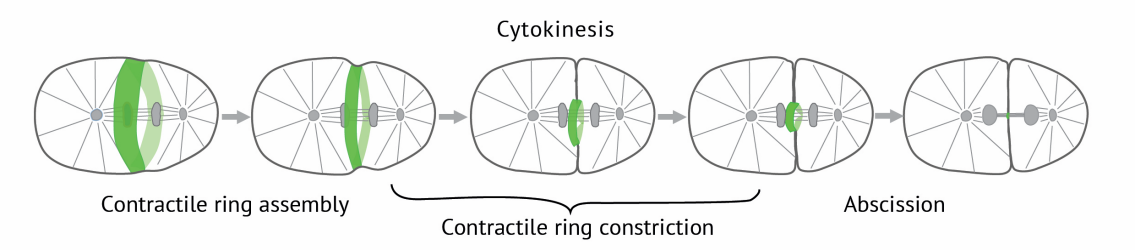

Figure 2- Schematic of cytokinesis.

The contractile ring (in green) is assembled after anaphase onset right beneath the plasma membrane (in dark grey). The contractile ring constricts bringing the plasma membrane behind it until only a narrow cytoplasmic bridge filled with bundled microtubules (light grey) connects the two daughter cells setting the stage for abscission. Image from the Cytoskeletal Dynamics Group, i3S.

3. The contractile ring

The contractile ring was early reported as being a thin (0.1-0.2 μm) filamentous layer, that assembles just beneath the plasma membrane at the cell equator, in a

circumferential way, parallel to the cleavage plane after anaphase onset (Schroeder 1968, 1972, 1973). It is composed of several proteins that are conserved among many organisms throughout evolution (Eggert, Mitchison, and Field 2006). Some of those proteins are actin, formins (that are involved in the nucleation of non-branched actin filaments), motor myosin (that slides actin filaments), anillin, septins, and some crosslinkers (such as filamin, spectrin, plastin, and others) (Figure 3) (Fujiwara et al. 2018; Sobral et al. 2021; Garno et al. 2021; Henson et al. 2017; Ding et al. 2017; Hartemink 2005; Green, Paluch, and Oegema 2012).

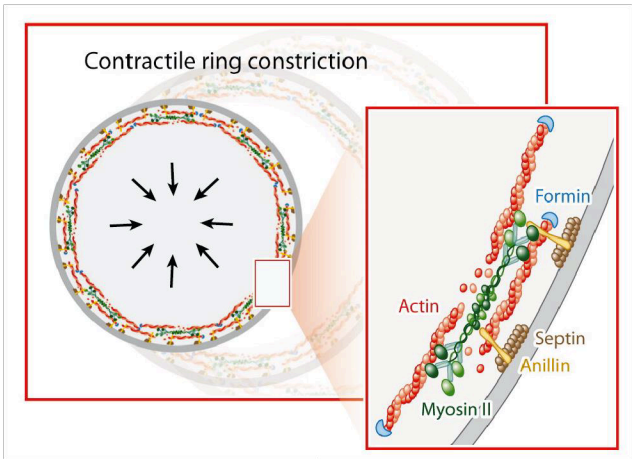

Figure 3- Schematic illustration of some contractile ring components.
The contractile ring is composed of parallel actin filaments that are nucleated by formins and interdigitate with non-muscle myosin II filaments. Anillin and septins are also part of the ring and may contribute to the anchoring of the contractile ring to the plasma membrane (Figure reprinted from Green, Paluch, and Oegema 2012; figure used under permission).

As the contractile ring constricts and its perimeter continuously decreases, its width and thickness are maintained (Carvalho, Desai, and Oegema 2009). During ring constriction, the cleavage furrow is tight with back-to-back plasma membranes in epithelial and embryonic cells but is open and broad in cultured vertebrate cells.

The contractile ring constricts at a constant rate for most of constriction and slows down when it approaches the central spindle microtubules (Carvalho, Desai, and Oegema 2009; Pelham and Chang 2002; Biron et al. 2004). At this point, the contractile ring compacts the midzone and astral microtubules in the furrow region, which fill the narrow cytoplasmic bridge connecting the sister cells, and transitions into a midbody ring once constriction stops. The compacted central spindle comprises a midbody central core that is a dense structure when visualized by electron microscopy and the midbody flank. Together with the midbody ring, the midbody central core and the midbody flank make up the midbody (Hu, Coughlin, and Mitchison 2012; Mierzwa and Gerlich 2014; Mullins and Biesele 1977;

Green, Paluch, and Oegema 2012). The midbody orchestrates the final step of cytokinesis by recruiting components of the abscission machinery (sections 5 and 6).

3.1. Contractile ring components

3.1.1. Actin

Actin is a globular protein that exists in monomers (G-actin) and can polymerize into filaments (F-actin).

The assembly of actin filaments is accomplished by the polymerization of the globular monomeric G-actin into double-stranded helical F-actin, through adenosine triphosphate (ATP) hydrolysis (Straub and Feuer 1950; Holmes et al. 1990; Oda et al. 2009; Fujii et al. 2010). Actin filament assembly/disassembly is a highly dynamic process, since, to rapidly adapt to intracellular and extracellular cues, F-actin has to be in constant polymerization and depolymerization (Harris, Jreij, and Fletcher 2018; Stossel, Fenteany, and Hartwig 2006). Actin monomers are always integrated into actin filaments in the same direction, giving rise to polarized filaments with two different ends (barbed (+) and pointed (-) ends). The addition of actin monomers into the barbed end (+) happens faster than at the pointed end (-), where disassembly takes place (Leite et al. 2019). F-actin is essential for the formation of a functional contractile ring once, the use of actin-depolymerizing drugs inhibits cytokinesis.

Several proteins regulate actin dynamics such as myosin, a motor protein, and others responsible to nucleate, elongating, branching, capping, severing stabilizing, or crosslinking F-actin (Blanchoin et al. 2014; Pollard, Blanchoin, and Mullins 2000; Shekhar, Pernier, and Carlier 2016). Cofilin is an actin-depolymerizing factor that severs and depolymerizes actin filaments. Formin is a protein responsible for nucleating and elongating linear F-actin within the contractile ring, whereas ARP2/3 is responsible for nucleating branched actin filaments that are present at the cell cortex during cytokinesis. Interestingly, the ARP2/3 complex counteracts formin activity within the cell cortex (Chan et al. 2019) but does not localize at the contractile ring, possibly not to interfere with formin activity (Jordan and Canman 2012; Pollard 2017). Capping proteins control the access of free G-actin to the barbed ends (+) of F-actin. Proteins exerting crosslinking activity of F-actin can bridge these filaments.

3.1.2. Myosin

Myosins are a superfamily of actin-based motor proteins, essential for the contraction of F-actin networks (Hartman and Spudich 2012). In the scope of this thesis, only non-muscle myosin II (NMY-II) (myosin, hereafter) will be mentioned. NMY-II is an hexameric complex composed of two myosin heavy chains (MHCs), two regulatory light

chains (RLCs), and two essential light chains (ELCs). The MHC contains a coiled-coil tail and a globular head where actin and ATP bind. The RLC is involved in the regulation of myosin motor activity and the ELC stabilizes the complex conformation (Vicente-Manzanares et al. 2009).

NMY-II transforms chemical energy into mechanical force through ATP hydrolysis, and translocates F-actin, through cyclic attachments and detachments. ATP binding to the myosin head causes the detachment of the myosin head from F-actin. Additionally, the myosin head converts ATP into ADP and inorganic phosphate (Pi) through ATPase activity. The energy released by ATP hydrolysis drives a conformational change of myosin head subdomains and in the lever arm. This results in a power stroke that leads to myosin moving toward the barbed-end of the actin filaments. In an interconnected network with anti-parallel actin filaments, these movements lead to network contraction (Leite et al. 2019).

Myosin activation mediated by RLCs is a key step for cytokinesis. To activate myosin, RLCs have to be phosphorylated at serine/threonine activation sites that start at anaphase and remain during cytokinesis. Several kinases, such as Rho-associated protein kinase (ROK or ROCK) and Citron Rho-interacting Kinase (CIT-K), that are RhoA effectors (see section 3.2.), can phosphorylate RLC at the activation sites. Once myosin is phosphorylated, its hexameric conformation opens up, and myosin forms bipolar filaments that can bind F-actin (Leite et al. 2019). Interestingly, myosin motor activity requirement for cytokinesis has been under debate. In budding yeast myosin motor activity is dispensable for cytokinesis completion (Lord, Laves, and Pollard 2005; Mendes Pinto et al. 2012). However in *Schizosaccharomycess pombe*, in *Dictyostelium discoideum* and in *C. elegans* myosin motor activity is required for ring constriction and successful cytokinesis (Osório et al. 2019; Sasaki, Shimada, and Sutoh 1998; Shimada et al. 1997; Laplante et al. 2015; Laplante and Pollard 2017; Palani et al. 2017).

3.1.3. Anillin

Anillin is a multifunctional protein that binds the plasma membrane and several components of the contractile ring and is capable of crosslinking F-actin in vitro (Piekny and Maddox 2010; D'Avino 2009). It is composed of a myosin-binding domain at the N-terminus, followed by an actin-binding domain (ABD) and an anillin-homology region (AHR) at the C-terminus, which includes RhoA, septin-binding sequences, and a membrane-binding pleckstrin homology domain (PH domain) (Field and Alberts, 1995; Oegema et al. 2000; Piekny and Glotzer, 2008).

Anillin also interacts with microtubules in biochemical studies and can co-localize with microtubules *in vivo* (Sisson et al. 2000; Hickson and O'Farrell 2008). Another interactor in *D. melanogaster* is RacGAP50c, a protein that belongs to the centralspindlin

complex (see section 4.1.). During cytokinesis, anillin binds RhoA. Despite anillin has been proposed to be a RhoA effector (Hickson and O'Farrell 2008), it should also function as a RhoA regulator or stabilizer, since anillin depletion in tissue cultured cells and *X. laevis* embryos dysregulate cortical RhoA distribution both at adherents junctions and at the cytokinetic furrow (Arnold, Stephenson, and Miller 2017; Budnar et al. 2019; Reyes et al. 2014; Piekny and Glotzer 2008). Moreover, anillin was propose to concentrate PI(4,5)P2 to retain membrane GTP-RhoA to promote effector recruitment (Budnar et al. 2019). Anillin and RhoA might stabilize one another, as RhoA depletion also perturbs anillin localization (Piekny and Glotzer 2008). Nevertheless, anillin is required to stabilize formin activation and localization at the cell equator and enhance formin-mediated F-actin nucleation activity at the contractile ring in HeLa cells (Chen et al. 2017; Watanabe et al. 2010).

Anillin localizes at the contractile ring and is important for cytokinesis (Oegema et al. 2000). Although the absence of anillin does not prevent contractile ring assembly, it can affect spindle positioning and contractile ring constriction speed in monkey kidney cells and leads to cytokinesis failure in HeLa cells and *D. melanogaster* S2 cells (Jinghe Liu et al. 2012; Oegema et al. 2000; Piekny and Maddox 2010; Echard et al. 2004; D'Avino 2009; Field et al. 2005; Pacquelet et al. 2015; Piekny and Glotzer 2008). Additionally, anillin depletion causes furrow oscillation at cell equator in HeLa cells (Zhao and Fang 2005; Piekny and Glotzer 2008) and *D. melanogaster* S2 cells (Hickson and O'Farrell 2008).

Besides anillin interaction with F- actin, myosin, membrane, and microtubules, it is well-known that anillin is required for septin recruitment to the plasma membrane in the ingressing furrow in HeLa cells (Jinghe Liu et al. 2012). Interestingly, in *D. melanogaster, C. elegans,* and *S. pombe* anillin acts upstream of septins to stabilize and recruit them to the contractile ring during cytokinesis (Field et al. 2005; Oegema et al. 2000; Maddox et al. 2005, 2007; Berlin, Paoletti, and Chang 2003; Tasto, Morrell, and Gould 2003). In *D. melanogaster,* anillin mutants failed to localize septin in the contractile ring and to the cellularization front during embryogenesis (Field et al. 2005; Oegema et al. 2000).

Anillin is also required for the last steps of cytokinesis, as anillin depletion in *D. melanogaster S2* cells leads to extensive blebbing around the midbody and reduced midzone microtubule integrity (Echard et al. 2004; Somma et al. 2002). Cells depleted of anillin present abnormal broad rings that ultimately, regress and fail cytokinesis (Echard et al. 2004; Kechad et al. 2012; Somma et al. 2002).

3.2. Specification of contractile ring positioning

The position where the contractile ring assembles is determined by positive and negative cues emerging from the mitotic spindle: signaling from the central spindle promotes local RhoA activation at the cell equator and astral microtubules suppress RhoA

activation at the cell poles (Basant and Glotzer 2018; Bement, Benink, and Von Dassow 2005; Foe and Von Dassow 2008; Von Dassow et al. 2009; Bringmann and Hyman 2005; Mangal et al. 2018). These signals are thought to work in parallel to provide a correct spatiotemporal RhoA activation. However, classic studies in Sea urchin eggs have suggest astral microtubules as being the ones capable of inducing furrow ingression.Studies led by Rappaport showed that cleavage can occur between appropriately positioned asters that are not connected by a spindle or chromosomes, favouring the hypothesis that astral microtubules are capable of inducing furrow ingression by their own (Rappaport 1961). In line with this, *Rieder et al.*, also observed in PtK1 cells that furrows can be formed between spindle poles in a process that is independent of chromosomes and central spindle (Rieder et al. 1997; Oegema and Mitchison 1997). Furrow formation was not prevented by placing obstacles like oil droplets between the central spindle and the cell cortex, which indicated that midzone microtubules were not responsible for inducing furrow initiation in these embryos (Rappaport and Rappaport 1983; Pollard 2004). Contrasting with this, studies performed in *D. melanogaster* spermatocytes and neuroblast indicate that central spindle microtubules, in the absence of astral microtubules, are sufficient to induce furrows (Bonaccorsi, Giansanti, and Gatti 1998; Giansanti, Gatti, and Bonaccorsi 2001), but not the other way around (Adams et al. 1998).

In *C. elegans* zygotes, the cleavage furrow can still ingress in the absence of signals from the central spindle (Mishima, Kaitna, and Glotzer 2002; Jantsch-Plunger et al. 2000; Raich et al. 1998; Lewellyn et al. 2010; Verbrugghe and White 2007), but not when asters are far from the cell poles (Lewellyn et al. 2010). This suggests that the central spindle is dispensable for furrow formation, as in the case of marine invertebrate embryos. The astral microtubule pathway remains poorly understood, however, it has been proposed that this pathway is involved in cortical contractility inhibition, by preventing contractility proteins from accumulating at cell poles. Work developed by *Werner et al*., (2007) showed that spindle formation next to one pole of the embryo led to NMY-II accumulation on the opposite side, indicating that astral microtubules prevent the accumulation of contractile ring proteins (Werner, Munro, and Glotzer 2007). Similar conclusions were achieved in grasshopper spermatocytes where positioning of asters on one side of the cell led to cortical actin flows towards the opposing side (Chen et al. 2008). This is explained based on local inhibition of contractility driven by aster microtubules that results in a gradient of contractility from the cell poles towards the cell equator, able to induce furrowing even in the absence of central spindle microtubules (Lewellyn et al. 2010; Verbrugghe and White 2007; Von Dassow et al. 2009; Dechant and Glotzer 2003). This gradient has been proposed to be accomplished by a gradient of Aurora-A at the poles, activated by TPXL-1, that prevents contractile ring component accumulation at the polar cortex in *C. elegans* 1-cell embryos (Mangal et al.

2018). Notably, a subset of astral microtubules that are equatorial-oriented might play a positive role in delivering contractility activators as is the case of the centralspindlin complex (Nishimura and Yonemura 2006).

Nevertheless, studies that used an ultraviolet laser to spatially separate spindle midzone from astral microtubules showed that in *C. elegans* zygotes the position of furrow assembly is a consequence of two consecutive pathways that work in parallel: first, the furrow is positioned by astral microtubules, and second, by signals derived from the spindle midzone (Bringmann and Hyman 2005; Bringmann et al. 2007). In line with the idea that the furrow position is driven by inhibitory signals coming from astral microtubules, and positive signaling emerging from the midzone, astral microtubule disruption by laser ablation in sea urchin eggs led to a broader RhoA active zone and contractile ring protein accumulation at the cell equator (Bement, Benink, and Von Dassow 2005; Foe and Von Dassow 2008; Von Dassow et al. 2009). Interestingly, the amount of active RhoA did not change, suggesting that astral microtubules did not inhibit RhoA activation but rather, confined it to the cell equator (Von Dassow et al. 2009).

RhoA is a small GTPase responsible for the two major functions required for contractile ring activity which consist in the elongation of non-branched actin filaments through formin activation (Kühn and Geyer 2014) and promotion of myosin activity by activation of ROK or ROCK (Matsumura 2005). RhoA can be bound to GTP or GDP which will determine its activation or inactivation, respectively, working as a switch. RhoA is activated by guanine nucleotide exchange factors (GEFs) that stimulate guanosine diphosphate (GDP) release, allowing guanine triphosphate (GTP) binding. RhoA is inactivated by GTPase-activating proteins (GAPs) that enhance the GTP hydrolysis rate, converting GTP into GDP (Rossman, Der, and Sondek, 2005; Tcherkezian and Lamarche-Vane, 2007). The main RhoA GEFs that contribute to cytokinesis in animal cells are epithelial cell transforming 2 (ECT2), GEF-H1, and MyoGEF, whereas the main cytokinesis GAPs are MgcRacGAP, p190RhoGAP, and MP-GAP (Chircop 2014; Jordan and Canman 2012). In the scope of this thesis, we will focus our attention on ECT2 and MgcRacGAP.

ECT2 localizes to the central spindle and interacts with the centralspindlin complex (section 4.1.), namely with MgcRacGAP (Kamijo et al. 2006; Yüce, Piekny, and Glotzer 2005; Mishima, Kaitna, and Glotzer 2002; Somers and Saint 2003). ECT2 phosphorylation by Cdk1 (cyclin-dependent Kinase) maintains ECT2 in an inactive conformation. Inactive ECT2 is not able to bind to MgcRacGAP preventing its precocious recruitment and RhoA activation (Chircop 2014). Upon anaphase onset, when Cdk1 activity decreases, ECT2 forms a complex with MgcRAcGAP and activates RhoA (Chircop 2014). In fact, MgcRacGAP GAP domain is the one responsible for interacting with ECT2 and to drive RhoA activation (Kamijo et al. 2006; Yüce, Piekny, and Glotzer 2005; Mishima, Kaitna, and

Glotzer 2002; Somers and Saint 2003; Loria, Longhini, and Glotzer 2012). However, the fact that MgcRacGAP and ECT2 interact and contributes for Rho activation is intriguing. As MgcRacGAP's name suggests, it should be a GAP for Rac, contributing for Rho inactivation. Indeed, studies perfomed in *X. laevis eggs* proposed that the GAP activity of MgcRacGAP was responsible to inactivate RhoA and maintain a focused zone for Rho activity through cytokinesis. This was called the Rho GTPase flux model (Miller and Bement 2009). In line with this, Canman *et al.* proposed a model in *C. elegans* where MgcRacGAP^{CYK-4} inactivates Rac, impeding actomyosin constriction (called the negative regulation). This negative regulation would operate in paralel with Rho activation pathway induced by ECT2 (called the positive regulation), and together, the negative and positive pathway, would contribute for ring constriction (Canman et al. 2009).

Thus, during cytokinesis, RhoA oscillates between active/inactive states driving contractile ring ingression (Miller and Bement 2009). RhoA activation is restricted to a narrow zone at the equatorial cell cortex upon anaphase onset (Yüce, Piekny, and Glotzer 2005; Bement, Benink, and Von Dassow 2005; Yonemura, Hirao-Minakuchi, and Nishimura 2004; Yoshizaki et al. 2003; Nishimura and Yonemura 2006). In *C. elegans* early embryos, RhoA activation is also driven by NOP-1, a poorly conserved nematode-specific protein (Glotzer and Basant 2017; Tse et al. 2012). NOP-1 promotes RhoA activation during polarization and seems to be capable of activating global RhoA in embryos (Figure 4).

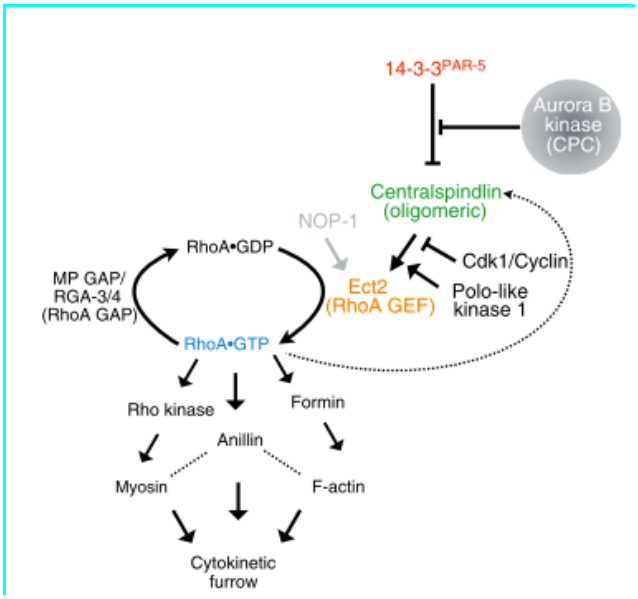

Figure 4- Schematic representation of the RhoA signaling pathway during cytokinesis.

GTP-bound RhoA drives formin and Rho kinase activation and binds anillin to generate a contractile ring. ECT2 is regulated by centralspindlin in a PLK-1 and Cdk1/cyclin-dependent manner. 14-3-3 proteins bind to MKLP1, a member of the centralspindlin complex, and prevent centralspindlin oligomerization. Aurora B prevents 14-3-3 binding to MKLP1,

promoting centralspindlin oligomerization. NOP-1 is a *C. elegans* specific ECT-2 activator (Basant and Glotzer 2018; figure used under permission).

4. The central spindle

During anaphase, chromosomes move towards the opposing cell poles and the midzone microtubules appear in the middle of the segregating chromatids, becoming more evident as they elongate and form bundles. Midzone microtubule nucleation originate on chromosomes and not centrosomes (Uehara and Goshima 2010). Augmin is an eight-subunit protein complex, that binds to a pre-existing microtubule and recruits γ-tubulin ring complex, promoting the nucleation of new microtubules forming a branch (Uehara et al. 2009; Štimac et al. 2022). Additionally, cytoplasmic linker-associated protein 1 (CLASP1), a microtubule-plus end-tracking protein, binds to tubulin dimers and promotes microtubule assembly (Pereira et al. 2006). It is primarily associated with kinetochores in early mitosis and during anaphase, it relocates to the central spindle (Maton et al. 2015; Jing Liu et al. 2009). CLASP1 interacts with protein regulator of cytokinesis 1 (PRC1) (section 7.3) (Jing Liu et al. 2009), a microtubule bundling protein (Mani et al. 2021). Interestingly, Aurora A kinase is required for proper midzone assembly by mediating phosphorylation of several proteins important for central spindle formation such as NEDD1, TACC3, HURP, and p150glued (Courthéoux et al. 2019; Lioutas and Vernos 2013; Reboutier et al. 2013). Inhibition of Aurora A activity results in abnormal spindles, chromosome misalignment, and centrosome defects (Hochegger, Hégarat, and Pereira-Leal 2013). Newly formed midzone microtubules are very dynamic (Vukušić et al. 2017; Yu et al. 2019), however as the cell cycle progresses, microtubules become more stable until they remain static in telophase cells (Saxton and McIntosh 1987; Landino and Ohi 2016; Murthy and Wadsworth 2008; Fermino et al. 2023). The trigger for static microtubule formation is given by cytokinesis progression and midzone proteins, namely PRC1 and KIF4A (section 7.3) (Fermino et al. 2023). Aurora B also plays an important role in midzone formation and cytokinesis. KIF4A phosphorylation mediated by Aurora B allows its interaction with PRC1 and suppresses midzone elongation of microtubule plus-end regulating the length of the midzone (Hu et al. 2011; Bastos et al. 2013).

However, how microtubules elongate during anaphase is under debate. Central spindle microtubules were proposed to elongate based on a “sliding filament” model (McIntosh, Helper, and Wie 1969) in which motor proteins slide adjacent microtubules similar to what happens for muscle myosin II during muscle contraction (Hugh and Hanson 1954). Nevertheless, electron microscopy (EM) studies revealed that this mechanism could not explain all the events happening during anaphase, namely, chromosome movement

towards the cell poles in anaphase A but it sustained the pole-to-pole separation happening during anaphase B that drives spindle elongation (Mcdonald et al. 1977; Winey et al. 1995).

There are five models to explain spindle elongation during anaphase: 1) midzone pushing model, 2) midzone braking model, 3) cortical pulling forces model, 4) microtubule plus end dynamics and polymerization model, and 5) microtubule minus end depolymerization/poleward flux model (Scholey, Civelekoglu-Scholey, and Brust-Mascher 2016).

The first model that consists of midzone pushing based on antiparallel microtubule sliding is especially appealing in diatom central spindle (Mcdonald et al. 1977; Cande and McDonald 1985), where laser destruction of microtubules at the presumptive sites of force generation at the midzone, but not at the poles, prevented spindle elongation (Leslie and Pickett Heaps 1983). Also, in fission yeast, laser microsurgery experiments revealed that midzone pushing is required and sufficient to support spindle elongation at anaphase B (Khodjakov, La Terra, and Chang 2004; Tolic-Norrelykke et al. 2004). In PtK1 culture cells, central spindle microtubules dynamics were studied using light microscopy and fluorescence recovery after photobleaching (FRAP), revealing that microtubule sliding apart was caused by force originated at the midzone microtubule overlap and that contributed to spindle elongation (Saxton and McIntosh 1987). Such a conclusion was reinforced by the observation that the microtubules minus ends of these cells did not reach the cell cortex, making it unlikely that cortical pulling forces drove spindle elongation (Mastronarde et al. 1993).

The second model predicts that the midzone functions as a brake for spindle elongation, counteracting antagonistic forces exerted by cortical pulling motors for example (Saunders et al. 2007; Peterman and Scholey 2009; Rozelle, Hansen, and Kaplan 2011; Shimamoto, Forth, and Kapoor 2015; Collins, Mann, and Wadsworth 2014; Tikhonenko et al. 2008). Indeed, experiments performed in *C. elegans* zygotes, using laser ablation of central spindle microtubules demonstrated that poles moved rapidly towards the cell cortex, indicating that the midzone is dispensable for spindle elongation but rather it works as a brake due to the action of bipolar kinesin-5 motors (Saunders et al. 2007) or the combined action of PRC1/Ase1p and kinesin-6 (Verbrugghe et al. 2004; Lee et al. 2015).

The third model defends the existence of pulling forces operating on the astral microtubules at the cell cortex that pull apart the associated spindle poles (Aist et al. 1991). Moreover, the pulling forces operating are proposed to be responsible for controlling pole-to-pole distance and the position of the entire spindle (Grill et al. 2001; Grill and Hyman 2005;Grill et al. 2003). There are several candidates for generating such forces which include cortically-anchored dynein or microtubule depolymerization (Fink et al. 2006; Saunders et al. 2007; Grishchuk et al. 2005).

Microtubule polymer dynamics, which is characterized by instability and microtubule flux toward the poles, constitutes a fourth model for explaining spindle elongation during mitosis (Desai and Mitchison 1997; Inoue and Salmon 1995). In PtK1 cells (Saxton and McIntosh 1987), *D. melanogaster* embryos (Cheerambathur et al. 2007), and *C. elegans* zygotes (Nahaboo et al. 2015; Dumont, Oegema, and Desai 2010), central spindles grow due to polymerization at microtubule plus ends as these slide apart. The microtubules plus ends are crosslinked by microtubule-associated proteins (MAPS) and motors to produce a more robust midzone.

In the last model, the suppression of poleward flux by inhibiting microtubules minus-end depolymerization, controls the rate of anaphase B spindle elongation in *D. melanogaster* embryos (Brust-Mascher et al. 2004, 2009) (Fifth model). However, the specificity of this model in this system or its applicability in other systems remains to be determined.

Notably, it is important to have in mind that these models do not work isolated one from others. Rather, a balance of opposing forces must be created to correctly explain midzone elongation as it was initially proposed by Ostergren (Hays, Wise, and Salmon 1982; Ostergren 1950). In *C. elegans* zygotes, cortical pulling forces acting on astral microtubules represent the major mechanism of outward-directed forces operating on the spindle (Grill et al. 2001; Grill et al. 2003). These forces are responsible for spindle positioning and spindle elongation (Hara and Kimura 2009; Cowan and Hyman 2004) and are generated by combining microtubule depolymerization and dynein-mediated movement towards the microtubules minus ends (Nguyen-Ngoc, Afshar, and Gonczy 2007; Cowan and Hyman 2004; Laan et al. 2012; Kozlowski, Srayko, and Nedelec 2007). PRC1 counteracts as a brake for spindle elongation (Lee et al. 2015). Female meiotic spindles are anastral, meaning that cortical pulling forces are unlikely to operate in these cases. In this case, a motor-driven midzone pushing mechanism that requires microtubule polymerization leads to pole-pole separation (Telley et al. 2012; McNally et al. 2016).

4.1. Central spindle components

Central spindle microtubules serve as a scaffold for important proteins involved in the positioning, assembly, and constriction of the contractile ring such as the chromosomal passenger complex (CPC) and the centralspindlin complex (Figure 5).

The PRC1, a protein that crosslinks midzone microtubules and keeps them bundled, which will be further detailed in section 7, is another component of the central spindle. The CPC, centralspindlin, and PRC1 are all required for proper midzone formation and maintenance, but their inhibition/depletion leads to different effects on cytokinesis, as will be described below.

The CPC is a four-protein complex composed of Aurora B kinase, INCENP, Survivin, and Borealin. It is localized at different places during mitosis and this allows its intervention in correcting chromosome-microtubule attachment errors, activation of spindle assembly checkpoint (SAC) and construction and regulation of the cytokinetic contractile ring (Carmena et al. 2012). Aurora B belongs to the Ser/Thr kinase family which includes: Aurora A, mentioned in the previous section as acting at mitotic spindle poles, Aurora B, which operates at the centromere, anaphase spindle, and cell cortex, and Aurora C, which resembles Aurora B function but in meiosis and mitosis in early development (Carmena, Ruchaud, and Earnshaw 2009). These kinases, together with CDKs and polo-like kinases (PLKs) are master regulators of cell division (Carmena, Ruchaud, and Earnshaw 2009; Lens, Voest, and Medema 2010). INCENP functions as a platform for CPC assembly and localization at centromeres, anaphase spindle midzone, and midbody (Vader et al. 2006; Jeyaprakash et al. 2007; Ainsztein et al. 1998; Klein, Nigg, and Gruneberg 2006). INCENP regulation is mediated by Aurora B and CDK1-cyclin B and its phosphorylation prevents CPC association with midzone before anaphase in budding yeast (Nakajima et al. 2011; Pereira and Schiebel 2003). Survivin contains an N-terminal Zn^{2+}-coordinated baculovirus IAP repeat (BIR) domain and mutations within this domain prevent CPC recruitment to the centromeres but do not affect protein localization from anaphase onward in vertebrates (Yue et al. 2008; Lens et al. 2006). Results gathered in *D. melanogaster* spermatocytes showed that a point mutation in the BIR domain prevents CPC localization to the spindle midzone without affecting its localization at centromeres (Szafer-Glusman, Fuller, and Giansanti 2011), suggesting that the BIR domain can also function in CPC localization during anaphase. Lastly, Borealin is involved in the regulation of cytokinesis and abscission by interacting with cytokinesis/abscission proteins (Carmena et al. 2012). Thus, disruption of the CPC by depleting or inactivating one of the proteins that forms this complex results in cytokinesis failure in multiple systems (Adams et al. 2001; Carvalho et al. 2003; Gassmann et al. 2004; Honda, Korner, and Nigg 2003).

The centralspindlin complex is a heterotetramer composed of two molecules of MgcRacGAP and two molecules of mitotic kinesin-like protein 1 (MKLP1). Centralspsindlin functions include central spindle assembly, regulation of Rho family GTPases (as discussed in section 3.2.), midbody assembly, and abscission (White and Glotzer 2012). Each of centralspindlin proteins alone cannot bundle microtubules to promote central spindle assembly during anaphase (Mishima, Kaitna, and Glotzer 2002; Mishima et al. 2004). Nevertheless, the first functions proposed to MKLP1 included microtubule crosslinking and sliding during anaphase and force generation to promote spindle elongation (Nislow et al. 1992). MKLP1 ortholog mutants in *D. melanogaster* embryos failed to initiate contractile ring assembly resulting in cytokinesis failure (Adams et al. 1998).

Perturbation of the *C. elegans* MKLP1 ortholog, ZEN-4, resulted in a lack of organized midzone microtubule bundles (Powers et al. 1998) but allowed contractile ring assembly but only partial furrow ingression followed by cytokinesis failure (Davies et al. 2014). Interestingly, ZEN-4 limits the extension of spindle elongation (Dechant and Glotzer 2003). Notably, MgcRacGAP, that was first identified in human cells as a Rho family GAP (Touré et al. 1998), and MKLP1 have been proposed to work together during embryogenesis (but not in germline development) (Lee et al. 2018).

Thus, inhibition of either CPC or centralspindlin results in cytokinesis failure in sand dollar eggs (Mabuchi et al. 1993), *D. melanogaster* embryos and Dmel2 tissue culture cells (Adams et al. 2001; Prokopenko et al. 1999), HeLa cells (Tatsumoto et al. 1999; Gassmann et al. 2004; Honda, Korner, and Nigg 2003; Hirose et al. 2001; Carvalho et al. 2003), and *C. elegans* embryos (Schumacher, Golden, and Donovan 1998; Davies et al. 2014). In HeLa cells, PRC1 perturbation resulted in cytokinesis failure either during or at the end of constriction (Jiang et al. 1998; Mollinari et al. 2005, 2002). Point mutations (feo^{EA86} and feo^{S27}) of PRC1^{FEO} in *D. melanogaster* S2 cells led to ring constriction problems during late telophase, with cells exhibiting partial furrow ingression followed by cytokinesis failure (Vernì et al. 2004). In fission yeast, PRC1^{Ase1} depletion showed defects in septum formation, and in the mechanism responsible for monitoring the formation and the integrity of medial actomyosin ring and septum, called cytokinesis checkpoint (Yamashita et al. 2005). Interestingly, no problems during cytokinesis were reported for PRC1^{SPD-1} depletion in *C. elegans* 1-cell embryos (Green et al. 2013). However, older reports indicate that PRC1^{SPD-1} inactivation causes cytokinesis failure in the EMS cell of the 4-cell *C. elegans* embryo after complete ingression of the furrow (Verbrugghe et al. 2004).

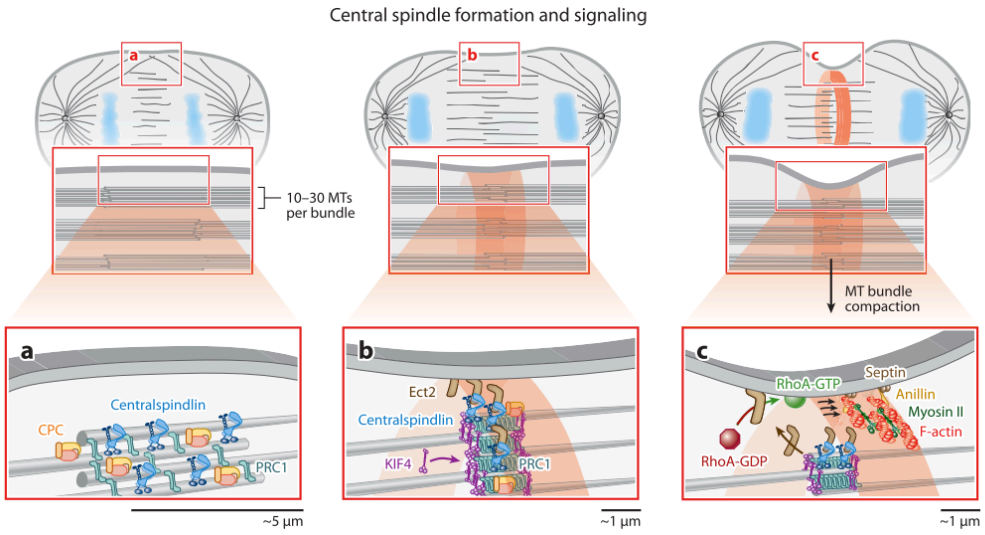

Figure 5- The central spindle and its main components.

(a) PRC1, centralspindlin, and the CPC are localized at the cell midzone. (b) PRC1 directly interacts and recruits the kinesin KIF4 to microtubule plus-ends (explained in section 7.2.). This interaction is required to limit the length of microtubule overlap. ECT2 interacts with centralspindlin at the midzone. (c) ECT2 activates RhoA by converting inactive RHOA-GDP into active RHOA-GTP at the cell membrane. This culminates in the assembly of the contractile ring (Green, Paluch, and Oegema, 2012; figure used under permission).

PLK1 is another protein that localizes to central spindle microtubules via PRC1, however, it is not required for central spindle formation (Neef et al. 2007; Petronczki et al. 2007; Brennan et al. 2007; Burkard et al. 2007). Nevertheless, PLK-1 inhibition leads to spindle elongation failure during anaphase (Brennan et al. 2007).

PLK1 also phosphorylates MgcRacGAP which allows the binding of MgcRacGAP to ECT2, and consequently Rho activation (Yüce, Piekny, and Glotzer 2005; Wolfe et al. 2009; Burkard et al. 2009). In addition to this, PLK1 can also bind ECT2, relieving its autoinhibited state (Niiya et al. 2006).

It has been proposed that two pools of centralspindlin exist in dividing HeLa cells: one at the equatorial cortex, where centralspindlin oligomerizes via Aurora B activity and activates RhoA (Basant et al. 2015; Adriaans et al. 2019); and another at the central spindle microtubules, where PRC1 directly interacts and sequesters MgcRacGAP in a PLK1-dependent manner (Ban et al. 2004; Lee et al. 2015; Adriaans et al. 2019). The latter pool is still able to bind and activate ECT2 and consequently RhoA. These two pools of centralspindlin operate independently and when one is disrupted the other can still compensate and the contractile ring can still ingress (Adriaans et al. 2019) (Figure 6).

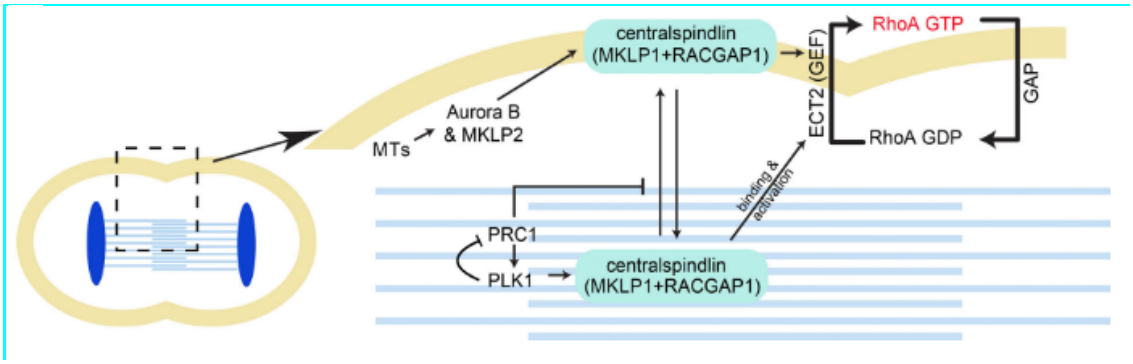

Figure 6- Schematic representation of a model for RhoA activation via two pools of centralspindlin in HeLa cells.

pools of centralspindlin exist: one at the equatorial cortex, which oligomerizes via Aurora B and drives RhoA activation, and another that relies on central spindle microtubules that can bind and activate ECT2 and RhoA. The central spindle pool is proposed to be sequestered by PRC1. Phosphorylation of PRC1 by PLK1 releases centralspindlin from the spindle

midzone making it available for Rho activation at the cell cortex (Adriaans et al., 2019; figure used under permission).

5. The midbody and the midbody ring

The midbody derives from the spindle midzone and is known to orchestrate the final steps of cytokinesis. While the central spindle matures into the midbody, the contractile ring transitions into the midbody ring.

The midbody components are partitioned into three groups especially well described in tissue culture cells: those in the midbody ring, in the midbody core, and the midbody flanking regions or midbody arms (Figure 7A) (Elia et al. 2011; Hu, Coughlin, and Mitchison 2012; Halcrow et al. 2022). PRC1 remains attached to central spindle microtubules in the region of microtubule overlap (midbody core) (Hu, Coughlin, and Mitchison 2012). Aurora B localizes in the midbody flanking regions (Gruneberg et al. 2004; Hu, Coughlin, and Mitchison 2012; Green, Paluch, and Oegema 2012). Contractile ring components such as anillin, septins, and RhoA localize in the midbody ring (Gai et al. 2011; Kechad et al. 2012; Hu, Coughlin, and Mitchison 2012). The localization of centralspindlin and Cep55, a protein required for ESCRT machinery recruitment, is less clear with some reports claiming they localize in the midbody core and others in the midbody ring (Figure 7) (Elia et al. 2011; Guizetti et al. 2011; Hu, Coughlin, and Mitchison 2012).

The transition from contractile to midbody ring is thought to involve molecular changes. However, what happens during this transition or when the transition starts remains largely unknown. A previous study has shown that in *D. melanogaster* S2 cells, this transition involves Anillin and Septins. As the contractile ring matures, anillin acquires different functions. Anillin N-terminus is required to connect to actomyosin structures and support the formation of a stable midbody ring. Notably, the contractile rings of anillin mutants lacking the C-terminus can fully constrict and form a midbody, but the plasma membrane detaches from it. Similar results were achieved when septin was depleted (Kechad et al. 2012). Indeed, septin was found to act on anillin C-terminus to remove the excess membrane-associated anillin molecules from the forming midbody ring (Amine et al. 2013). These indicated that the C-terminus of anillin and septins are required to anchor the midbody ring to the plasma membrane (Kechad et al. 2012). Additionally, the centralspindlin subunit MgcRacGAP binds to PtdIns4P and PtdIns(4,5)P_2 allowing the anchorage of the ingression furrow during abscission (Lekomtsev et al. 2012). Interestingly, while MKLP1 N-terminus can associate with central spindle microtubules, its C-terminus can directly bind Arf6 (a small GTPase) that tethers to the plasma membrane in mouse embryonic fibroblasts (Makyio et al. 2012).

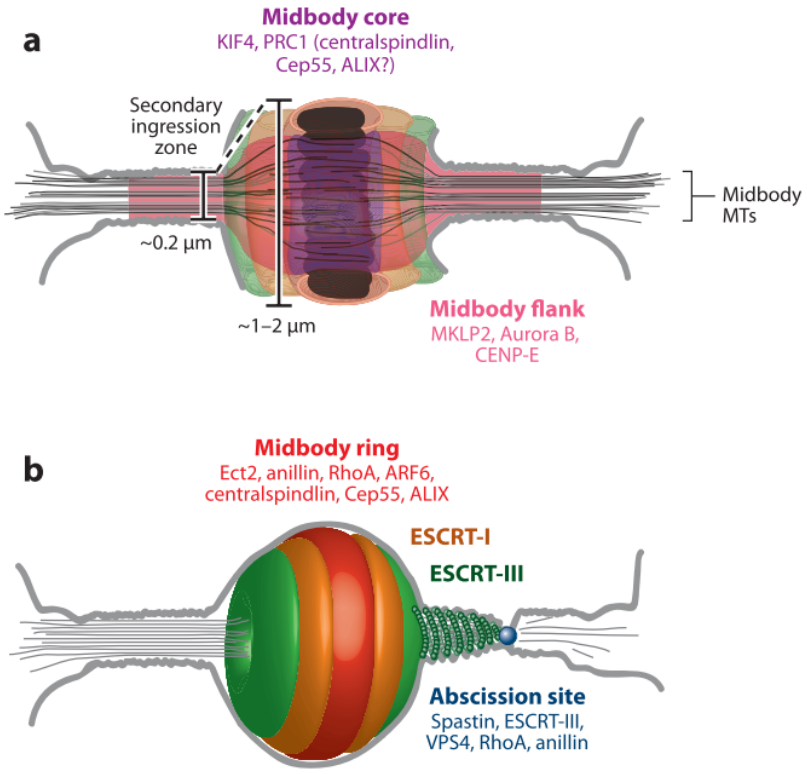

Figure 7- Midbody structure in HeLa cells.

(a) Schematic illustrating the midbody core and midbody flank components. (b) Schematic illustrating midbody ring components and ESCRT machinery organization. Midbody MTs represent midbody microtubules (Green, Paluch, and Oegema 2012; figure used under permission).

6. Abscission

Abscission is the process that completes cytokinesis by sealing the final gap between the two sister cells. What happens during abscission is better understood in tissue culture cells, namely HeLa cells, and in the *C. elegans* 1-cell embryo. While this process involves the formation of ESCRT filaments in HeLa cells, in *C. elegans* zygotes ESCRTs are not necessary (Guizetti et al. 2011; König et al. 2017; Green et al. 2013).

ESCRT machinery involved in abscission is mainly composed of three complexes: ESCRT-I, ESCRT-II, and ESCRT-III complex.

ESCRT-I complex is constituted by several different subunits: MVB-12 A, B, VPS-37 A-D, VPS-28, TSG-101, and UBAP1L. TSG-101 is responsible for recruiting the remaining ESCRT-I proteins to the midbody and VPS-37 contributes to the binding of the complex to the membrane. However, no functions have been attributed yet to MVB-12, VPS-28, or UBAP1L subunits, although a possible role in establishing interactions with ESCRT-III subunit VPS-20 has been proposed for VPS-28 (Hurley 2011).

The role of the ESCRT-II complex in cytokinesis has been poorly discussed and it is controversial. ESCRT-II is constituted of three subunits: VPS22, VPS25, and VPS36. Live-cell imaging of Madin-Darby canine kidney (MDCK) cells has revealed that ESCRT-II is required for successful abscission (Goliand et al. 2014). VPS25 subunit was shown to bind and interact with the ESCRT-III subunit, CHMP6, recruiting it to the midbody (Goliand et al. 2014; Im et al. 2009). Thus, ESCRT-II was suggested to bridge ESCRT-I and III, being a downstream effector of ESCRT-I machinery (Christ et al. 2016).

Once ESCRT-III subunit CHMP6 is target to the abscission site, the process of ESCRT-III complex assembly initiates (Schiel and Prekeris 2010). First, CHMP4B is recruited and recruits downstream subunits, CHMP2, CHMP3, CHMP1, and IST1 that were described to polymerize into filaments *in vitro* (Christ et al. 2017; Schiel and Prekeris 2010). *In vitro* studies suggest that VPS4 promotes ESCRT-III disassembly but is not important for membrane fission reaction (Wollert et al. 2009). In contrast, in cells, VPS4-ESCRT-III binding contributes to membrane neck narrowing (Adell et al. 2014) and VPS4 accumulates at the midbody before abscission, releasing IST-1 protein (Agromayor et al. 2009; Bajorek et al. 2009; Elia et al. 2011). IST-1 is known to inhibit VPS4 activity.

Thus, ESCRT machinery is thought to be recruited sequentially. It all starts with the interaction between the centralspindlin subunit MKLP1 with CEP-55 during late cytokinesis, at least in human cells (Bastos and Barr 2010; Carlton and Martin-Serrano 2007; Hyung et al. 2008; Morita et al. 2007). CEP-55 interacts either with TSG-101 and ALIX, and that allowed ESCRT-III complex to be recruited to the midbody in human cells (Carlton and Martin-Serrano 2007; Hyung et al. 2008). TSG-101 and ALIX were proposed to compete for CEP-55 binding (Hyung et al. 2008). Since TSG-101 and ALIX are both essential for cytokinesis in HeLa cells (Carlton and Martin-Serrano 2007; Morita et al. 2007), Hyung *et al.*, proposed that multiple CEP-55 dimers must exist to bind ALIX and TSG-101 (Hyung et al. 2008). Interestingly, while the absence of CEP-55 does not compromise mouse embryonic development nor division of fibroblasts, it affects the survival and abscission of neural progenitors (Tedeschi et al. 2020; Little et al. 2020). Whether CEP-55 is required to recruit ESCRTs into the midbodies of mouse brain cells differs between reports (Little et al. 2020; Tedeschi et al. 2020). Interestingly, *D. melanogaster* and *C. elegans* lack CEP-55 homologs suggesting that other mechanisms are involved in the recruitment of the ESCRT machinery to the midbody. In *D. melanogaster* it was shown that centralspindlin directly recruits ALIX and TSG-101 to the midbody allowing successful cytokinesis (Lie-Jensen et al. 2019).

Currently, 3 models attempt to explain how membrane scission is promoted (Figure 8). The first model defends that ESCRT-III spirals are assembled in the abscission site with a gradual decrease of their diameter extending from the midbody until the place where

abscission will be promoted (Guizetti et al. 2011). The second model postulates that part of ESCRT-III filaments are released from the midbody, possibly in a VPS4-dependent manner, accumulate in the secondary ingression site, and constrict the cortex (Elia et al. 2012). The third model proposes a model where ESCRT-III binds and stabilizes the membrane deformations, generated by other processes such as vesicle secretion (Schiel et al. 2012).

Actin filament disassembly has been suggested to be required for abscission (Mierzwa and Gerlich 2014). Actin filament disassembly in the abscission sites is achieved through RhoA inactivation that is mediated by PKCε kinase and 14-3-3 protein (Saurin et al. 2008). Also, changes in membrane lipid composition and delivery of endosomal vesicles containing Rab11 and FIP3 contribute to actin disassembly and the formation of the secondary ingression sites (Schiel et al. 2012; Dambournet et al. 2011). This promotes high membrane curvature allowing ESCRT-III recruitment (Schiel et al. 2012).

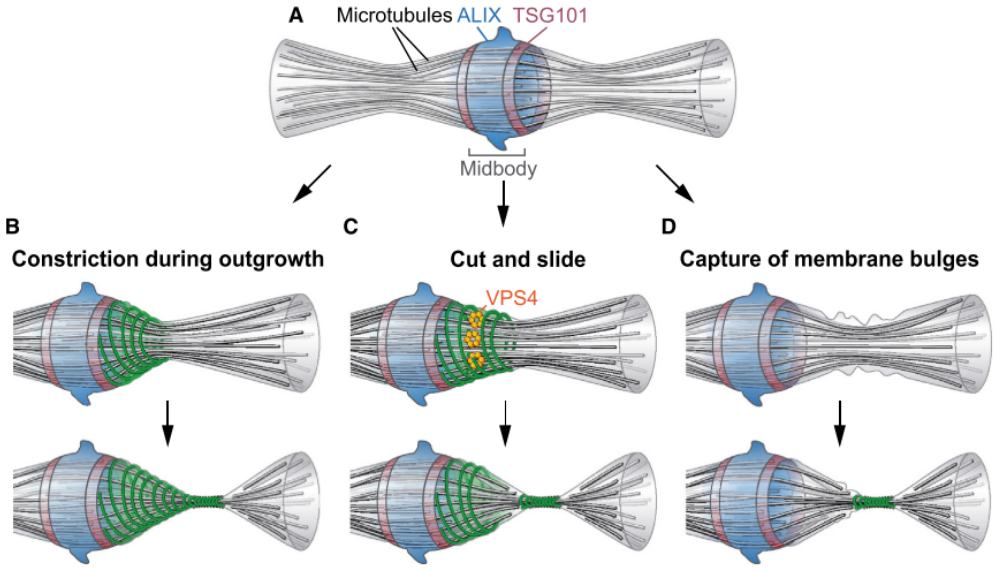

Figure 8- Models for membrane scission in HeLa cells.
(A) ALIX and TSG101 allow ESCRT-III (green spirals) recruitment to the midbody. (B-D) Proposed models for membrane constriction. (B) ESCRT-III filaments gradually narrow forcing the membrane curvature away from the midbody. (C) ESCRT-III filaments form cylindrical spirals that are eventually split by VPS4, constricting away from the midbody. (D) ESCRT-III capture membrane bulges generated by other processes such as vesicle secretion (Mierzwa and Gerlich 2014; figure used under permission).

It is known that abscission timing is regulated by mitotic kinases and mechanical tension in HeLa cells. PLK1 was first implicated in preventing abscission by phosphorylating CEP-55 avoiding its association with the centralspindlin complex (Bastos and Barr 2010). Thus, PLK1 needs to be degraded in order to CEP-55 is recruited to the midbody and abscission takes place (Bastos and Barr 2010). However, a more recent report has

suggested that PLK1 is important to phosphorylate ALIX and to release it from the close to open conformation (Sun et al. 2016). By opening its conformation, ALIX is able to recruit ESCRT complex and abscission takes place. Thus an apparent contradiction between PLK1 role during last stages of cytokinesis exists and remains to be elucidated whether PLK1 promotes or inhibits abscission (Sun et al. 2016; Bastos and Barr 2010). Also, Aurora B functions as a negative regulator of abscission since it is a major player in the abscission checkpoint (Carlton et al. 2012). Abscission checkpoint was firstly identified in budding yeast *S. cerevisiae* as the "NoCut checkpoint", and then in HeLa cells and in *C.elegans* embryos (Steigemann et al. 2009; Mendoza et al. 2009; Norden et al. 2006; Bembenek et al. 2013; Carlton et al. 2012). In the presence of chromatin bridges or lagging chromosomes, abscission is delayed, preventing the chromatin breakage or tetraploidiztion, and this is called the abscission checkpoint (Norden et al. 2006; Mierzwa and Gerlich 2014; Steigemann et al. 2009). Indeed, other triggers for abscission checkpoint activation were more recently identified such as: nuclear pore defects, DNA replication stress or high midbody tension (Mackay, Makise, and Ullman 2010; Mackay and Ullman 2015; Lafaurie-Janvore et al. 2013). In tissue culture cells, mechanical tension release seems to favour abscission since severing of the connecting bridge between the two sister cells by laser microsurgery triggers ESCRT-II accumulation and abscission (Lafaurie-Janvore et al. 2013).

Gathered evidence indicates that central spindle microtubules are required to set the stage for the abscission machinery to function but they need to be disassembled for abscission to complete in tissue culture cells. Indeed, the addition of nocodazole, a microtubule depolymerization agent, during cleavage furrow ingression has been shown to cause furrow regression in rat epithelial cultured cells (Wheatley and Wang 1996). However, when cells are treated with microtubule depolymerizing agents at a time when only a thin cytoplasmic bridge, filled with microtubules, connects the two sister cells, abscission does not fail. In fact, in these situations cytoplasmic bridge narrowing happens faster indicating that that central spindle microtubules need to be disassemble for abscission takes place (Guizetti et al. 2011; Schiel et al. 2012).

In the *C. elegans* zygote, abscission has been described to occur in two steps: 1) cytoplasmic isolation (early abscission) and 2) midbody release (late abscission) (Green et al. 2013). Cytoplasmic isolation, which is septin-dependent, occurs immediately after contractile ring ingression stalls (Green et al. 2013). Midbody release also relies on septin and ESCRT machinery (namely TSG-101) (Green et al. 2013). However, contrasting with mammalian cells, where ESCRT helical structures were first identified (Guizetti et al. 2011), tomograms of *C. elegans* 1-cell embryos failed to detect ESCRT filaments within the abscission site (König et al. 2017), suggesting alternative abscission mechanisms.

Nevertheless, many members of the abscission machinery are conserved. These data reveal that ESCRT-independent ways of performing abscission exist.

Contrasting with conclusions gathered in HeLa cells, midbody microtubules were proposed to be dispensable for abscission in *C. elegans* 1-cell embryo (Hirsch et al. 2022; Green et al. 2013; König et al. 2017). The authors showed indeed that abscission machinery can still be recruited directly to the midbody ring in the absence of central spindle microtubules (Green et al. 2013). These conclusions were taken from experiments of $PRC1^{SPD-1}$ depletion, which as will be discussed in the results section, may not be fully penetrant. Furthermore, it was recently shown that a functional midbody still forms in *C. elegans* zygotes lacking the CENP-F–like proteins HCP-1/2, which are required for central spindle formation (Hirsch et al. 2022). In this situation, the authors proposed that this is possible via contractile ring-mediated compaction of bundled astral microtubules that traverse the equatorial region. Nevertheless, $PRC1^{SPD-1}$ is essential for cytokinesis in the EMS cell (K. J. C. Verbrugghe et al. 2004) indicating that PRC1 requirement may vary with cell type.

During abscission, midbody remnants can either be attached to cells or released. After release the midbody remnant can be inherited specifically by one of the daughter cells. The presence of a midbody remnant has been associated with the “stemness” of mouse neural stem cells (McNeely and Dwyer 2020). HeLa cells containing midbody remnants were shown to upregulate genes directly linked to cell proliferation (Peterman et al. 2019). This promotes the pluripotency and the tumorigenicity of cancer cells (Kuo et al. 2011). Additionally, the position of midbody remnants can affect cell polarity (Luján et al. 2016; Lujan et al. 2017) and tissue epithelial architecture in *D. melanogaster* follicle cells (Morais-De-Sá and Sunkel 2013). In *C. elegans* embryos, midbody remnants were shown to direct spindle rotation in P1 cells and mediate dorsal-ventral axis specification (Singh and Pohl 2014; Hyman 1989; Waddle, Cooper, and Waterston 1994; Keating and White 1998).

Midbody inheritance can be associated with where membrane scission occurs in HeLa cells. If the abscission machinery accumulates on only one side of the midbody, the opposing daughter cell inherits the midbody remnant (Chen et al. 2013). This asymmetric inheritance seems to occur in a centrosome-age-dependent manner (Salzmann et al. 2014; Kuo et al. 2011). Of note, in HeLa, MDCK, and mouse cortical neuronal stem cells, membrane scission sequentially occurs on both sides (Guizetti et al. 2011; Elia et al. 2011; McNeely and Dwyer 2020). In *D. melanogaster* germline (Salzmann et al. 2014) and imaginal disk epithelium (Daniel et al. 2018) asymmetric inheritance of the midbody was reported. In *C. elegans* early embryos, midbody remnant inheritance is also asymmetric and controlled by cortical tension – cells with lower cortical tension inherit it (Singh and Pohl, 2014). Interestingly, membrane scission occurs on both sides of the midbody with the

midbody remaining in the middle and later being engulfed into the posterior cell (König et al. 2017). Whether membrane scission occurs first on the anterior or posterior side is random (König et al. 2017). Nevertheless, midbody inheritance in *C.elegans* does not affect cell fate (Ou, Gentili, and Gönczy 2014). In *C. elegans* Q neuroblast divisions, the midbodies are released into the extracellular space, being later internalized and degraded (Chai et al. 2012).

7. PRC1: a microtubule bundler protein

The first PRC1 ortholog was discovered in 1993 in cytoplasmic extracts of miniprotoplasts from tobacco Bright Yellow-2 (BY-2) cells and was named MAP65 (microtubule-associated protein 65) (Chang-Jie and Sonobe 1993). It was reported to co-localize with microtubules along the cell cycle (Chang-Jie and Sonobe 1993). Later, other MAP65 orthologues were identified and are summarized in Table I.

Table I- Microtubule-associated proteins orthologs.

Species	*H. sapiens*	*D. melanogaster*	*C. elegans*	*S. cerevisiae/pombe*
Protein Name	PRC1	Feo	SPD-1	Ase1p/Ase1
Reference	(Jiang et al. 1998)	(Vernì et al. 2004)	(Verbrugghe et al. 2004)	(Pellman et al. 1995; Loıodice et al. 2005; Yamashita et al. 2005)

In mammalian cells, PRC1 localization was first determined by immunofluorescence studies that revealed that it localizes in the nucleus during interphase, and on the central spindle and midbody during mitosis (Jiang et al. 1998). A similar localization pattern is found in *C. elegans* embryos expressing SPD-1::GFP (Verbrugghe et al. 2004). In *D. melanogaster,* PRC1 (Feo) is cytoplasmic during interphase in brain cells and accumulates in the central spindle in mitotic cells (Vernì et al. 2004). In fission yeast, PRC1 (Ase1) can colocalize with microtubules either in interphase (cytoplasmic microtubule array) or during mitosis (microtubule organizing center and spindle midzone) (Yamashita et al. 2005). By contrast, in budding yeast, PRC1(Ase1p) did not present any specific staining but during mitosis, it localizes along the spindle (but not at centrosomes) (Pellman et al. 1995).

PRC1 and its orthologues SPD-1 and Ase1p bridge and bundle microtubules *in vitro* (Schuyler, Liu, and Pellman 2003; Chang-Jie and Sonobe 1993; Mollinari et al. 2002; Lee et al. 2015).

In vivo, PRC1 has been proposed to operate during different phases of the cell cycle with a special emphasis on anaphase. PRC1 was shown to be required for microtubule overlap during metaphase that directly impacts chromosome alignment in U2OS cells (Jagrić et al. 2021). Moreover, PRC1 depletion or overexpression impedes spindle twist, indicating that PRC1 plays a role in regulating spindle torques in HeLa-Kyoto BAC cells (Trupinić et al. 2022). Lack of PRC1/SPD-1 function consistently leads to unbundled central spindle microtubules in anaphase across experimental systems (Zhu et al. 2006; Jiang et al. 1998; Mollinari et al. 2002; Maton et al. 2015; Verbrugghe et al. 2004). In budding yeast, *Saccharomyces cerevisiae,* Ase1p was shown to be required for viability and anaphase spindle elongation (Pellman et al. 1995). Ase1p loss leads to premature mitotic spindle disassembly while preventing its degradation results in delayed spindle disassembly (Juang et al. 1997; Schuyler, Liu, and Pellman 2003). Feo mutant flies exhibit poorly constricted contractile rings (Vernì et al. 2004). Also, Feo mutation (EA86 and S27 mutation) causes very small testes and decreased dividing spermatocytes (Vernì et al. 2004). Notably, *C. elegans* carrying a temperature-sensitive mutation (*oj5*) in the *spd-1* gene present defects in the germline gonads, exhibit poor mobility, lay dead embryos, and possess vulval defects, evidencing the importance of SPD-1 for *C. elegans* development (O'Connell, Leys, and White 1998).

7.1. PRC1 structure

PRC1 is a homodimer constituted by an N-terminal dimerization domain followed by a rod and a spectrin domain, and a disordered domain at the C-terminus. Part of dimerization domain, the entire rod domain and the N-terminal region of spectrin domain of PRC1 shares 21% of similarity with SPD-1 (Verbrugghe et al. 2004).

Moreover, the N-terminal region of PRC1 is predicted to contain multiple coiled-coil motifs that in *spd-1*(*oj5*) mutant is predicted to be disrupted, at least, one of them (Mollinari et al. 2002; Verbrugghe et al. 2004).

The rod domain is flexible when the protein is attached to a single microtubule, however, it adopts a specific orientation when it crosslinks microtubules (Kellogg et al. 2016; Subramanian et al. 2010). Dimerization and rod domains are required to orient spectrin and C-terminal domains towards the opposing microtubules. Within the spectrin domain a set of conserved residues are responsible for PRC1 binding to microtubules (Portran et al. 2013; Subramanian et al. 2010; Mollinari et al. 2002). This latest domain regulates the geometry of a microtubule array (Kellogg et al. 2016). Moreover, a conserved motif localized within the microtubule binding region is common among species (Portran et al. 2013; Schuyler, Liu, and Pellman 2003). Interestingly, previous studies using truncated versions of PRC1 revealed that the C-terminus of rod domain together with spectrin domain and part of

disordered domain are required for PRC1 localization at microtubules *in vivo* during interphase (Mollinari et al. 2002; Kellogg et al. 2016). Nevertheless, the N-terminus of PRC1 including the dimerization and the rod domain are both necessary for PRC1 localization at the midzone and at the midbody in HeLa cells (Mollinari et al. 2002; Kellogg et al. 2016). Interestingly, the same region of PRC1 directly binds KIF4 (section 7.2. and 7.3.) (Kurasawa et al. 2004).

The PRC1 C-terminal region contains a disordered domain hypothesized to enhance the microtubule-binding activity through electrostatic interactions with neighbour protofilaments (Subramanian et al. 2010; Kellogg et al. 2016). Additionally, also in the C-terminus, PRC1 contains two nuclear localization signals (NLSs) responsible for PRC1 localization in the nucleus (Jiang et al. 1998; Mollinari et al. 2002) and CDK1 phosphorylation sites (Mollinari et al. 2002). Mitotic PRC1 phosphorylation by CDK1 decreases the affinity of PRC1 to microtubules possibly by reducing the positive charge of the domain thus impairing the electrostatic interaction that it establishes with microtubules (Subramanian et al. 2010). Thus, PRC1 mutated for CDK phosphorylation sites causes extensive bundling of microtubules and block the mitotic progression (Mollinari et al. 2002). Additionally, PRC1 mitotic phosphorylation is responsible for PRC1 oligomerization (Fu et al. 2007). PLK1 docking sites can also be found in the C-terminus, and PRC1 mutated for PLK1 docking sites is unable to recruit PLK1 to the midzone and prevents cytokinesis (Neef et al. 2007).

Finally, PRC1 also contains several motifs for ubiquitination-dependent proteolysis required for cell-cycle-dependent degradation (She et al. 2019).

7.2. PRC1 regulation

For the cell to enter mitosis, cyclin-dependent kinase 1, CDK1, has to be activated by Cyclin B during the G2 phase. Once chromosomes are correctly aligned in the metaphase plate, Cyclin B is degraded, and consequently, CDK1 activity is compromised. CDK1 phosphorylates PRC1 at residues Thr-470 and Thr481 in HeLa cells (Jiang et al. 1998). However, the CDK1 phosphorylation site in PRC1 is not well conserved in budding yeast (Jiang et al. 1998). PRC1 expression also varies throughout the cell cycle, presenting high levels during S and G2/M phases in HeLa cells (Pellman et al. 1995; Jiang et al. 1998). In *S. pombe,* PRC1 degradation is required for spindle disassembly (Juang et al. 1997).

PRC1 is recruited to the interdigitated central spindle microtubules by its binding partner kinesin family member 4 (KIF4) during the metaphase-to-anaphase transition (Kurasawa et al. 2004; Zhu and Jiang 2005). At this time, CDK1 activity starts to drop and PRC1 becomes dephosphorylated by the action of mitotic phosphatase Cdc14A or protein phosphatase 1 gamma (PP1Y) (Zhu and Jiang 2005), which was found in a midbody

interactome in HeLa cells (Capalbo et al., 2019). Dephosphorylation allows for PRC1 dimerization and consequently microtubule bundling, with a PRC1 mutant carrying mutated CDK1 phosphorylation sites leading to extensive bundling of microtubules *in vivo* (Mollinari et al. 2002).

PRC1 phosphorylation by CDK1 during metaphase impedes PRC1 interaction with PLK1 in HeLa cells (Neef et al. 2007). In anaphase, after the decrease in CDK1 activity, PLK1 binds its docking sites in PRC1, which increases its microtubule-binding activity (Neef et al. 2007), and allows for its localization at the central spindle (Neef et al. 2007). *In vitro* experiments showed that PRC1 phosphorylation by PLK1 is stimulated by microtubule density, suggesting that when microtubule density is high PLK1 negatively regulates PRC1 (Hu et al. 2012a). If microtubule density is low, PRC1 becomes less phosphorylated by PLK1 allowing microtubule crosslinking mediated by PRC1 (Hu et al. 2012a). Moreover, it was proposed that PRC1 phosphorylation by PLK1 contributes to centralspindlin release from the central spindle allowing for ECT-2 activation at the equatorial cortex in HeLa cells (Adriaans et al. 2019).

7.3. PRC1 interactors and central spindle formation

Citron kinase is responsible to recruit and maintain anillin in the midbody (Amine et al. 2013; Gai et al. 2011) and has been implicated in midbody stabilization through the interaction that it establishes with MKLP1 and KIF14 (Bassi et al. 2013; Gruneberg et al. 2006; Watanabe et al. 2013). Citron kinase and KIF14 can interact with PRC1 (Gruneberg et al. 2006; Bassi et al. 2013).

PRC1 tags microtubule plus ends through KIF4-mediated transport. *In vitro* assays showed that the number of PRC1-KIF4 tags is directly proportional to microtubule length (Subramanian et al. 2013). PRC1-KIF4 tags at microtubule plus ends allow microtubule capping, stabilization, and recruitment of more regulators such as PLK1, kinesin-6, and CLASP (Duellberg et al. 2013; Subramanian et al. 2013). Interestingly, Aurora B can interact with both KIF4 and PRC1 during cytokinesis in HeLa cells (Özlü et al. 2010). Aurora B phosphorylates KIF4 and this promotes the KIF4-PRC1 interaction, allowing proper microtubule elongation in HeLa and MCAK cells (Özlü et al. 2010; Bastos et al. 2013).

PRC1-CLASP1 interaction is required for central spindle microtubule stabilization and chromosome segregation by mediating the initial bipolar spindle formation (Rincon et al. 2017; Jing Liu et al. 2009).

PRC1 can directly interact with centralspindlin in HeLa cells and *C. elegans* (Ban et al. 2004; Lee et al. 2015). This interaction was proposed to keep the mechanical robustness of the midzone to sustain the pulling cortical forces acting on both spindle poles (Lee et al. 2015).

In HeLa cells, PRC1 also interacts with centromeric-associated protein-E (CENP-E), which is a mitotic spindle motor protein belonging to the kinesin superfamily, and this was shown to be required to regulate CENP-E ATPase activity *in vitro* and guarantees PRC1 localization in the midbody core (Ohashi, Ohori, and Iwai 2016).

In breast cancer cell lines, PRC1 was found to interact with KIF2C/mitotic centromere-associated kinesin (MCAK) (Shimo et al. 2007). This interaction was hypothesized to be important for PRC1 movement along the central spindle microtubules (Shimo et al. 2007). PRC1 directly interacted with M-phase phosphoprotein 1 (MPHOSPH1) in several bladder cancer cell lines (Kanehira et al. 2007). The biological significance of such interaction was not revealed.

Feo interacting protein (FIP) was identified in *D. melanogaster* as being a binding partner of Feo (Swider et al. 2019). FIP is required for proper Feo localization and successful cytokinesis in *D. melanogaster* S2 cells (Swider et al. 2019).

In fission yeast, Ase1 physically interacts and recruits Kinesin-6 (Klp9p) to the central spindle (Fu et al. 2009). This interaction promotes microtubule sliding and spindle elongation during anaphase B and is dependent on the phosphorylation states of both Klp9p and Ase1 (Fu et al. 2009).

Taken it all together, PRC1 can establish interactions with several proteins to maintain central spindle and midbody integrity. PRC1 disruption leads to cytokinesis failure in a variety of systems, and its mechanisms of action are important to continue to be elucidated. Indeed, PRC1 deregulation has been linked to many cancer types, probably by promoting cytokinesis defects, chromosomal instability, and aneuploidy (Li et al. 2018; She et al. 2019).

8. *Caenorhabditis elegans*: an ideal model system

8.1. *C. elegans* as an animal model

In 1963, Sydney Brenner and colleagues first proposed *C. elegans* as a eukaryotic work model to develop studies on neuronal development. Since then, this nematode has been widely used to develop studies in several research fields such as genetics, neuroscience, evolution, cell biology, and aging.

C. elegans is a small and transparent nematode that can be found in soils worldwide and is approximately 1 mm long at the adult stage. It is a multicellular organism, and most of its cellular and molecular processes are well conserved among species. It can be easily maintained in the laboratory using inexpensive NGM (nematode growth medium) plates, seeded with a standard strain of *Escherichia coli* (*E. coli)*, used as food supply, and grown between 15°C and 26°C (Stiernagle 2006). The reproductive rate of these worms depends on the temperature, with worms growing faster at higher temperatures, and slower at lower

temperatures. Worms are usually grown at 20°C, and under these conditions, their reproductive cycle takes ~3 days and each worm produces approximately 300 offspring.

C. elegans has five pairs of autosomes and one pair of sex chromosomes. This nematode exists in two forms: hermaphrodites with two X chromosomes (XX) and males containing one X chromosome (X0- in *C. elegans* the Y chromosome does not exist). Self-fertilization occurs in hermaphrodites, the most abundant form. Males arise from the loss of chromosome X and occur either spontaneously in <0.2% of the progeny, or by heat shock of L4 hermaphrodites (exposing the worms for a few hours to 30-34°C) (Corsi, Wightman, and Chalfie 2015). Males can be easily distinguished from hermaphrodites by their triangular tail shape and they can be used to cross strains to obtain new strains following Mendelian segregation rules. When mating hermaphrodites with males, the F1 generation will consist of 50% males and 50% hermaphrodites.

After oocyte fertilization, an eggshell is formed around the egg and mitotic divisions start. Embryonic development in the uterus can take 14-16h until the egg is laid. Newly L1 larvae hatch at the end of embryogenesis and measure about 1/6 of the length of an adult worm. L1 larvae progressively develop into L2, L3, and then L4 larvae, and then become adults that can produce embryos. Under stress conditions, such as lack of food, L2 larvae will enter the dauer stage, where it can persist for up to six months (Cassada and Russell 1975). Dauer will transition to the L4 stage when the conditions are favorable again (Figure 9) (Meneely, Dahlberg, and Rose 2019). L1 larvae can be frozen at -80°C for several years, allowing efficient strain management. Defrosted larvae can recover within a few hours, in the presence of food (Stiernagle 2006).

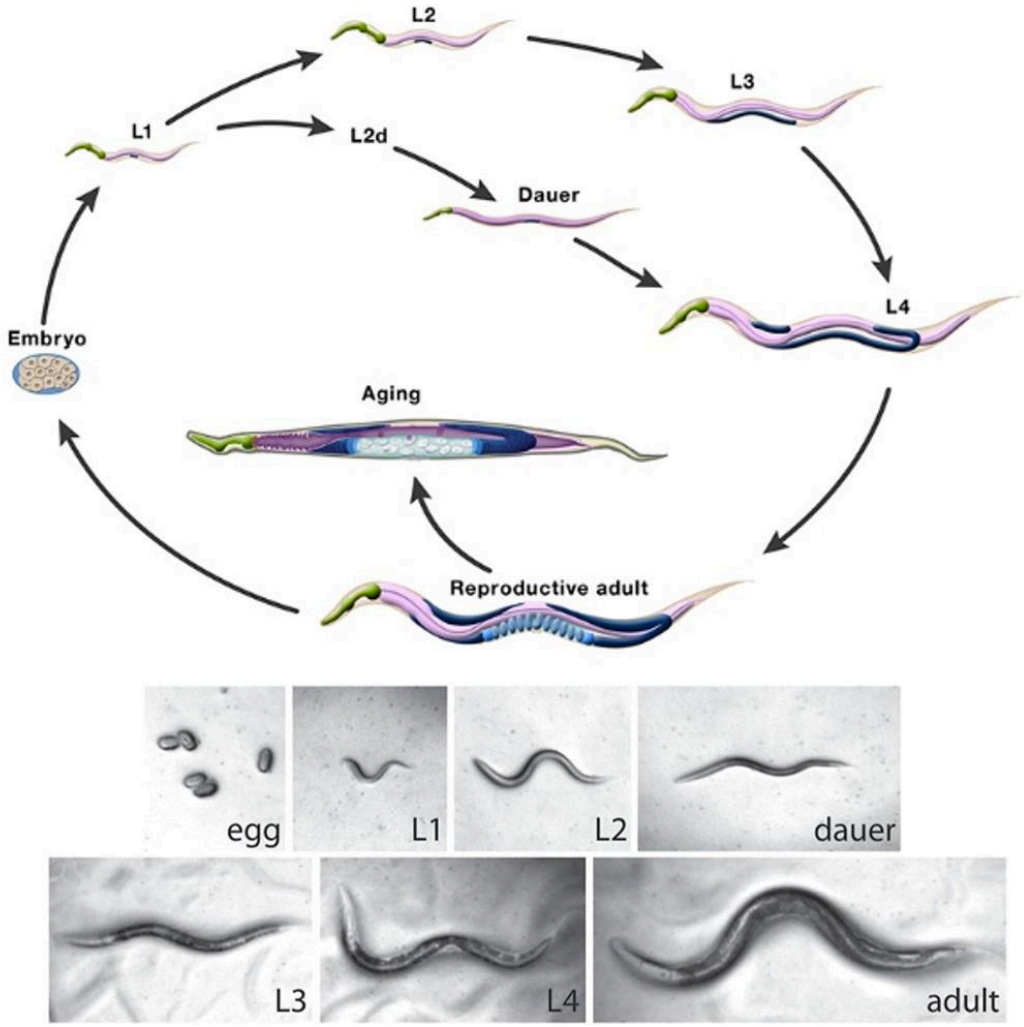

Figure 9- Schematic of the *C. elegans* life cycle.

After embryonic development, *C. elegans* eggs hatch and pass through different larva stages (L1, L2, L3, and L4 larva) culminating in adult worms that can reproduce for a certain period. Under stress conditions, the L1 larva might enter into the Dauer stage, allowing long-term survival, until it reaches a more favourable environment and molts again into L4, following the rest of the life cycle. (Figures used under permission (Herndon et al. 2018); bottom: images illustrating different worm developmental stages (Figures used under permission (Fielenbach and Antebi 2008).

Besides the cheap maintenance, easy handling, and storage, the *C. elegans* nematode is transparent, providing an optimal observation of its cells and subcellular structures under Nomarski microscopy. Mutation and protein tags can be easily introduced in the *C. elegans* genome, allowing the phenotype characterization in diving embryos under microscopy imaging. The number of somatic cells is invariable, allowing the characterization and mapping of the cell shape and fate of each cell between fertilization and adulthood

(Sulston and Horvitz 1977; Kimble and Hirsh 1979; Sulston et al. 1983; Giurumescu and Chisholm 2011).

The *C. elegans* genome was completely sequenced (*C. elegans* Consortium (1998)) and most of the genes are well conserved among species including humans (Kaletta and Hengartner 2006). These enable precise genetic manipulation, mutant generation, or the use of RNA interference (RNAi) to deplete the gene of interest (Fire et al. 1998). Finally, the *C. elegans* research community benefits from a database (Wormbase) containing information about all *C. elegans* genes and their sequences, phenotypes, genetic interactions, mutants, and strains characterized so far. Any *C. elegans* strain can be deposited at the *Caenorhabditis* Genetics Center (CGC) and is available to the research community upon request. Also, a collection of peer-reviewed chapters on different aspects of *C. elegans* biology is available online in open access (WormBook).

8.2. Advantages of using *C. elegans* early embryos to study cytokinesis

C. elegans is a powerful model to study cytokinesis since most of the cytokinesis players are conserved in this species (table II).

Table II- Proteins required for cytokinesis in *C. elegans* embryos (Pintard and Bowerman 2019; table used under permission).

C. elegans protein	*C. elegans* gene	Vertebrate ortholog	Brief description of localization and function	TS alleles (* indicates fast acting)
NMY-2	*nmy-2*(F20G4.3)	nonmuscle myosin II	Localizes to the contractile ring during cytokinesis as well as the other cortical contractile structure	*ne3409**, *ne1490**
MLC-4	*mlc-4*(C56G7.1)	nonmuscle myosin II regulatory light chain	Regulates the ability of myosin II to form filaments and interact with actin; localizes to the contractile ring during cytokinesis as well as the other cortical contractile structure	
LET-502	*let-502*(C10H11.9)	Rho-binding kinase (ROK)	Rho-binding serine/threonine kinase; promotes myosin II contractility by increasing the phosphorylation of MLC-4; localizes to the contractile ring	
MEL-11	*mel-11*(C06C3.1)	Myosin phosphatase targeting subunit (MYPT)	Regulatory subunit of myosin phosphatase; inhibits cortical contraction by de-phosphorylating the regulatory light chain of myosin II; LET-502 and MEL-11 colocalize in cleavage furrows	
RHO-1	*rho-1*(Y51H4A.3)	RhoA	Small GTPase that connects signaling by the ana-phase spindle to assembly and ingression of a cortical contractile ring; localizes to the furrow	
RGA-3/4	*rga-3(K09H11.3)*; *rga-4(Y75B7AL.4)*	Not identified	Rho GTPase activating proteins regulating RHO-1 in the early embryo	
ECT-2	*let-21*(T19E10.1)	Ect2	Guanine nucleotide exchange factor; activates RHO-1; uniformly distributed over the cortex but presumably activated at the furrow	
CYK-1	*cyk-1*(F11H8.4)	formins	A member of the formin family of proteins, promotes actin assembly in response to activation of Rho family GTPases; localizes to the cleavage furrow and is required to initiate furrow ingression	*or596**
PFN-1	*pfn-1*(Y18D10A. 20)	profillin	One of three *C. elegans* homologs of the actin binding protein profilin	
ANI-1	*ani-1*(Y49E10.19)	Anillin	One of the three *C. elegans* anillins; required for contractile events in the early embryo	
UNC-59;UNC-61	*unc-59*(W09C5.2); *unc-61*(Y50E8A.4)	septins	*C. elegans* homologs of the septins form nonpolar membrane-associated filaments	
NOP-1	*nop-1(F25B5.2)*	Not identified	Contributes to RHO-1 activation	
UNC-60A	*unc-60*(C38C3.5)	cofilin	Regulates actin filament dynamics	
ZEN-4	*zen-4*(M03D4.1)	kinesin-6 family member MKLP1	Interacts with CYK-4 to form the centralspindlin complex; localizes microtubule bundles in the spindle midzone and midbody	*or153**
CYK-4	*cyk-4*(K08E3.6)	MgcRacGAP	Interacts with ZEN-4 to form the centralspindlin complex; localizes microtubule bundles in the spindle midzone and midbody	*or749**
AIR-2	*air-2*(B0207.4)	Aurora B	Mitotic serine threonine kinase part of the chromosome passenger complex (CPC)	*or207**
ICP-1CeINCENP	*icp-1*(Y39G10AR. 13)	INCENP	Part of the chromosome passenger complex (CPC)	*or663**
BIR-1	*bir-1*(T27F2.3)	Survivin	Part of the chromosome passenger complex (CPC)	
CSC-1	*csc-1*(Y48E1B.12)	Borealin, Dasra A/B	Part of the chromosome passenger complex (CPC)	
SPD-1	*spd-1*(Y34D9A.4)	PRC1	Microtubule bundling factor; localizes to microtubule bundles in the spindle midzone	

Besides all the advantages previously mentioned, *C. elegans* embryonic divisions are stereotypical. *C. elegans* embryos are relatively large (around 50 μm long and 30 μm wide), which facilitates microscopy imaging. Proteins can be progressively depleted using increasing timing of RNAi treatment. In addition, temperature-sensitive mutants of several cytokinesis players exist, which allows for protein inactivation at restrictive temperatures specifically at the time of interest (Fire et al. 1998; Davies et al. 2014). Several drugs (e.g. latrunculin and nocodazole) can be used to study cytokinesis and embryos can be treated with these after permeabilizing the eggshell (Carvalho et al. 2011).

8.3. The RNA interference pathway in *C. elegans*

The RNA interference (RNAi) pathway has been widely used in *C. elegans* since 1998 when Fire et al. unveiled how the RNAi pathway works using this system (Fire et al. 1998). It is present in most eukaryotic cells where they use small double-stranded RNA (dsRNA) molecules to specifically silence a certain gene activity vis a homology-dependent pathway. Long dsRNA molecules are recognized by Dicer, an RNA endonuclease, that cuts the dsRNA into small fragments (small interference RNAi or siRNAs). These fragments bind to the RNA-induced silencing complex (RISC) in which Argonaute protein is included. RISC together with the siRNAs is directed to the target messenger RNA (mRNA), which pairs with the siRNAs by complementary homology. Paired siRNA-mRNAs are fragmented by Argonaute protein, and degraded (Figure 10) (Kim and Rossi 2008; Neumeier and Meister 2021).

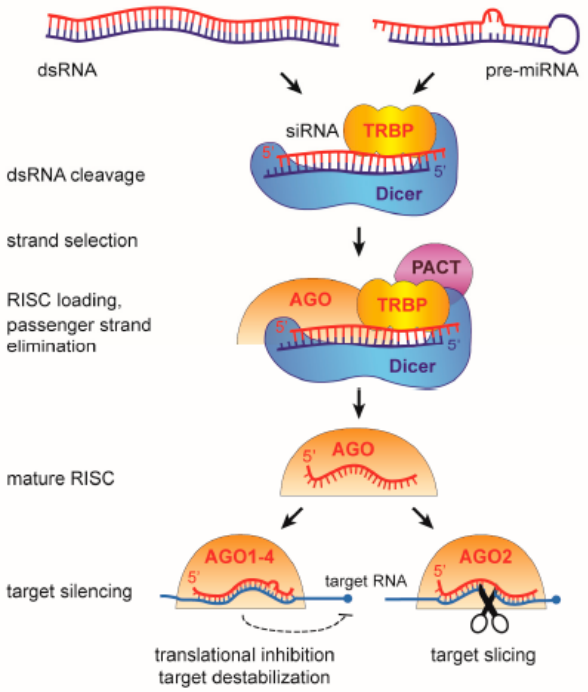

Figure 10- The RNAi pathway.

Dicer processes long dsRNA into siRNAs. siRNAs are loaded into Argonaute containing RISC complex and one of the strands is degraded. The remaining strand is retained and guides Argonaute onto the target RNA that will be cleaved or the target RNA is destabilized or translational inhibited in the case of miRNA (Schuster, Miesen, and van Rij 2019; figure used under permission).

In *C. elegans*, the administration of dsRNA for RNAi can be done by injection, feeding, or soaking. Protein depletion induced by feeding is achieved by cloning the specific cDNA into a bacterial expression vector between opposing phage T7 polymerase promoter sites. This vector is then transformed into an *E.coli* HT115 strain providing IPTG inducible

expression of the phageT7 RNA polymerase. Interestingly, this *E. coli* strain lacks the *Rnc* gene, that encodes RNase III, preventing dsRNA degradation. These bacteria are prepared and seeded into NGM plates containing IPTG. Finally, worms are placed on these plates, fed with bacteria expressing the desirable dsRNA, and adult animals or progeny is evaluated (Conte et al. 2015). mRNA degradation in the germline gonad is gradual: new oocytes and embryos will be progressively loaded with less and less target protein until all the protein is depleted (Oegema and Hyman 2006). The penetrance of the protein depletion directly correlates with the protein halftime, thus proteins that have long halftime are more difficult to deplete. Moreover, double and triple RNAi depletions can be combined simultaneously in *C. elegans.* Lastly, protein depletion by RNAi can be assessed by immunoblotting, reverse-transcription (RT)-PCR, and/or phenotypical analysis.

8.4. Protein inactivation in *C. elegans*

Temperature-sensitive mutants are powerful tools to study transient processes such as cytokinesis, as they usually allow rapid convert an active protein into an inactive protein, by simply shifting the temperature at a precise time. At the permissive temperature, the worms develop normally and are viable. However, at restrictive temperatures, the proteins lose their function and their roles become compromised (Davies et al. 2017).

A collection of fast-acting temperature-sensitive mutants implicated in cytokinesis was identified in classical forward genetic screens (Canman, Desai, Bowerman, and Oegema, 2008; Encalada et al., 2000; Kemphues, Priess, Morton, and Cheng, 1988; O'Connell et al., 1998; O'Rourke et al., 2011; Raich, Moran, Rothman, and Hardin, 1998). The degree of functionality of these mutants can be tuned using a range of temperatures between 16 ºC and 26ºC. The mutants exhibit higher activity at lower temperatures and lower activity at higher temperatures (Davies et al., 2014; Davies et al., 2017). Also, protein inactivation in fast temperature-sensitive is reversible, allowing the reactivation of the inactive protein by shifting to permissive temperatures.

All these characteristics make fast-inactivating mutants very appealing tools to study embryonic cytokinesis, especially because cytokinesis is a highly transient process, lasting about ~500 seconds in the early *C. elegans* embryo. Also, cytokinesis players are often involved in other stages of the cell cycle and during oogenesis/spermatogenesis, so their timely-controlled inactivation allows for their function during embryonic cytokinesis to be specifically examined. Moreover, fast inactivation allows for the dissection of the roles of its players during contractile ring assembly, constriction, or abscission.

Precise and rapid temperature shifts can be achieved using commercially available thermally fluidic control setups (Figure 11).

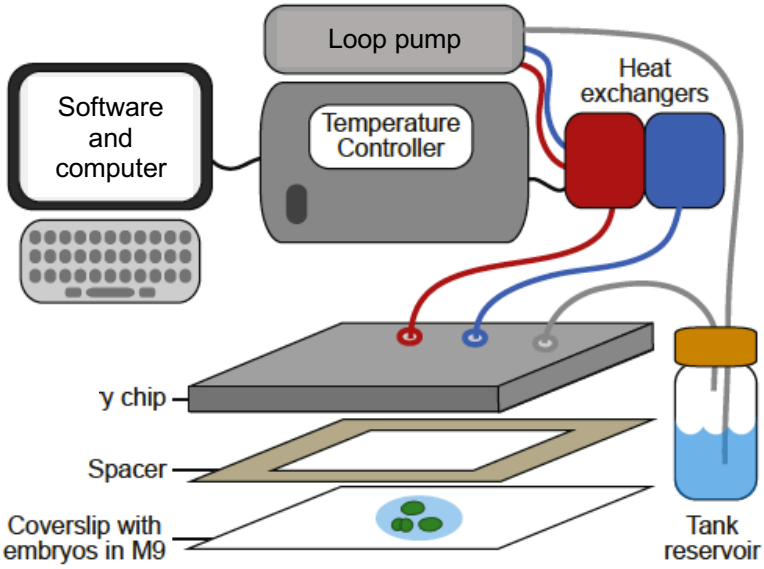

Figure 11- Schematic representation of a commercially available device that allows for rapid temperature changes on the sample.

The temperature on a chip is controlled by dedicated software that operates changes on the fluid heat. A coverslip with embryos in M9 medium is placed on the microscope. On top of that, a spacer is added to avoid the embryo's squeeze. The commercially available chip is placed on top of the spacer to allow precise temperature control (Davies et al., 2017; figure used under permission).

CHAPTER II

AIMS AND OVERVIEW

Aims and Overview

During the later stages of cytokinesis, the cleavage furrow approaches and compacts the central spindle microtubules. The impact of the central spindle on the constricting contractile ring is not well understood. To address this knowledge gap, my studies focused on characterizing the behavior of the contractile ring and its components during the second half of furrow ingression in unperturbed conditions or when the central spindle microtubule bundler PRC1/SPD-1 was depleted or inactivated. Bundling of central spindle microtubules is essential for cytokinesis in cultured cells but previous reports demonstrated that SPD-1 inhibition does not prevent cytokinesis completion in the *C. elegans* zygote but prevents cytokinesis in the EMS cell of the *C. elegans* 4-cell embryo.

To characterize contractile ring behavior during the second half of ring constriction in unperturbed conditions the distribution profiles of the contractile ring and central spindle fluorescent markers were analyzed, from the point when the contractile ring approached the central spindle until the ring stopped constricting. Also, midbody organization in control embryos was characterized and compared to previous reports in HeLa cells. For some contractile ring proteins, their turnover was assessed by photobleaching experiments either in unperturbed conditions or when SPD-1 was depleted. In a brief biochemical incursion to reveal potential SPD-1 interactors with other cytokinesis machinery members, I also conducted a yeast two-hybrid assay.

To characterize the role of bundled central spindle microtubules during cytokinesis, I revisited the phenotypes of SPD-1 inhibition in the 1-cell and 4-cell embryos by high-resolution live fluorescence imaging. This led to the conclusion that SPD-1 perturbation leads to the formation of elongated intercellular bridges during the last stages of ring constriction that were characterized. A synergy between a contractile ring protein, anillin, and SPD-1 was observed during the second half of ring constriction and the operating mechanism behind it was investigated.

CHAPTER III

MATERIAL AND METHODS

Materials and Methods

C. elegans strains

The strains used in this study are listed in Table III. Strains carrying the temperature-sensitive alleles *spd-1(oj5)* or *nmy-2(ne3409)* were maintained at 16°C and the others at 16°C or 20°C on nematode growth medium (NGM) plates seeded with OP50 *E. coli*.

RNA interference

RNAi was performed by feeding hermaphrodites with HT115 E. coli bacteria expressing double-stranded RNA (dsRNA) of interest from the L4440 vector. To deplete SPD-1 by feeding RNAi, a 1590 bp region of the SPD-1 locus was amplified from N2 genomic DNA with the primers: 5'-CCCGGATCCATGTCCCGAAGGCACAGC-3' and 5'-CCCGGATCCTCACAAAAACTGATTTCG, digested with BamHI restriction enzyme and cloned into L4440 in the BglII restriction enzyme site. The final plasmid was sequenced and transformed into HT115 E. coli. These bacteria were used to prepare RNAi feeding plates as previously reported (Silva et al. 2016). L4 animals were placed in the RNAi plates and incubated at 20°C for 44-48 hours or at 26°C for 32h before dissection for imaging. To deplete ANI-1, EFA-6, and GPR1/2, L4440 vectors carrying part of the sequence of ani-1, efa-69, and gpr1/2 respectively were obtained from the Ahringer library ((Kamath et al. 2003) distributed by Source BioScience, United Kingdom) and sequenced to confirm the gene target. L4 animals were fed with bacteria expressing double-stranded RNA either against ani-1 and efa-6, and incubated at 16°C for 61h-64h or against gpr-1/2 and incubated at 16ºC for 30-33h, before being dissected in cold M9 medium.

Live imaging

1-cell, 4-cell, or ~16-cell *C. elegans* embryos were dissected from adult hermaphrodites and filmed. *spd-1(RNAi)* depleted embryos were either imaged under compression on 2% agarose pads overlaid with a coverslip in a room acclimatized to 20°C, or under no compression in a drop of M9 medium (86 mM NaCl, 42 mM Na_2HPO_4, 22 mM KH_2PO_4, and 1 mM $MgSO_4.7H_2O$) placed on the CherryTemp chip set to 16°C, 22°C or 26°C. *spd-1(oj5)* and *nmy2(ne3409)* animals were filmed under no compression in a drop of cold M9 medium placed on the CherryTemp chip set to 16°C, 22°C, or 26°C. The temperature in the CherryTemp chip was controlled by dedicated software (CherryBiotech), as explained in the text. In *spd-1*(*oj5*) EMS cells, the temperature was upshifted when chromosome condensation started, when the equatorial cortex started to deform at the beginning of furrow ingression (shallow deformation), or halfway through cleavage furrow

ingression, as indicated in the figures. In ABa, ABp, and P2 cells, the temperature was upshifted at the time of contractile ring assembly in the ABa cell; in P0 cells, the temperature was upshifted at nuclear envelope breakdown. Assessment of cytokinesis failure or success was done in the strains GCP380 and GCP691, in movies that covered the entire process of furrowing until the following cell division, when both sister cells entered anaphase (Fig. 17C, 17G, 26A, 27A, 33D).

For fluorescence recovery after photobleaching (FRAP) experiments (Fig. 15), a FRAPPA photobleaching module (Andor Technology) placed between the spinning disk head and the microscope was used. Photobleaching was performed by 3 sweeps of a 405 nm laser with 100% power and 40 µs dwell time.

The rest of the images were acquired on a spinning disk confocal system (Andor Revolution XD Confocal System; Andor Technology) with a confocal scanner unit (CSU-X1; Yokogawa Electric Corporation) mounted on an inverted microscope (Ti-E, Nikon) equipped with a 60x oil-immersion Plan-Apochromat objective (N.A. 1.4) and solid-state lasers of 488 nm (50 mW) and 561 nm (50 mW). An electron multiplication back-thinned charge-coupled device camera (iXon Ultra 897; Andor Technology) with 1x1 binning was used. Acquisition parameters, shutters, and focus were controlled by Andor iQ3 software. Images were acquired in sets of ten z-planes 0.5- or 1-µm apart, every 10, 20, or 30 seconds.

Image analysis and statistics

All measurements and image processing were done using Fiji (ImageJ; (Schindelin et al. 2012)). Z-stacks were projected using the maximum intensity projection tool. Graph plotting and statistical analyses were performed with Prism 9.5.0 (GraphPad Software). All error bars represent the 95% confidence interval of the mean Statistical significance was determined using a two-tailed Mann-Whitney test.

Images in Figure 22 were obtained using the Imaris program (Imaris (RRID:SCR_007370))

Measurement of furrow ingression profiles, instantaneous contractile ring constriction rate, and point when the contractile ring approaches the central spindle

The contractile ring diameter was determined in EMS cells expressing NMY-2::GFP and mCherry::PH (Fig.12B, 17D-E, 26D, 27B, 25C) or GFP::PH (Fig. 28A), by manually tracing a straight line between the two tips of the cleavage furrow on the z-plane where this was the widest for each time point and plotted against time after anaphase onset (the first point when two masses of segregated chromatids were observed immediately after

metaphase, as judged by chromosome labeling using the histone marker mCherry::HIS-58, or negative myosin labeling, which is cytoplasmic and absent from chromatin). Data from multiple rings were temporally aligned and averaged. The values were normalized to the diameter of the embryo measured at the cell equator at anaphase onset.

Percent ingression was considered to be 0% before furrow ingression initiated and 100% when it completed.

For the graphs of instantaneous constriction rate, the rate of ring constriction was calculated for pairs of consecutive time points by dividing the difference in diameter by the time interval. Individual rate measurements from all imaged embryos were pooled and the mean rate for the data points falling in overlapping 2-µm intervals was plotted against the contractile ring diameter at the center of each interval. Segmental linear regression (GraphPad) was used to determine the point of abrupt deceleration, which was considered to be the intersection of the line segment during which the constriction rate is decreasing only slightly and the line segment during which the constriction rate starts decreasing significantly.

In Figure 28B, the point when the contractile ring approached the central spindle was determined in EMS cells expressing NMY-2::mKate2 and GFP::TBB-2 or NMY-2::mKate2 and SPD-1::GFP, by manually tracing a straight line between the two tips of the cleavage furrow (as judged by NMY-2::mKate2 signal) on the z-plane where this was the widest, at the time point when the signal of NMY-2 and TBB-2 or SPD-1 first overlapped. The midzone length was determined by manually tracing a straight line between the two edges of the central spindle (as judged by TBB-2 or SPD-1 signal) at the time point just before it started being compacted by the advance of the cleavage furrow.

In Figure 25B, a line of 1.8 µm width was drawn over the two sides of the cleavage furrow at a point of 70% ingression in control and a *ani-1(RNAi)* EMS cell expressing NMY-2::GFP, and the mean GFP fluorescence along the line was quantified.

Measurement of DNA-DNA and Pole-to-Pole distance

All measurements were performed on maximum projection movies of embryos expressing H2B::mCherry, or TBB-2::mCherry. The DNA-DNA and the pole-to-pole distance were determined by manually tracing a straight line between the center of the two masses of chromosomes or the two centrosomes, respectively, in Fiji and reading the length of the line. Data from multiple examples were temporally aligned to anaphase onset or shallow deformation and averaged by calculating the arithmetic mean.

Quantification of protein levels in the contractile ring

To compare protein levels of contractile rings during the second half of constriction (Fig. 12D), analyses were done in ABa and ABp cells starting when the contractile ring perimeter was 20 µm. NMY-2::GFP, UNC-59::GFP, LifeAct::GFP, ANI-1::GFP, and CYK-1::GFP levels were analyzed by drawing a segmented line, with a constant width, on top of the contractile ring on each time point. When the contractile ring perimeter was smaller than 5 µm a circle (with variable size) was drawn on top of the contractile/midbody ring until the P2 furrow has ingressed 50%, and the reference point was chosen to finish the analysis. For the CYK-4::mNeonGreen probe, a circle was drawn using the inner part of the contractile ring as a template for each timepoint, and the area mean fluorescence was calculated. The cytoplasmic signal of the P2 cell (measured in a 10-pixel diameter circle) was subtracted from the mean fluorescence (Fig. 12C).

Measurement of protein turnover in the contractile ring

Photobleaching experiments were performed to analyze contractile ring dynamics during constriction in control and SPD-1-depleted AB cells. Embryos expressing CYK-1::GFP, ANI-1::GFP, and NMY-2::GFP were photobleached in a portion of the arc (~3.5-4.5 µm in length). The bleached area was monitored by collecting 8 z-planes 1−µm apart every 1.7 or 10 seconds before and after photobleaching.

Analysis was performed on maximum intensity projections by drawing a segmented line with a fixed length and thickness on top of the bleached area, before and after bleaching (Fig.15A). A circle with a fixed perimeter was drawn in the center of the ring to determine the background fluorescence for each timepoint, before and after bleaching (Fig.15A).

To determine the fluorescence in the arc, the mean GFP fluorescence per pixel in the arc after bleaching was subtracted from the mean background fluorescence in the center of the ring after bleaching. This was normalized for the mean GFP fluorescence per pixel in the arc before bleaching subtracted to the mean background fluorescence in the center of the ring before photobleaching (Fig. 15A). The fluorescence intensity before bleaching correspond to the average of three consecutive timepoints.

Characterization of intercellular bridges

In Figure 18C, the period of bridge elongation corresponds to the interval of time between the point when the intercellular bridge started to form (the frame in which the furrow tip started to broaden) and the time when it reached its maximum length (as judged by mCherry::PH signal); the period of bridge shortening corresponds to the interval of time between the point when the intercellular bridge was the longest to the point when the two

ends of the bridge joined together. The point of sister cell juxtaposition corresponded to the time point when the two sister cells became completely juxtaposed, as in control embryos. The end of furrowing was considered to be the point when the distance between the two sides of the furrow was minimal. The point of furrow regression was considered to be the time frame when the two sides of the furrow separated. All reference points were determined in a minimum of 10 examples and the values shown correspond to the mean.

In Figure 23D, midbody shedding corresponded to the point when some signal of anillin or myosin was released from the midbody, and midbody release was the time when the entire midbody separated from the back-to-back plasma membranes separating the sister cells.

Embryonic viability

Embryonic viability tests were performed by feeding RNAi at 20°C or by growing N2 or *spd-1*(*oj5*) worms at 16°C or 26°C (Fig. 30).

L4 stage animals of the strain N2 were grown in SPD-1 feeding RNAi plates for 40 hours at 20 ºC. Animals were then singled out onto fresh RNAi plates and let to lay eggs for eight hours. After this period, the adults were removed and laid embryos were left to hatch for 24 hours. The number of unhatched (dead) and hatched embryos were counted and the embryonic viability was calculated by dividing the number of hatched embryos by the total number of progeny. In the case of *spd-1(oj5)* animals, L4 stage animals of the strain WH12 were grown in OP50 *E. coli* NGM plates for 27 hours at 26°C or 53 hours at 16ºC, and after a period of 5.5 or 11 hours, respectively, adults were removed and unhatched and hatched embryos were counted 24 or 36 hours later, respectively.

Yeast-two-Hybrid assay

In figure 16, yeast two-hybrid assays were performed according to the manufacturer's guidelines (Matchmaker; Invitrogen). cDNAs of SPD-1, ANI-1, UNC-59, UNC-61, NMY-2, MLC-4, CYK-7, CYK-1 fragments (F1 1-GBD-FH3-675 and F2 670-FH1-FH2-DAD-1437), CYK-4, ZEN-4, PLK1, AIR-2, BIR-1, ICP-1 CSC-1, CLS-2, and TSG-101 were cloned into bait pGBKT7 or prey pGADT7 vectors. pGBKT7 and pGADT7 carry cassettes that lead to the synthesis of Tryptophane and Leucine, respectively. Yeast-containing bait and prey vectors with the cDNAs of interest were plated on -Leu/-Trp plates to test for growth and in -Leu/-Trp/-His plates to select for interactions, as the interaction between proteins encoded by prey and bait plasmids leads to the additional synthesis of Histidine.

Table III- List of *C. elegans* strains used in this thesis.

Strain	Genotype	Source
N2	*Ancestral*	*Caenorhabditis* Genetics Center
WH12	*spd-1(oj5) I*	*Caenorhabditis* Genetics Center
RZB250	*[cyk-1 (knu83 C-terminal GFP, unc-119 (+)); unc-119(ed3)] III; zuIs151 (Nmy-2::mCherry); ltIs37 [pie-1::mCherry::his-58 + unc-119(+)] IV*	Zaidel-Bar lab
QM88	*pie-1::mCherry::tub::pie-1; cyk-4(ok1034) III; xaSi2[cyk-4::gfp cb-unc-119(+)] IV*	(Lee et al. 2015)
QM89	*pie-1::mCherry::tub::pie-1; cyk-4(ok1034) III; xaSi11[cyk-4CΔ::gfp cb-unc-119(+)] IV*	(Lee et al. 2015)
QM90	*pie-1::mCherry::tub::pie-1; cyk-4(ok1034) III; xaSi10[cyk-4EAE::gfp cb-unc-119(+)] IV*	(Lee et al. 2015)
JDU21	*ijmSi8[pJD362; Pmex-5::egfp::tbb-2; mCherry::his-11; cb-unc-119(+)] II; unc119(ed3) III*	(Barbosa et al. 2021)
JDU33	*ijmSi11[pJD359/pCFJ151;SPD-1p::SPD-1::sfGFP; cb-unc-119(+)]II; unc-119(ed3) III*	(Hirsch et al. 2022)
JCC637	*nmy-2(ne3409)I; unc-119(ed3)(?); ltIs38 [pAA1; pie-1/GFP::PH(PLC1delta1); unc-119 (+)] III; ltIs37 [pAA64; pie-1/mCherry::his-58; unc-119 (+)] IV*	(Davies et al. 2014)
OD3686	*ltSi849 [pKL120; Pmex-5::mCherry::PH(PLC1delta1)::tbb-2 3'UTR; cb-unc-119(+)] I; ltSi1124[pSG092; Pcyk-4::CYK4reencoded::mNeonGreen::cyk-4 3'-UTR; cbunc-119(+)] II; unc119(ed3) III*	(Lee et al. 2018)

TMR08	*unc-119(ed3)III; ddIs186[WRM0631C_D06::S000126_R6K-pCFJ496-000032-mos1([240][31816]tsg-101::S000138_R6K-2×TY1-wSNAP-eGFP 3×FLAG); unc-119^{+}]; ltIs44[pAA173; pie-1p-mCherry::PH(PLC1Δ1) + unc-119^{+}])*	(König et al. 2017)
LP229	*nmy-2(cp52[nmy-2::mKate2 + LoxP unc-119(+) LoxP]) I; unc-119(ed3) III*	(Dickinson et al. 2017)
OD27	*unc-119(ed3) III; ltIs14 [pASM05; pie-1/GFP-TEV-STag::air-2; unc-119 (+)] IV*	(Lewellyn et al. 2011)
MG685	*mgSi43 [cyk-4p::cyk-4::GFP::pie-1 3'UTR + Cbr-unc-119(+)] II*	(Zhang and Glotzer 2015a)
GCP13	*unc-119(ed3) III; prtSi2[pAC71; Pnmy-2:nmy-2reencoded::mCherry::StrepTagII::3'UTRnmy-2; cb-unc-119(+)]II*	Our lab
GCP113	*nmy-2(cp13[nmy-2::gfp + LoxP]) I; unc-119(ed3) III (?); ltIs37 [pAA64; pie-1/mCherry::his-58; unc-119 (+)]*	(Sobral et al. 2021)
GCP380	*nmy-2(cp13[nmy-2::gfp + LoxP]) I; unc-119(ed3) III (?); ltIs44 [pAA173; pie-1/mCherry::PH(PLC1delta1); unc-119 (+)]; ltIs37 [pAA64; pie-1/mCherry::his-58; unc-119 (+)]*	Our lab
GCP456	*prtSi2[pAC71; Pnmy-2:nmy-2reencoded::mCherry::StrepTagII::3'UTRnmy-2; cb-unc-119(+)] II; unc-119(ed3) III (?); ddIs186[WRM0631C_D06::S000126_R6K-pCFJ496-000032-mos1([240][31816]tsg-101::S000138_R6K-2×TY1-wSNAP-eGFP 3×FLAG); unc-119+]*	This study
GCP528	*unc-119(ed3)III (?); ltIs44 [pAA173; pie-1/mCherry::PH(PLC1delta1); unc-119 (+)]; ltIs37 [pAA64; pie-1/mCherry::his-58; unc-119 (+)]; Si37[pEZ98; Pani-1:GFP::ani-1; cb-unc-119(+)] IV*	This study

GCP556	*spd-1(oj5) I; nmy-2(cp13 [nmy-2::gfp + LoxP]) I; unc-119(ed3) III (?); ltIs37 [pAA64; pie-1/mCherry::his-58; unc-119 (+)]*	This study
GCP615	*spd-1(oj5) I; unc-119(ed3)III (?); ltIs44 [pAA173; pie-1/mCherry::PH(PLC1delta1); unc-119 (+)]; ltIs37 [pAA64; pie-1/mCherry::his-58; unc-119 (+)]; Si37[pEZ98; Pani-1:GFP::ani-1; cb-unc-119(+)] IV*	This study
GCP691	*nmy-2(cp13 [nmy-2::gfp + LoxP]) I; spd-1(oj5) I; unc-119(ed3) III (?); ltIs37 [pAA64; pie-1/mCherry::his-58; unc-119 (+)]; ltIs44 [pAA173; pie-1/mCherry::PH(PLC1delta1); unc-119 (+)]*	This study
GCP720	*nmy-2(cp52[nmy-2::mKate2]) I;unc-119(ed3)III; pEZ60; PPlk1::PLK1::GFP::Plk1; cb-unc-119(+)]II ; ltIs37 [pAA64; pie-1/mCherry::his-58; unc-119 (+)] IV*	This study
GCP725	*nmy-2(cp52[nmy-2::mKate2+ LoxP unc-119(+) LoxP] I; ijmSi8 [pJD362; Pmex-5::gfp::tbb-2; mCherry::his-11; cb-unc-119(+)] II; unc-119(ed3) III (?)*	This study
GCP730	*nmy-2(cp52[nmy-2::mKate2+ LoxP unc-119(+) LoxP] I; unc-119(ed3) III (?); ltIs14 [pASM05; pie-1/GFP-TEV-STag::air-2; unc-119 (+)] IV; ltIs37 [pAA64; pie1/mCherry::his-58; unc-119 (+)]*	This study
GCP744	*nmy-2(cp52[nmy-2::mKate2+ LoxP unc-119(+) LoxP] I; ltSi1124 [pSG092; Pcyk-4::cyk-4reencoded::mNeonGreen::cyk-4 3'-UTR; cbunc-119(+)] II; unc-119(ed3) III (?)*	This study
GCP941	*spd-1(oj5) I; ijmSi8 [pJD362; Pmex-5::gfp::tbb-2; mCherry::his-11; cb-unc-119(+)] II; unc-119 (ed3) III (?)*	This study
GCP942	*spd-1(oj5) I; ltSi1124[pSG092; Pcyk-4::cyk-4reencoded::mNeonGreen::cyk-4 3'-UTR; cbunc-119(+)] II; unc-119 (ed3) III; ltIs37 [pAA64; pie-1::mCherry::his-58 +unc-119(+)] IV*	This study

GCP950	*ltSi1124[pSG092; Pcyk-4::cyk-4reencoded::mNeonGreen::cyk-4 3'-UTR; cbunc-119(+)] II; unc-119 (ed3) III; ltIs37 [pAA64; pie-1::mCherry::his-58 +unc-119(+)] IV*	This study
GCP1203	*nmy-2(cp52[nmy-2::mKate2]) I; ijmSi11 [pJD359/pCFJ151; spd-1p::spd-1::sfGFP; cb-unc-119(+)]II; unc-119(ed3) III (?)*	This study
GCP1353	*mgSi43 [cyk-4p::cyk-4::GFP::pie-1 3'UTR + Cbr-unc-119(+)] II; unc-119(ed3) III; ltIs44 [pAA173; pie-1/mCherry::PH(PLC1delta1); unc-119 (+)]*	This study
GCP1354	*spd-1(oj5) I; unc-119(ed3) III (?)*; mgSi43 [cyk-4p::cyk-4::GFP::pie-1 3'UTR + Cbr-unc-119(+)] II; unc-119(ed3) III; ltIs44 [pAA173; pie-1/mCherry::PH(PLC1delta1); unc-119 (+)]*	This study
GCP1505	*spd-1(oj5) I; unc-119(ed3) III (?)*; nmy-2(cp52[nmy-2::mKate2+ LoxP unc-119(+) LoxP] I; unc-119(ed3) III (?)*; ltIs14 [pASM05; pie-1/GFP-TEV-STag::air-2; unc-119 (+)] IV; ltIs37 [pAA64; pie1/mCherry::his-58; unc-119 (+)]*	This study

unc-119(ed3) III (?) - the presence of this allele was not verified after completion of the genetic cross

CHAPTER IV

MICROTUBULE BUNDLING ACTIVITY IS REQUIRED FOR LAST STAGES OF CYTOKINESIS IN *C. ELEGANS*

Microtubule bundling activity is required for last stages of cytokinesis in *C. elegans*

9. An increase in NMY-2, ANI-1, UNC-59, and CYK-4 levels is observed in the contractile ring during the second half of constriction

Contractile ring to midbody ring transition is thought to involve molecular changes (Kechad et al., 2012). To determine when, and which molecular changes operate, we decided to characterize ring constriction. We measured the contractile ring perimeter over time, described the contractile ring shape, and analyzed the distribution profiles of fluorescent markers of the contractile ring and central spindle in the ABa and ABp cells. The ABa and ABp cells are two of the four cells in the 4-cell embryo that usually divide perpendicular to the imaging plane, and consequently, the whole circumference of their constricting rings can be visualized in projections of a few z-planes (Fig. 12A).

By measuring the contractile ring perimeter over time, we confirmed that the ring constriction rate is constant until it reaches a perimeter of 19 µm, the point at which the rate slows down, in agreement with a previous study (Carvalho, Desai, and Oegema, 2009) (Fig. 12B and B'). This decrease in the rate of constriction has been previously shown to be due to the proximity of the ring to the central spindle microtubules (Carvalho, Desai, and Oegema, 2009). Interestingly, we also observed that shortly after the ring starts to slow down, it also changes shape: during early constriction the ring seems to be attached to cell-cell contacts adopting a "triangular shape", whereas it detaches from cell-cell contacts adopting a more circular shape at approximately 12 µm (Fig. 12A and B').

By examining distribution profiles of contractile ring and central spindle components during ring constriction, we found that: formin (CYK-1) and actin (as judged by LifeAct) levels remained constant when ring´s perimeter was below ~20 µm until 240s after the furrow has completely closed; non-muscle myosin II (NMY-2) and one of the septins (UNC-59) increased in concentration when the ring perimeter was ~10 µm, but stabilized soon after; and anillin (ANI-1) and a centralspindlin component (CYK-4) levels started to increase when the ring perimeter was ~20 µm and continued to increase when the ring perimeter was below 5 µm (Fig. 12D).

These observations suggest that topological and molecular changes that set the stage for abscission, occur during the second half of contractile ring constriction.

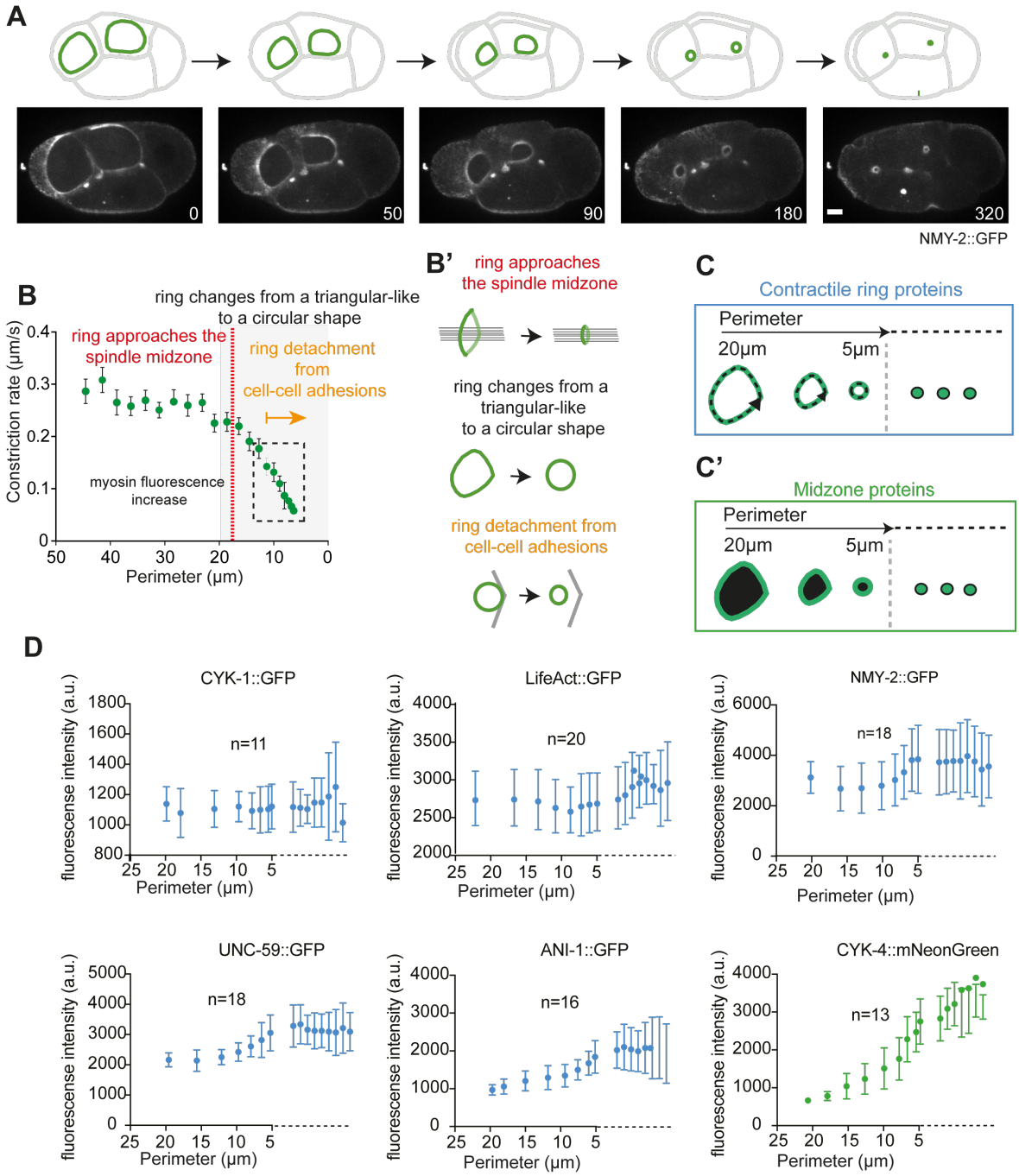

Figure 12- Analysis of contractile ring behavior during the second half of constriction.

(A) Schematic illustrating a 4-cell *C. elegans* embryo where the contractile ring (in green) of ABa and ABp cells is constricting. Schematics are followed by stills of a time-lapse video of an embryo expressing NMY-2::GFP. Numbers in stills indicates times in seconds. Scale bar, 5 µm. **(B)** Graph showing mean constriction rate versus ring perimeter. The x-axis is reversed to represent progression from larger to smaller perimeters during ring constriction. Error bars are the 95% confidence interval of the mean. The grey box depicts the window of ring perimeters during which the ring approaches the central spindle microtubules

(dashed red line), the dashed black outline and the orange arrow represents time when the ring changes from “triangular” to circular shape, and when the ring detaches from cell-cell contacts **(B’). (C, C’)** Schematic illustrating how contractile ring and central spindle protein levels were quantified before and after the contractile ring reached a perimeter 5 µm. To quantify contractile ring probes, a segmented line with a fixed width was drawn over the constricting ring, and the mean fluorescence intensity along the line was determined. For CYK-4, a circle covering the area inside of the ring was drawn, and the mean fluorescence intensity in that region was determined after subtraction of the cytoplasmic background. For ring perimeters below 5 µm, the ring and the region inside it were too small to be traced in separate, and thus a circle covering the entire region was drawn for quantification purposes. **(D)** Fluorescence intensity per unit length of contractile ring (blue) and central spindle (green) proteins against decreasing ring perimeter. The black dashed line on the x-axis starts at ring perimeters below 5 µm. Error bars, 95% CI.

10. Composition of the midbody in *C. elegans* EMS cells is similar to that in tissue culture cells and SPD-1 behaves like PRC1

The composition of the midbody is well known in tissue culture cells where proteins are distributed in 3 different compartments: midbody core, midbody flanking regions/midbody arms, and midbody ring (Elia et al. 2012; Green, Paluch, and Oegema 2012; Hu, Coughlin, and Mitchison 2012). These regions are well-established and easily identified in HeLa cells. In *C. elegans* embryos, the distribution within three regions has not been carefully looked at (Green et al. 2013; König et al. 2017).

To evaluate if midbody architecture in *C. elegans* embryos is similar to that described in HeLa cells, we imaged midbodies in the EMS cell in 4-cell embryos expressing fluorescent GFP tagged SPD-1 (PRC1), CYK-4 (MgcRacGAP); AIR-2 (Aurora B), NMY-2 (non-muscle myosin II), and ANI-1 (anillin). EMS cells divide parallel to the imaging plane, thus two sides of the contractile ring can be visualized when acquiring images of the center of the cell.

During the first steps of cytokinesis, NMY-2 and ANI-1 accumulate at the cell equator. As the ring constricts and gets smaller they concentrate at the tip of the furrow until the midbody forms. NMY-2 and ANI-1 remain at the midbody even when this is released (Fig.13A,B, and A,B’). During midbody formation, these two proteins adopt a more peripheral localization than TBB-2, AIR-2, SPD-1, PLK-1, and TSG-101 (Fig. 13C, D, E, G and H).

SPD-1::GFP starts to appear at the midzone (22±6 s after anaphase onset; n=10). As the contractile ring constricts, and compacts the central spindle, SPD-1 progressively

compacted until co-localizing with NMY-2::mKate2 at the midbody. After complete furrow ingression, the SPD-1 signal starts to decrease 540±61s after anaphase onset (n=10), while the NMY-2 signal remains constant (Fig.12D; Fig. 13E).

CYK-4 appears at the midzone right after anaphase onset but its intensity increases as cytokinesis progresses until the furrow has completely ingressed, indicating its different behavior when compared to that of SPD-1 (Fig. 13F). CYK-4 signal seemed to be predominantly in the central spindle but we cannot exclude that at least some transferred to the contractile ring at the last stages of ring constriction, as it has been described (Basant et al., 2015; Elia et al., 2011; Hu et al., 2012b; Zhang and Glotzer, 2015).

AIR-2::GFP localizes on the centromeres of chromosomes at the metaphase plate and translocates to the central spindle right after anaphase onset. As the contractile ring constricts and the midbody forms, AIR-2 localizes in the inner region of the midbody and on the midbody flanking regions (Fig. 13D), resembling what happens in HeLa Cells. As the midbody matures, the AIR-2::GFP signal starts to fade especially from the midbody flanking regions, and localizes only at the midbody center. Since AIR-2 and SPD-1 localize to central spindle microtubules, we checked whether the decrease of their signal could coincide with midzone microtubule depolymerization. EMS cells co-expressing GFP::TBB-2 and NMY-2::mKate2 were imaged and the time of microtubule depolymerization, as judged by GFP::TBB-2 signal loss from the midzone was determined. We found that the GFP::TBB-2 signal disappears from the midzone 670±96s (n=11) after anaphase onset, which is similar to that of AIR-2::GFP loss from the midbody flanking regions (615±34s, n=4) (P value = 0,3178, ns). SPD-1::GFP signal decrease (540± 61s, n=10) coincides also with AIR-2::GFP loss from the midbody flanking regions (P value = 0,3178, ns) (Fig. 13C, D and E). These data indicate that SPD-1 and Aurora B levels at the midbody probably decrease due to microtubule depolymerization.

As PLK-1 (a protein that localizes to central spindle microtubules) and TSG-101 (a protein belonging to the ESCRT-I machinery) have been implicated in abscission in different systems (Carlton and Martin-Serrano 2007; Bastos and Barr 2010; Green et al. 2013; König et al. 2017), we decided to explore their localization during the last stages of cytokinesis. PLK-1 localizes on chromosomes and centrosomes at anaphase onset (data not shown; n=20), as previously reported (Budirahardja and Gönczy 2008). It appears at the midzone 154±33s after anaphase onset and its signal progressively increases until 537±87s after anaphase onset when its intensity starts to decrease. TSG-101 starts to accumulate at the midzone 310±61s (n=9) after anaphase onset and its concentration progressively increases as the midbody matures, and remains at the midbody remnants when they are released. PLK-1 and TSG-101 signals were internal to that of NMY-2::GFP (Fig. 13G and H).

Our data indicate that the midbody in *C. elegans* is composed of a midbody core (containing microtubules, AIR-2, SPD-1, PLK-1, TSG-101 and CYK-4), midbody arms (containing microtubules, and AIR-2), and a midbody ring (containing NMY-2 and ANI-1) (Fig.14). Moreover, SPD-1 localization at the midbody core is in accordance with what was previously reported for PRC1 in HeLa Cells (Hu et al., 2012b; Jiang et al., 1998).

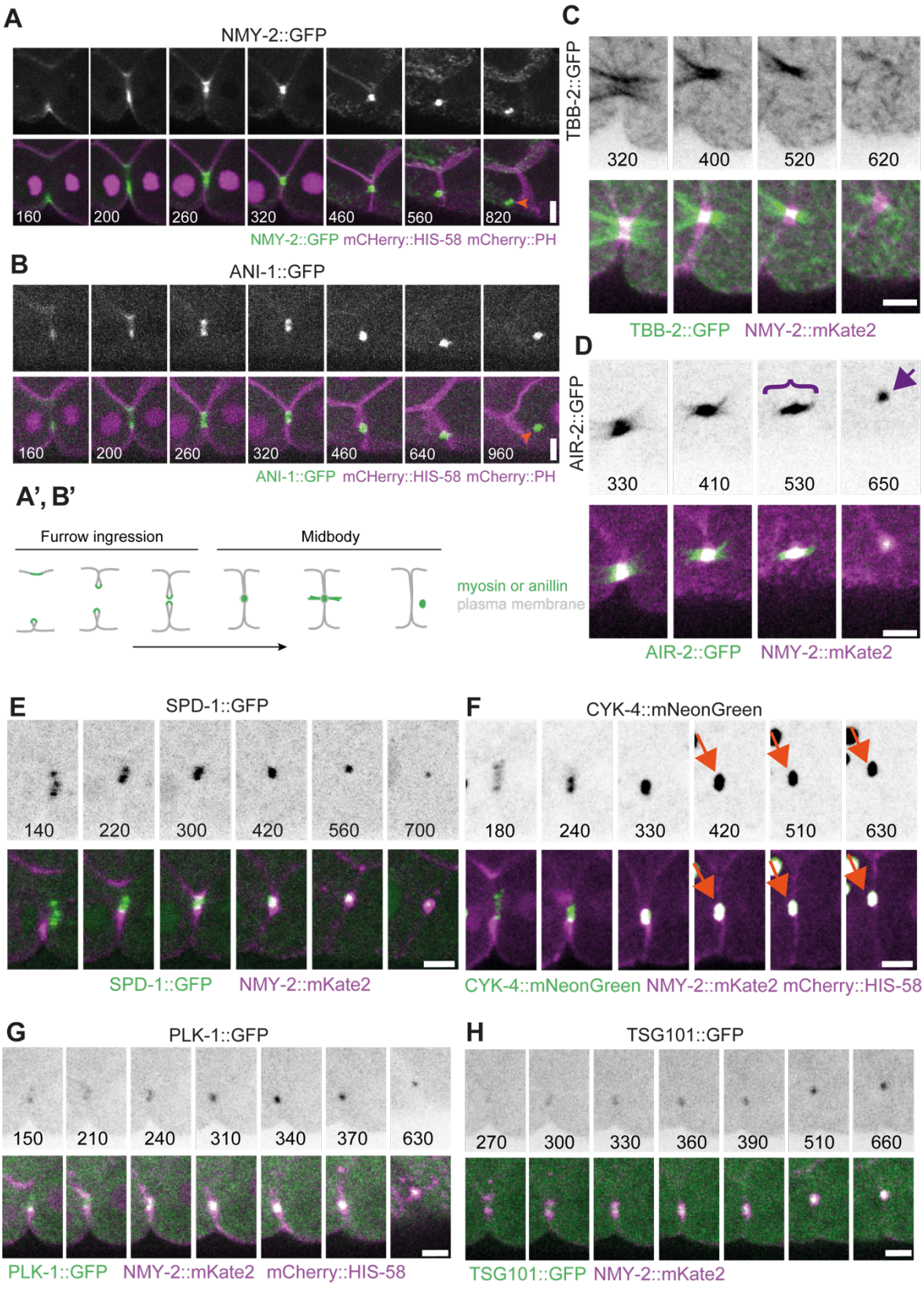

Figure 13- Characterization of midbody in the EMS cell.

(A-H). Images of time-lapse videos of the region of the furrow of EMS cells expressing NMY-2::GFP (A), ANI-1::GFP (B), TBB-2::GFP (C), AIR-2::GFP (D), SPD-1::GFP (E), CYK-4::mNeonGreen (F), PLK1::GFP (G), and TSG-101::GFP (H). Cells co-express the plasma

membrane probe (mCherry::PH) and the histone (mCherry::HIS-58) in panels (A) and (B), NMY-2::mKate2 in panels (C), (D), (E), and (H) or NMY-2::mKate2 and mCherry::HIS-58 in panels (F) and (G). Numbers on stills are time in seconds after anaphase onset. **(A, B')** Schematic illustrating the behavior of the cleavage furrow with back-to-back plasma membranes and the contractile ring at its tip (green), and the midbody that persists after completion of furrow ingression in control cells; some myosin and anillin shed away from the midbody before its release. Orange arrows in panel (A) and (B) point at the midbody being released. Purple brace symbol in panel (D) illustrates AIR-2::GFP spread along the midbody arms and midbody core pointed with purple arrow. Orange arrow in panel (F) illustrates CYK-4 accumulation at the midbody ring/core. Scale bars, 5 µm. Panels (A), (B) and (B') correspond to panels (A) and (A') from figure S3 in Santos and Silva et al., 2023. Panel in (E) was adapted from panel (B) in figure 1 in Santos and Silva et al., 2023.

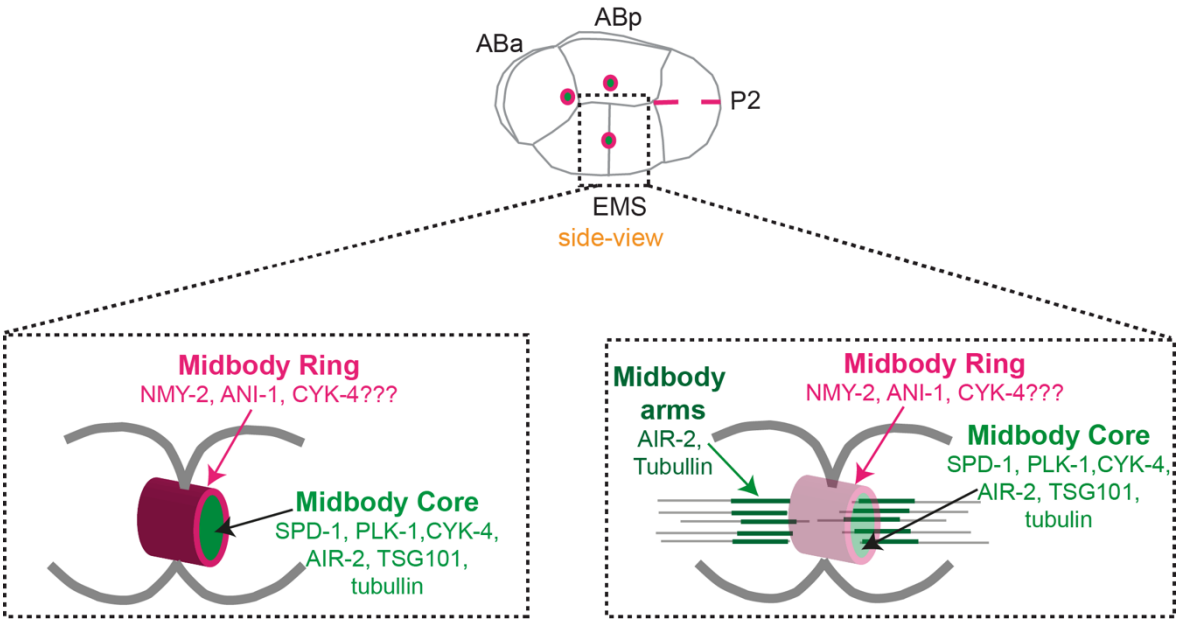

Figure 14- The midbody in the EMS cell of the early *C. elegans* embryo shares similar architecture to that in HeLa Cells.

Midbody proteins are distributed along the midbody ring, midbody core, and midbody arms. The midbody ring contains NMY-2, ANI-1, and probably CYK-4 (in pink), the midbody core contains SPD-1, PLK-1, CYK-4, AIR-2, TSG-101, and tubulin and the midbody arms contain AIR-2 and tubulin (in green).

11. SPD-1 depletion affects ANI-1, but not CYK-1 or NMY-2 turnover during contractile ring constriction

Differences in contractile ring protein behavior were identified during the second half of constriction (section 9), when the contractile ring encounters the central spindle

microtubules. To check whether the proximity between the two structures could have an impact on the dynamics of proteins in the contractile ring, we characterized ANI-1::GFP, NMY-2::GFP and CYK-1::GFP dynamics after *spd-1*(*RNAi*) by measuring the fluorescence recovery after photobleaching (Fig. 15C). A small region of ABa or ABp constricting contractile rings of 38±10 µm of perimeter was photobleached. The average GFP signal within a box of constant width and length manually drawn over the photobleached region was determined for every time point to monitor protein recovery. As the contractile ring constricted, these boxes also covered the flanking regions of the photobleached area. For smaller ring perimeters, it became difficult to draw the boxes, thus we stopped measuring the GFP signal when the rings reached a perimeter of 14±6µm. Plotting the mean of fluorescence recovery over time shows that a plateau was not reached in some conditions, which prevented us from quantitatively determining the half-time recovery (Fig. 15C). Nevertheless, analysis of the curves obtained show that ANI-1 recovery is substantially slowed down after *spd-1(RNAi)*.

These results indicate that the presence of central spindle microtubules is required for normal ANI-1 dynamics during the last phases of contractile ring constriction and that central spindle microtubules contribute to molecular changes in the constricting ring.

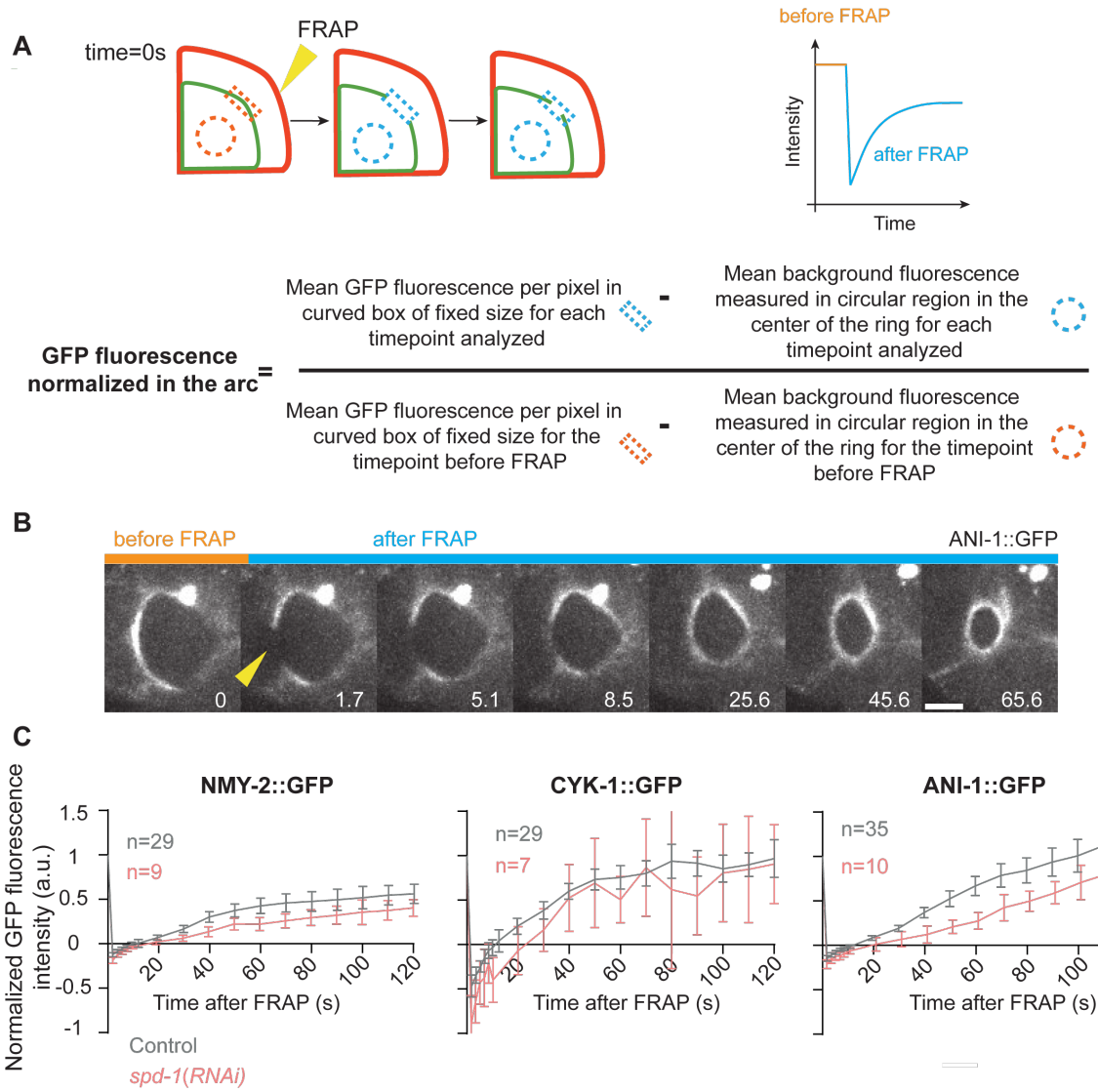

Figure 15- SPD-1 depletion affects ANI-1 dynamics during contractile ring constriction.

(A) Schematic illustrating the measurements and quantifications of fluorescence recovery after photobleaching (FRAP) in ABa or ABp contractile rings. A box with constant width and length was drawn before (orange rectangle) and after (blue rectangle) FRAP. A circle with a constant size was drawn on the cytoplasm for each time point before (orange) and after (blue) FRAP to measure the background intensity. The results were normalized to the values before FRAP. **(B)** Images of a time-lapse video showing the contractile ring before and after FRAP. Scale bar, 5 μm. Numbers on stills correspond to time in seconds. **(C)** Mean GFP fluorescence normalized as explained in (A) plotted versus time. Error bars, 95% CI.

12. SPD-1 interacts with the contractile ring, central spindle, and abscission proteins in a yeast two-hybrid assay

To search for possible interactions of SPD-1 with other proteins that might be relevant to its function, we used a yeast-two-hybrid assay. This is a system that consists in having two yeast strains: one with a plasmid with one of our proteins of interest and the activation domain (AD) of a transcription factor (prey plasmid); and another yeast strain transformed with a plasmid that encodes for the other protein of interest fused to the DNA binding domain (BD) of the transcription factor (bait plasmid). If the proteins cloned as bait and prey do not interact, the transcription factor will not be functional and a reporter gene will not be transcribed. If the two proteins of interest interact, the AD and BD come close and the transcription factor becomes functional resulting in the transcription of the reporter gene (Fig. 16A). In our case the reporter gene is HIS3, coding an enzyme involved in histidine biosynthesis, an essential amino acid. Yeast strains containing bait and prey plasmids were mated and then supplemented in a medium lacking histidine. Only yeast containing proteins that physically interact will be able to synthesize histidine, thus will be able to grow in a medium that is not supplemented with this amino acid.

In our lab, a library of yeast expressing several members of the cytokinesis machinery was already available. We searched for possible interactions with SPD-1, using this as prey, and the other possible interactors as bait (Fig. 16B). As a control for autoactivation empty vector was used as prey and as bait. Unpublished work from our lab indicated that SPD-1 could interact with CYK-1 full length, thus we decided to map this interaction by generating two CYK-1 fragments: one containing the N-terminal GTPase Binding Domain (GBD) and the Formin Homology Domain 3 (FH3) (CYK-1 F1); and the other containing the Formin Homology Domains 1 and 2 (FH1 and FH2) and the diaphanous autoregulatory domain (DAD) (CYK-1 F2). We found that, in this assay, SPD-1 can interact with the contractile ring proteins ANI-1 and CYK-1 F1, midzone proteins CYK-4, PLK-1, CLS-2, and SPD-1 itself, and the abscission protein TSG-101 (Fig. 16B and C). Some of these interactions, such as SPD-1-CYK-4, PRC1^{SPD-1}-PLK1, and PRC1^{SPD-1}-CLASP^{CLS-2} have already been described validating our assay (Hu et al. 2012a; Patel, Nogales, and Heald 2012; Lee et al. 2015; Jing Liu et al. 2009; Neef et al. 2007).

These data suggest that SPD-1 functions in *C. elegans* might go beyond its microtubule bundling capacity and might contribute to cytokinesis/abscission by interacting directly with contractile/midbody ring and abscission machinery.

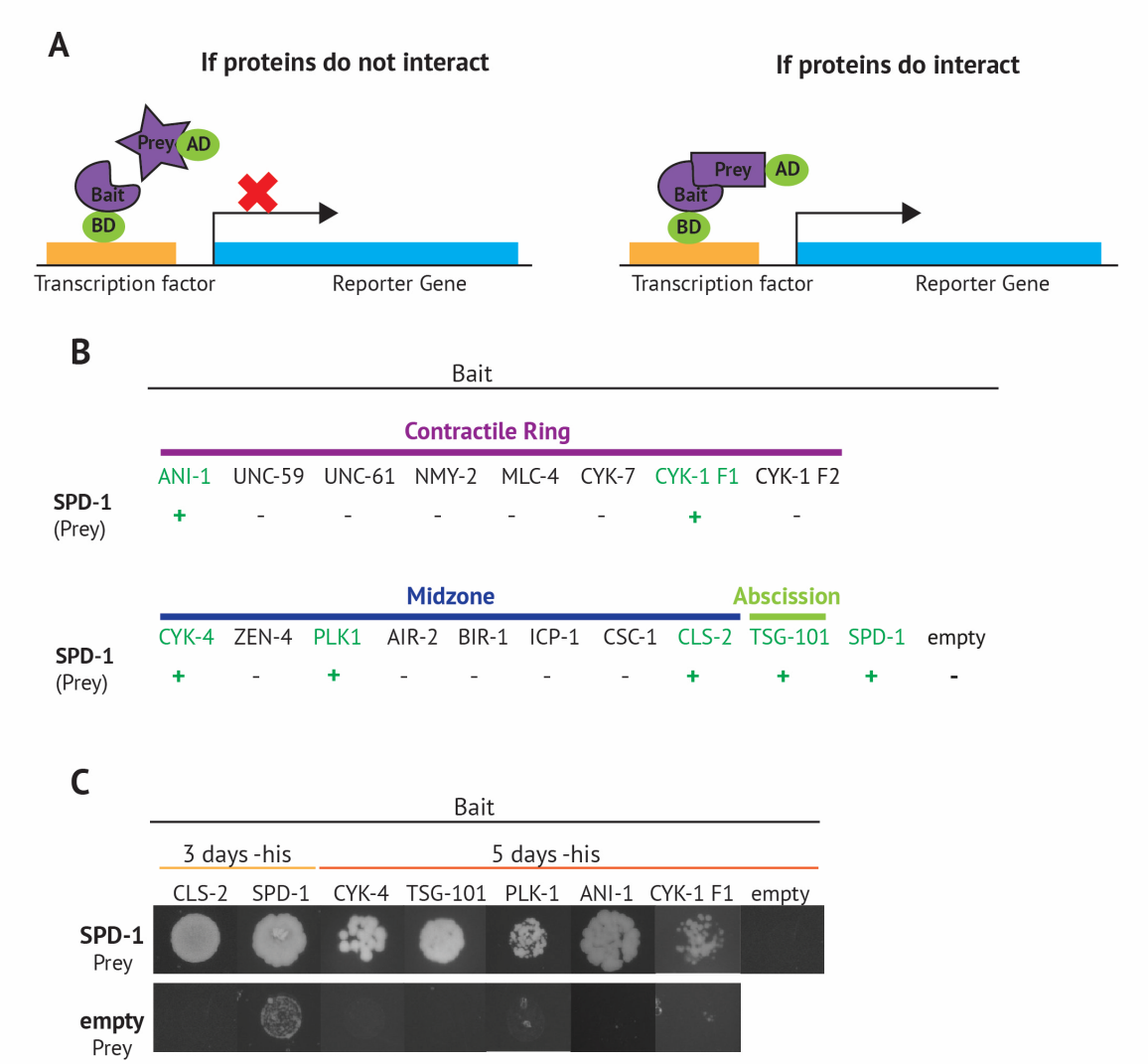

Figure 16- SPD-1 interacts with contractile ring, midzone, and abscission proteins in a yeast-two-hybrid assay.

(A) Schematic representations of the AD, activation domain and BD, DNA binding domain. **(B)** List of proteins tested as possible SPD-1 interactors. Positive and negative interactions are indicated by a green + or a black - signal, respectively. **(C)** Images of yeast two-hybrid assay showing that SPD-1 interacts with CLS-2, CYK-4, TSG-101, PLK1, ANI-1 and CYK-1 F1. Mated yeast was grown for 3 or 5 days in a medium lacking histidine. Empty prey plasmid was used as control. These experiments were repeated 3-4 times for every SPD-1 interaction.

13. Penetrant SPD-1 inhibition in the *C. elegans* early embryo results in frequent cytokinesis failure

To study the requirement of SPD-1 for cytokinesis in the *C. elegans* early embryo, we took advantage of the temperature-sensitive mutant *spd-1(oj5)*, which permits rapid inactivation by upshifting the temperature from 16°C to 26°C (Verbrugghe et al. 2004). For

comparison, we depleted SPD-1 by RNAi (Fig. 16A). After anaphase onset, SPD-1 localizes to the bundled microtubules of the midzone and persists at the midbody (Fig. 13E). Penetrant inhibition of SPD-1 is expected to result in two separated half spindles with no overlapping microtubules in the way of the ingressing cytokinetic furrow (Fig. 17B).

When SPD-1 was depleted by RNAi at 20°C or 26°C in embryos expressing fluorescent myosin (NMY-2::GFP), a marker for the plasma membrane (mCherry::PH(PLC1δ1)) and a marker for chromosomes (mCherry::HIS-58), the majority of EMS cells completed cytokinesis, and the rate of contractile ring constriction was unaffected (Fig. 17C,D). In contrast, and in agreement with a previous study (Verbrugghe et al. 2004), 78% of *spd-1(oj5)* EMS cells failed cytokinesis when upshifted to 26°C during prophase (Fig. 17C). Cytokinesis typically failed after complete furrow ingression, which occurred at the same rate as in controls (Fig. 17E). Inactivation of *spd-1(oj5)* at the beginning of furrowing or at 50% of furrow ingression resulted in a similar phenotype, which reveals that SPD-1 activity is required during the last stages of cytokinesis (Fig. 17C). At 26°C *spd-1(oj5)* also caused cytokinesis failure in the zygote and the other cells of the 4-cell embryo (ABa, ABp, P2), but the failure rate was not as high as in the EMS cell (41%, 53%, 40%, and 30% of cytokinesis failure, respectively; Fig. 17F). We conclude that SPD-1 is required for cytokinesis in the *C. elegans* early embryo and that the EMS cell is particularly sensitive to SPD-1 inactivation.

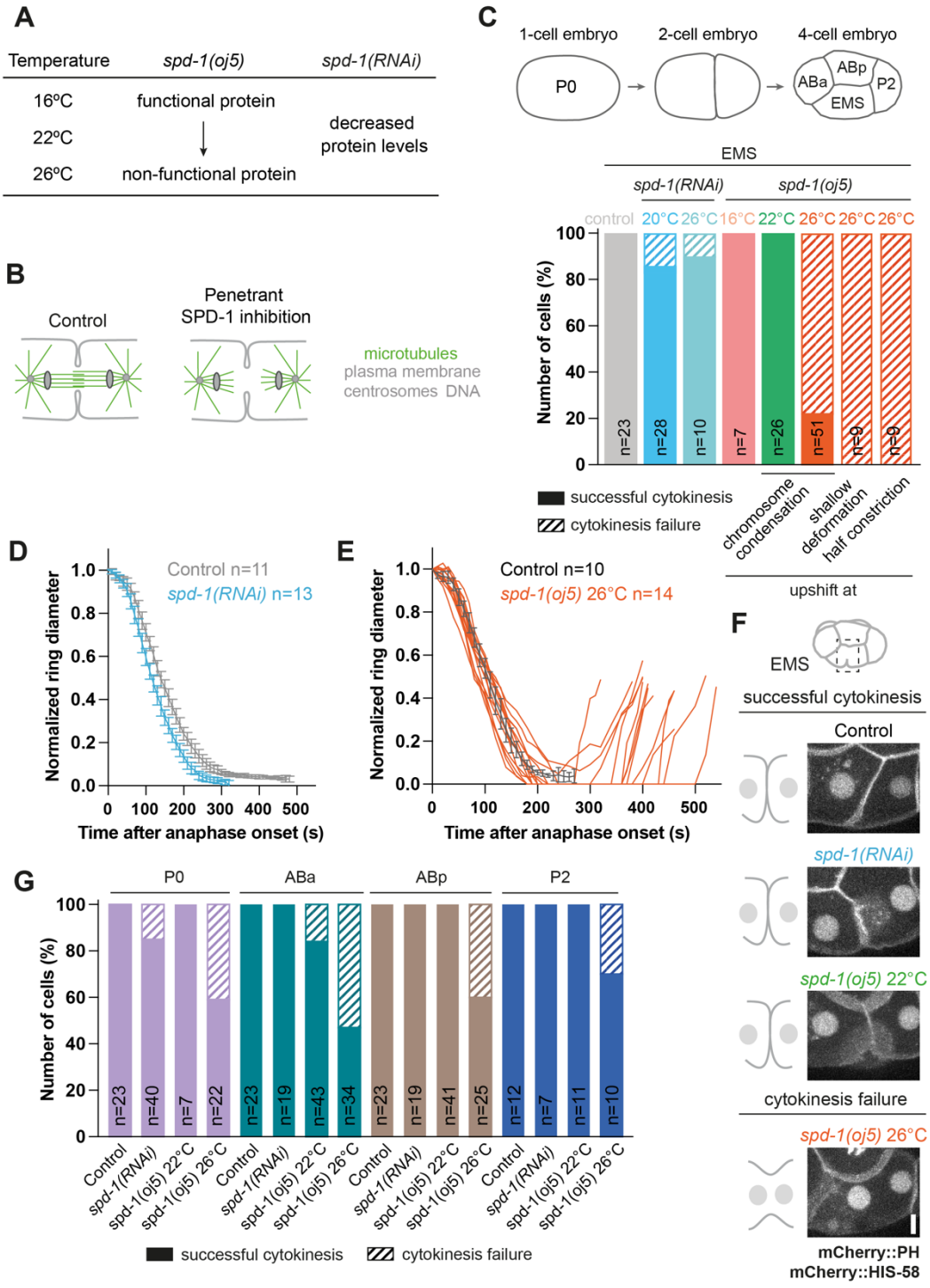

Figure 17- SPD-1 is required for cytokinesis in the *C. elegans* early embryo.

(A) List of conditions used to study SPD-1 function. **(B)** Schematic illustrating that SPD-1 full inhibition is expected to result in two separated half spindles with no bundled microtubules in the midzone. **(C)** Percentage of EMS cells that fail cytokinesis for each condition. *spd-1(oj5)* embryos were upshifted from 16°C to 22°C or 26°C at a point when nuclear chromatin is condensing at the beginning of mitosis, equatorial cortex starts to

deform at the beginning of furrow ingression (shallow deformation), or half way through cleavage furrow ingression. **(D)** Mean contractile ring diameter over time in EMS *spd-1(RNAi)* cells and corresponding control filmed at 20ºC (mean ± 95% CI). **(E)** Individual curves of contractile ring diameter over time after anaphase onset in *spd-1(oj5)* EMS cells at 26°C. Average curve (mean ± 95% CI) is shown for the corresponding control. In *(D)* and *(E)* ring diameter is normalized to ring diameter before ingression, time zero corresponds to anaphase onset, and *n* is the number of cells analyzed. **(F)** Selected images of time-lapse videos showing cytokinesis success or failure in control, *spd-1(RNAi)*, *spd-1(oj5)* at 22°C and *spd-1(oj5)* at 26°C EMS cells expressing a probe for the plasma membrane (mCherry::PH) and a probe for chromosomes (mCherry::HIS-58). Scale bar, 5µm. **(G)** Percentage of P0, ABa, ABp, and P2 cells that fail cytokinesis for each condition. In *(C)*, *(D)*, *(E)* and *(G) n* is the number of cells analyzed. This figure was adapted from figure 1 in Santos and Silva et al., 2023.

14. SPD-1 inhibition leads to formation of an elongated intercellular bridge during the last stages of cleavage furrow ingression

To characterize the impact of SPD-1 inhibition on cytokinesis in more detail, we focused on the EMS cell in embryos co-expressing mCherry::HIS-58 and mCherry::PH(PLC1δ1). In control cells, a tight cleavage furrow forms and sister cells are juxtaposed with back-to-back plasma membranes until the end of furrow ingression. Different temperatures changed the duration of cytokinesis but not the tight furrowing (Fig. 19 and Fig. 18A, A'). In contrast, SPD-1 inactivation at 26°C or *spd-1(RNAi)* at 20°C resulted in broadening of the cleavage furrow tip and in the creation of an elongated intercellular bridge between sister cells at the last stages of constriction (Fig. 18A, A'). In *spd-1(RNAi)* cells, the intercellular bridge elongated and thinned, and the bridge then shortened until the sister cells became juxtaposed. At this point, sister cells resembled those in control embryos (Fig. 18A, C). In the majority of *spd-1(oj5)* EMS cells at 26°C, the intercellular bridge thinned but did not seal, as after bridge shortening the cleavage furrow regressed and cytokinesis failed (424+50 s after anaphase onset, n=10). The phenotype of *spd-1(oj5)* at the semi-restrictive temperature of 22°C was similar to that of *spd-1(RNAi)* (Fig. 17C, 18B-C and 20), suggesting that *spd-1(RNAi)* results in partial inhibition of SPD-1. The formation of an elongated intercellular bridge between sister cells was also observed during cytokinesis of the ABa, ABp, and P2 cell, the 1-cell embryo (P0), and cells of older embryos (16-32-cell stage) (Fig. 18D). These results reveal that SPD-1 is required to maintain the ingressing cleavage furrow in a tight back-to-back configuration.

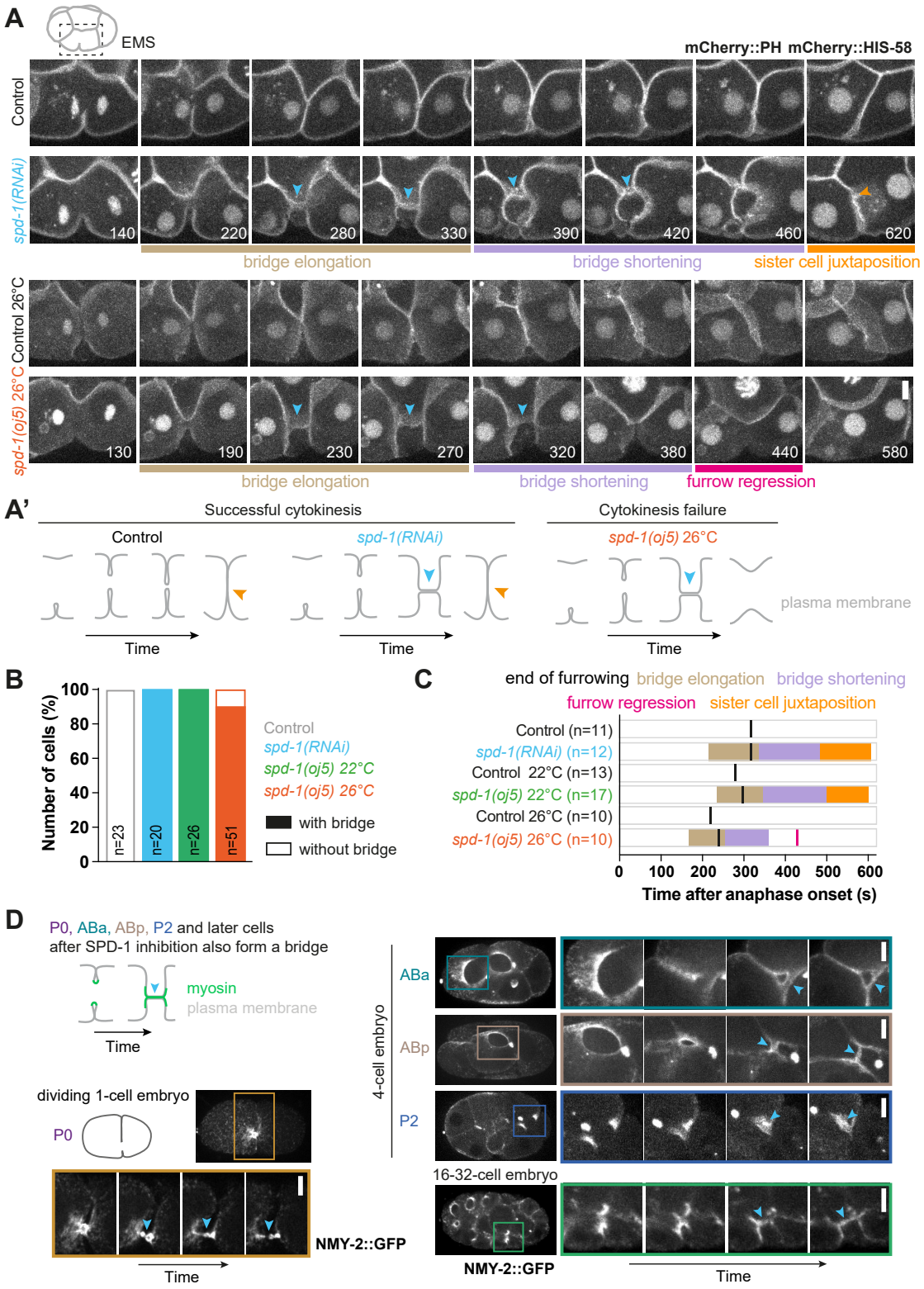

Figure 18- SPD-1 inhibition leads to the formation of an elongated intercellular bridge at the end of furrow ingression.

(A) Images of time-lapse videos in control, *spd-1(RNAi)* and *spd-1(oj5)* at 26°C EMS cells expressing a probe for the plasma membrane (mCherry::PH) and a probe for chromosomes (mCherry::HIS-58). Periods of intercellular bridge elongation and shortening, as well as

sister cell juxtaposition are indicated. Blue and orange arrowheads point to the intercellular bridge and juxtaposed sister cells, respectively. Numbers correspond to time in seconds after anaphase onset. Scale bar, 5 µm. **(A')** Schematic illustrating intercellular bridge formation and successful furrowing completion or furrow regression in *spd-1(RNAi)* and *spd-1(oj5)* at 26°C, respectively. **(B)** Percentage of EMS cells that formed an elongated intercellular bridge. *n* is the number of cells analyzed. **(C)** Diagram showing intervals of intercellular bridge elongation and thinning, bridge shortening, sister cell juxtaposition, mean point of furrowing completion and furrow regression for the different conditions and corresponding controls (n≥10). **(D)** Images of time-lapse videos of embryos expressing myosin (NMY-2::GFP) showing that elongated intercellular bridges also form in P0, ABa, ABp, P2, and later cytokinesis, as illustrated on the top left. Single images of the entire embryos indicate the position of the cells shown in the insets. Blue arrowheads point to the intercellular bridge. ABa and ABp cells start dividing vertically, providing an end-on view of the entire contractile ring, and rotate during furrow ingression, when only two sides of the contractile ring and the intercellular bridge can be observed. Scale bars, 5 µm. This figure corresponds to figure 2 in Santos and Silva et al., 2023.

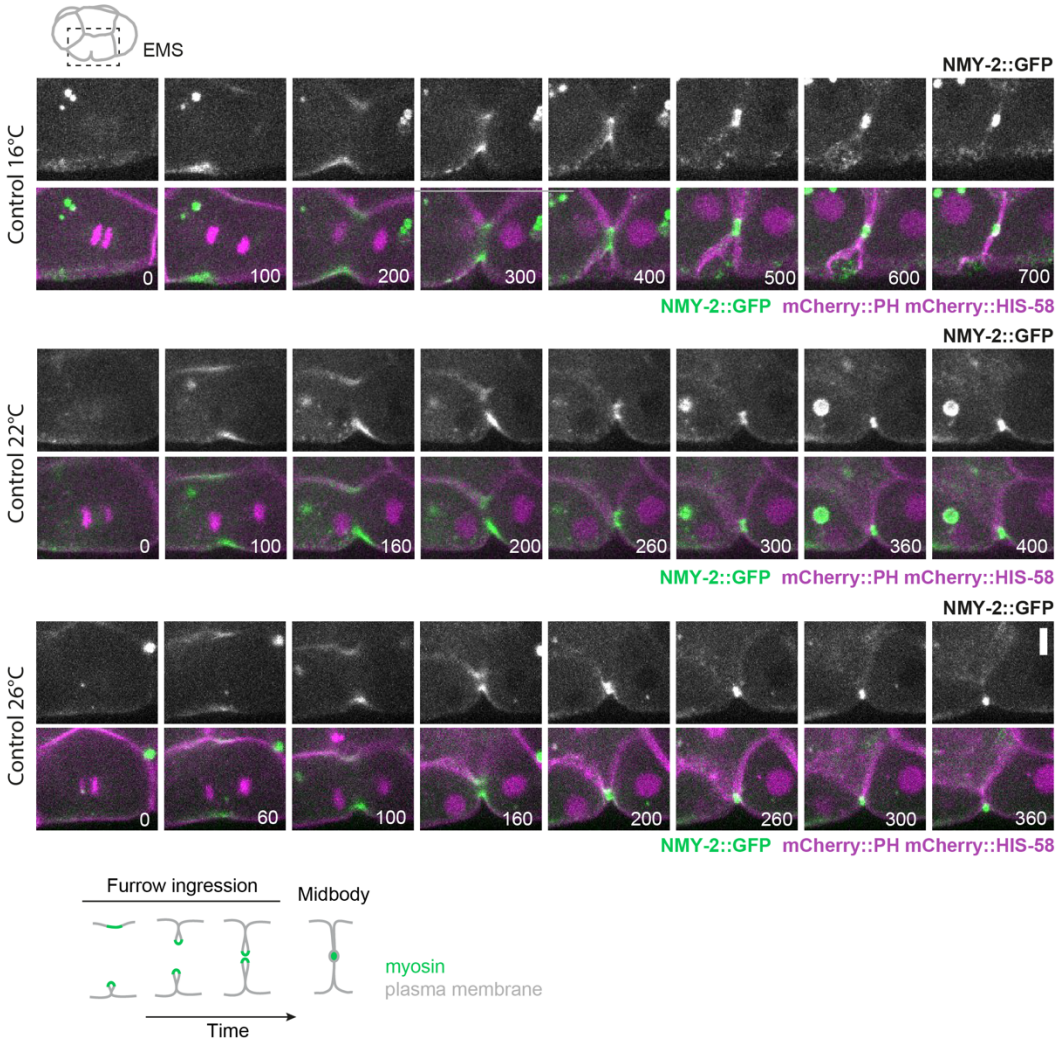

Figure 19- Duration of cytokinesis varies depending on the temperature.

Images of time-lapse videos in control EMS cells expressing myosin (green or gray, NMY-2::GFP), a probe for the plasma membrane (magenta, mCherry::PH), and a histone (magenta, mCherry::HIS-58). Numbers correspond to time in seconds after anaphase onset. Schematic at the bottom illustrates the behavior of the cleavage furrow with back-to-back plasma membranes and the contractile ring at its tip (green), and the midbody that persists after completion of furrow ingression in control cells. Scale bar, 5 μm. This figure corresponds to figure S1 in Santos and Silva et al., 2023.

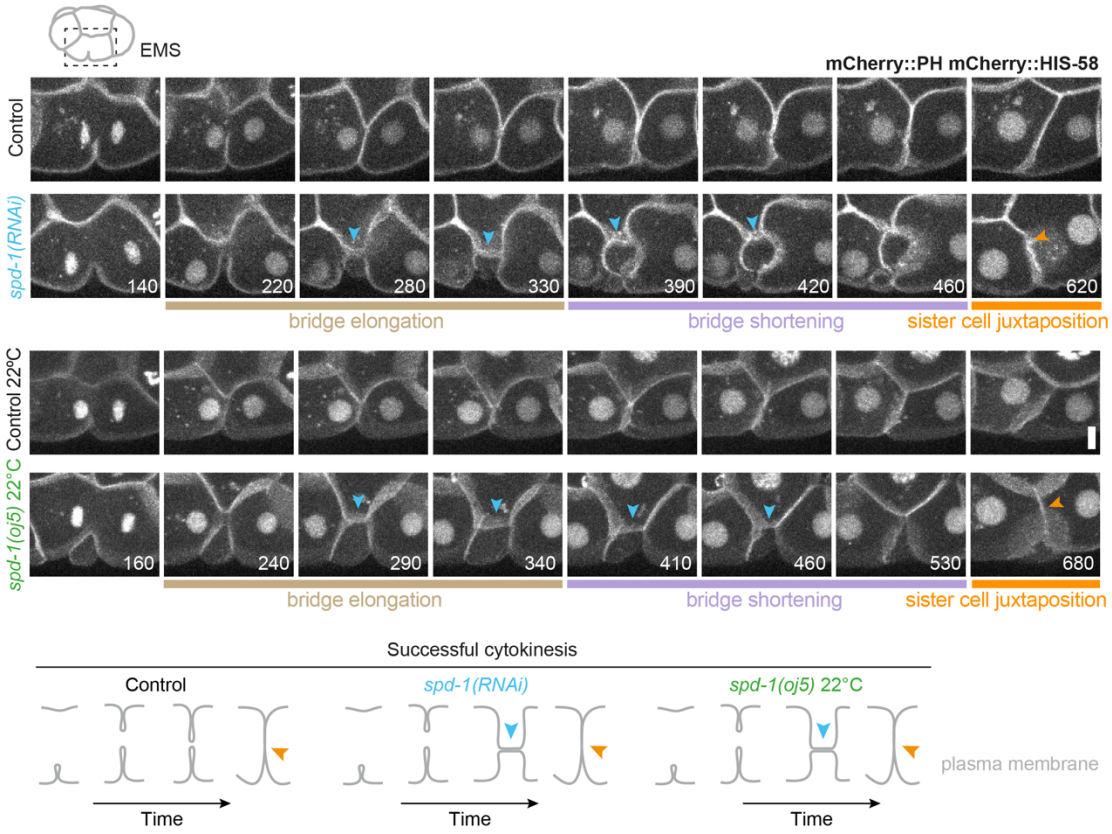

Figure 20- The cytokinesis phenotype of *spd-1(oj5)* at the semi-restrictive temperature of 22°C is similar to that of *spd-1(RNAi)*.

Images of time-lapse videos in *spd-1(RNAi)* and *spd-1(oj5)* at 22°C EMS cells expressing a probe for the plasma membrane (mCherry::PH). Periods of intercellular bridge elongation and shortening, as well as sister cell juxtaposition are indicated. Blue and orange arrows point at the intercellular bridge and juxtaposed sister cells, respectively. Numbers correspond to time in seconds after anaphase onset. Scale bar, 5 µm. This figure corresponds to figure S2 in Santos and Silva et al., 2023.

15. Contractile ring components disperse along the intercellular bridge after SPD-1 inhibition, and successful cytokinesis after partial SPD-1 inhibition correlates with formation of a mini-midbody

To understand why partial SPD-1 inhibition allows cytokinesis to complete while penetrant inhibition does not, we examined the state of midzone microtubules. Bundled midzone microtubules were abundant in control embryos, were substantially decreased at the semi-restrictive temperature, and were undetectable at the restrictive temperature (Fig. 21A). For *spd-1(RNAi)* and corresponding control EMS cells, imaging could be performed under compression, which improves image quality because the spindle is situated closer to the coverslip (Fig. 21B). As in *spd-1(oj5)* at the semi-restrictive temperature, residual

microtubule bundles were detected at the midzone after *spd-1(RNAi)* (Fig. 21B). In agreement with this, residual Aurora B (AIR-2::GFP) and centralspindlin (CYK-4::mNeonGreen) signal was detected in the intercellular bridge in *spd-1(oj5)* at 22°C and after *spd-1(RNAi)*. At the restrictive temperature neither AIR-2::GFP nor CYK-4::GFP were detected in the midzone of *spd-1(oj5)* cells. We conclude that cytokinesis completion after *spd-1(RNAi)* or in *spd-1(oj5)* at 22°C correlates with the presence of a residual central spindle (Fig. 21A-C).

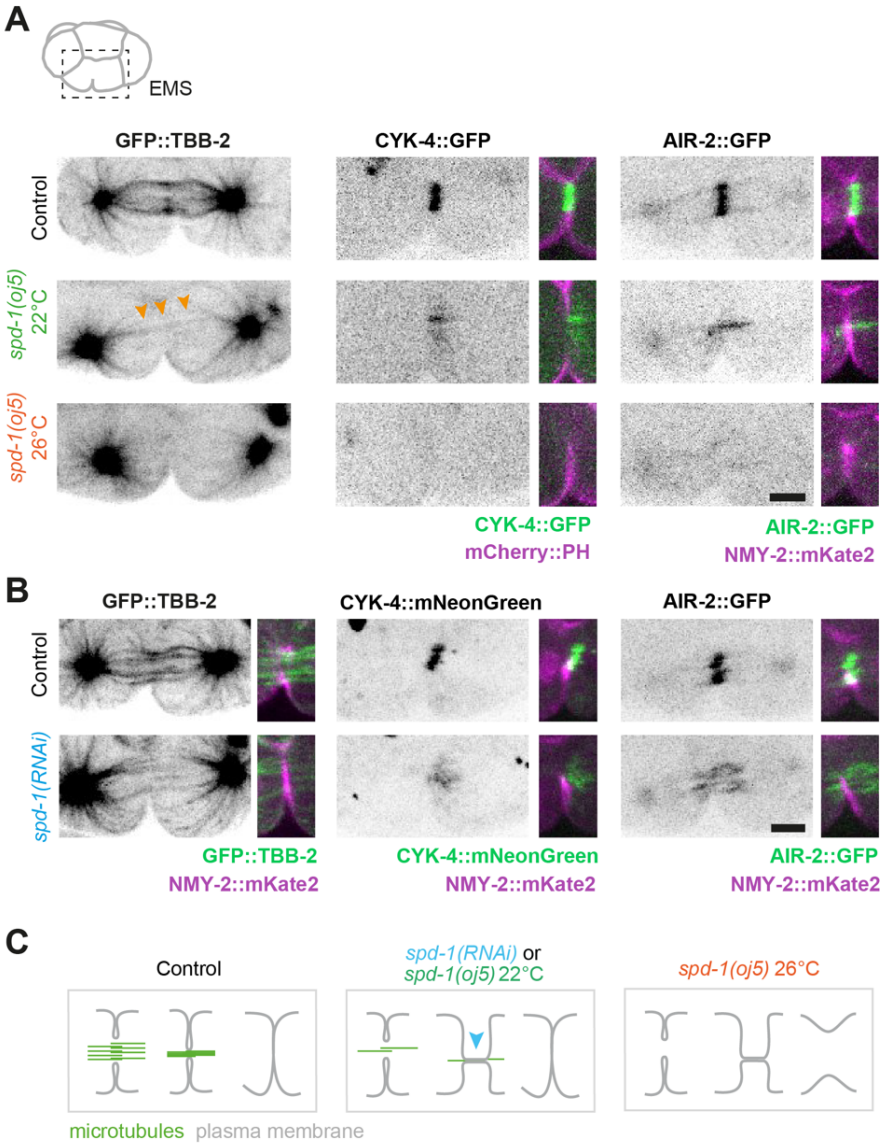

Figure 21- Residual midzone microtubules are observed after SPD-1 depletion and partial inactivation of *spd-1(oj5)* at 22°C in EMS cells.

(A,B) Images of tubulin-labeled microtubules (GFP::TBB-2), centralspindlin component CYK-4 (CYK-4::mNeonGreen) and chromosomal passenger protein AIR-2 (AIR-2::GFP) in control, *spd-1(oj5)* at 22°C, *spd-1(oj5)* at 26°C and *spd-1(RNAi)* at 20°C EMS cells co-expressing either a probe for the plasma membrane (mCherry:PH) or for the contractile ring

(myosin, NMY-2::mKate2) filmed under no compression *(A)* or under compression *(B)*. Orange arrows point at residual microtubules traversing the midzone. Scale bars, 5 µm. **(C)** Schematic illustrating the presence of residual bundled microtubules when SPD-1 is partially inhibited (*spd-1(RNAi)* and *spd-1(oj5)* at 22°C) and their absence when SPD-1 is fully inhibited (*spd-1(oj5)* at 26°C). Scale bars, 5 µm. This figure corresponds to figure 3 in Santos and Silva et al., 2023.

To better characterize the distribution of the chromosomal passenger protein complex (as judged by AIR-2::GFP) and the centralspindlin complex (as judged by CYK-4::mNeonGreen) within the elongated intercellular bridges observed upon SPD-1 perturbation, we performed 3D spatial reconstructions. We observed that NMY-2::mKate2 formed a hollow cylinder filled with AIR-2::GFP and CYK-4::mNeonGreen during bridge elongation (Fig. 22). We did not find strong evidence that CYK-4::mNeonGreen signal also overlapped with that of NMY-2::mKate2. This analysis suggests that the remaining AIR-2 and CYK-4 present in the bridges is attached to residual central spindle microtubules and not to the broadened contractile ring.

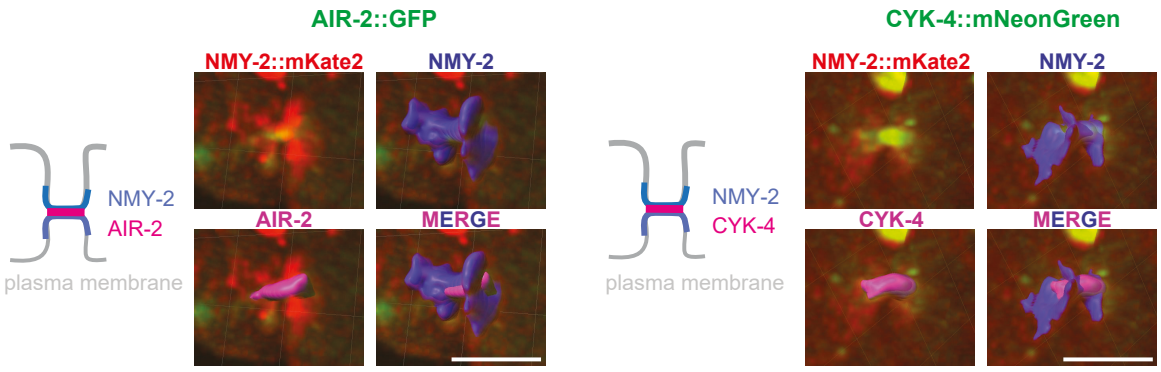

Figure 22- AIR-2 and CYK-4 localize in the inner part of the elongated intercellular bridges after SPD-1 inhibition.
Stills of the EMS cell rotated in different orientations, from embryos co-expressing AIR-2::GFP or CYK-4::mNeonGreen, NMY-2::mKate2 and a probe for chromosomes (mCherry::HIS-58) in an SPD-1 depleted embryo during bridge formation. A reconstructed surface is observed in blue based on NMY-2 fluorescence or in magenta based on AIR-2 or CYK-4 fluorescence. The stills are accompanied by schematics representing the bridge stage. Scale bar,5 µm.

We next examined how SPD-1 inhibition affects contractile ring components. During cytokinesis in control EMS cells, the contractile ring folds back onto itself at the tip of the cleavage furrow. Myosin (NMY-2::GFP) and anillin (ANI-1::GFP) localized in the contractile

ring throughout constriction and persisted at the midbody. A fraction of myosin and anillin was shed from the midbody 582±28 s after anaphase onset (n=12), but most of the signal persisted at the midbody even after the midbody was released 1046±162 s after anaphase onset (n=7; Fig. 23D, D'). In contrast, myosin and anillin became dispersed along the intercellular bridge and spread into the lateral sides of the furrow in *spd-1(oj5)* cells at 22°C and 26°C (Fig. 23A-C). When the bridge reached its maximum length, the continuous myosin and anillin signal became fragmented and decreased over time. Residual myosin and anillin concentrated at the center of the bridge in a midbody-like structure in *spd-1(oj5)* at 22°C, which persisted during sister cell juxtaposition (Fig. 23A). The presence of residual Aurora B, and centralspindlin at the center of the bridge after *spd-1(RNAi)* and *spd-1(oj5)* at *22°C* supports the idea that partial inhibition of SPD-1 allows for formation of a mini-midbody (Fig. 24). In agreement with this, residual ESCRT-I (TSG-101::GFP) was observed in the mini-midbody after *spd-1(RNAi)*. In *spd-1(oj5)* at 26°C, no mini-midbody was observed, and myosin and anillin completely disappeared from the bridge shortly before furrow regression (Fig. 23B, and 24B). These results suggest that the residual microtubule bundles observed in *spd-1(RNAi)* and *spd-1(oj5)* at 22°C support the formation of a mini-midbody, which in turn allows bridge sealing and completion of cytokinesis.

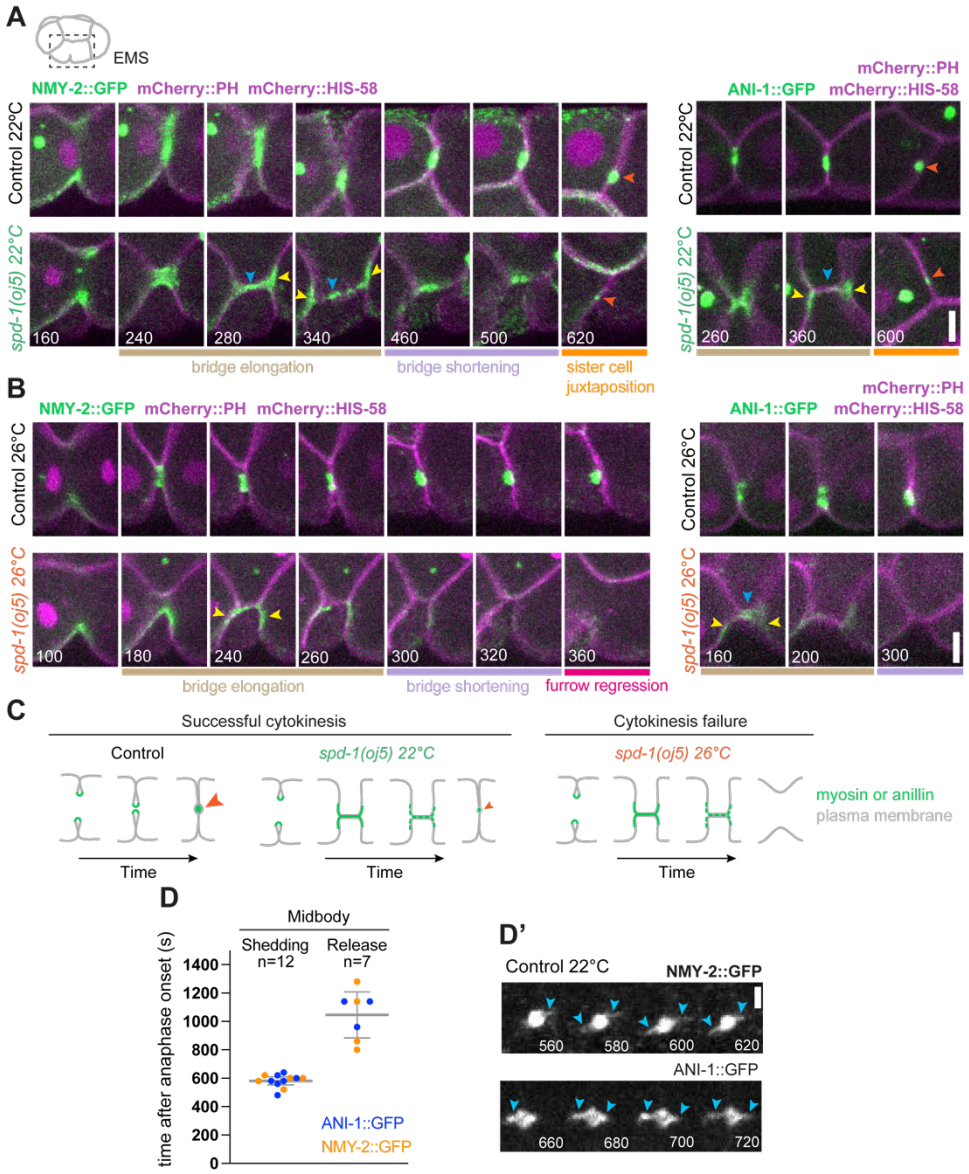

Figure 23- Myosin and anillin distribute along intercellular bridges after SPD-1 inhibition and the formation of a mini-midbody ensures cytokinesis completion after partial SPD-1 inhibition.

(A,B) Images of time-lapse videos of the region of the furrow in control and *spd-1(oj5)* at 22°C *(A)* or control and *spd-1(oj5)* at 26°C EMS cells *(B)* expressing myosin (green, NMY-2::GFP, left) or anillin (green, ANI-1::GFP, right), the plasma membrane probe mCherry::PH and the DNA probe mCherry::HIS-58. Periods of intercellular bridge elongation and shortening, as well as sister cell juxtaposition are indicated. Yellow arrowheads point at the myosin/anillin signal on the laterals of the furrow, blue arrowheads point at the myosin/anillin that persists within the intercellular bridge, and orange arrowheads point at the midbody or mini-midbody. Numbers correspond to time in seconds after anaphase onset. **(C)** Schematic illustrating that some myosin/anillin signal persists in a mini-midbody in *spd-1(oj5)* at 22°C but it completely disappears in *spd-1(oj5)* at 26°C, which leads to furrow

regression and cytokinesis failure. **(D)** Mean time after anaphase onset (mean ± 95% CI) when some NMY-2::GFP (orange circles) and ANI1::GFP (blue circles) shed from the midbody and when midbody release happens in control EMS cells, at 22°C. *n* is the number of cells analyzed. **(D')** Images of time-lapse videos of the region of the midbody showing shedding events at 22°C, indicated by the blue arrowheads. Numbers in images correspond to time in seconds after anaphase onset in (A), (B) and (D'). Scale bars, 5 µm. This figure was adapted from figure 4 and figure S3 in Santos and Silva et al., 2023.

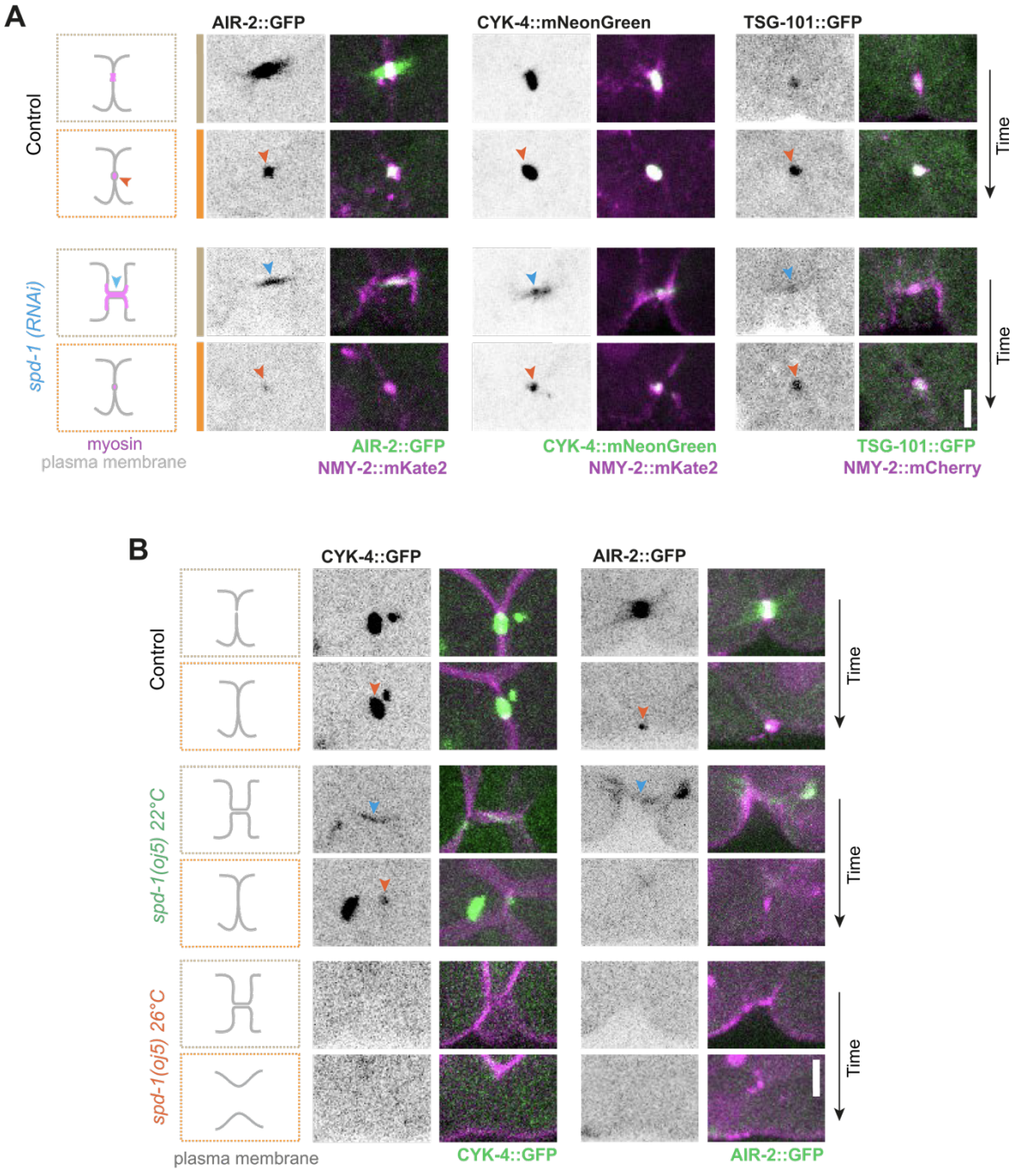

Figure 24- CYK-4 and AIR-2 are able to accumulate in intercellular bridges of *spd-1(RNAi)*, *spd-1(oj5)* EMS cells at 22ºC but not at 26ºC.

(A) Images showing that reduced chromosomal passenger protein AIR-2 (AIR-2::GFP), centralspindlin component CYK-4 (CYK-4::mNeonGreen), and ESCRT-I component TSG-101 (TSG-101::GFP) are present in the mini-midbody observed after *spd-1(RNAi)* in EMS cells co-expressing NMY-2::mKate2 or NMY-2::mCherry. Orange arrowheads point at the midbody or mini-midbody and blue arrowheads point at AIR-2, CYK-4 and TSG-101 in the intercellular bridge. Two time points during bridge elongation and sister juxtaposition are shown for each case. **(B)** Images of centralspindlin component CYK-4 (CYK-4::GFP) and chromosomal passenger protein AIR-2 (AIR-2::GFP) in control, *spd-1(oj5)* at 22°C and *spd-1(oj5)* at 26°C EMS cells co-expressing a probe for the plasma membrane (mCherry:PH) or a probe for the contractile ring (myosin, NMY-2::mKate2). Orange arrowheads point at the midbody or mini-midbody and blue arrowheads point at AIR-2 and CYK-4 in the intercellular bridge. Two time points during bridge elongation and sister juxtaposition are shown for each case. Scale bars, 5 µm. This figure was adapted from figure 4 and figure S3 in Santos and Silva et al., 2023.

16. Anillin depletion aggravates cytokinesis in SPD-1-inhibited cells

Anillin is involved in coordinating the transition from contractile ring to midbody ring during late cytokinesis in *D. melanogaster* S2 cells (Kechad et al. 2012). In the *C. elegans* early embryo, however, the anillin ANI-1 is not essential for cytokinesis (Maddox et al. 2007). *C. elegans* also expresses two additional anillin paralogs (ANI-2 and ANI-3), but these have not been implicated in embryogenesis (Maddox et al. 2005). We next investigated how co-inhibition of ANI-1 and SPD-1 impacts cytokinesis in EMS cells. ANI-1 depletion on its own resulted in symmetric furrow closure (Fig. 25A, B), a slower second half of contractile ring constriction, and an even slower final phase of constriction (Fig. 25C). Central spindle microtubules were unaffected (Fig. 25D), and cytokinesis completed in all cells (n=20).

Strikingly, ANI-1 depletion in *spd-1(oj5)* at 22°C severely aggravated cytokinesis failure in EMS cells, with 88% of furrows not completing ingression (Fig. 26A). The presence of residual microtubule bundles at the midzone suggested that ANI-1 depletion in *spd-1(oj5)* at 22°C did not further compromise central spindle formation beyond the defects observed in *spd-1(oj5)* (Fig. 26B). Although an intercellular bridge formed in the double inhibition, it did not elongate or thin out as much as the intercellular bridge in *spd-1(oj5)* cells (Fig. 26C), reaching a maximum length of 3.5±0.5 µm (versus 5.6±0.5 µm in *spd-1(oj5)* cells at 22°C; n=10 and n=33, respectively; P=0.0001). After reaching a maximum of 97% ingression, furrow ingression in the double inhibition stalled until regression ensued (Fig. 26D). Mini-midbodies were not observed at any point (Fig. 26C). At 26°C, all *ani-1(RNAi);spd-1(oj5)*

EMS cells failed cytokinesis. 87% already stopped furrowing at 70±6% ingression (n=20), and, after a period of pause, their furrows regressed (Fig. 26A, B). We conclude that depletion of ANI-1 in SPD-1-inhibited cells aggravates cytokinesis defects without aggravating defects in central spindle formation.

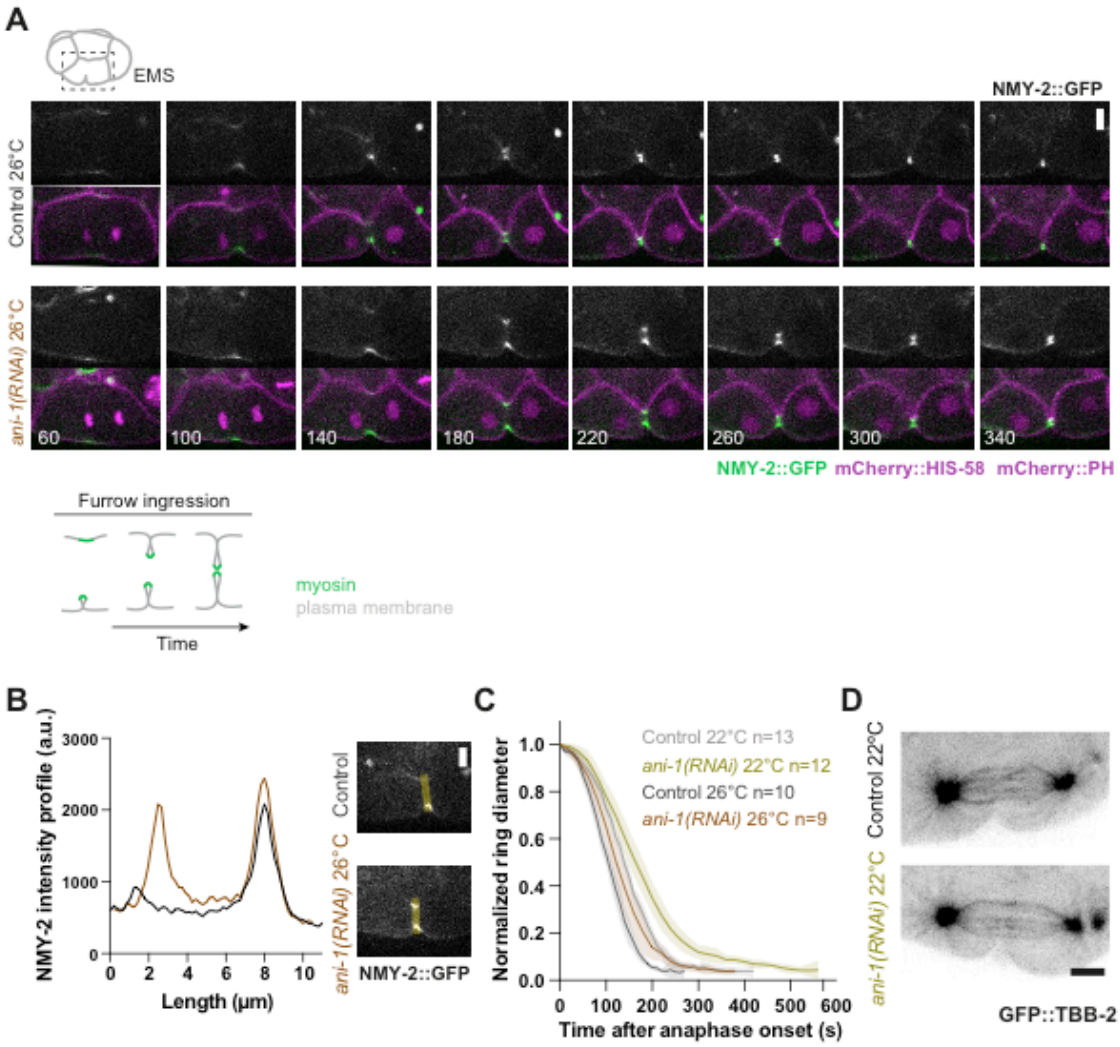

Figure 25- *ani-1(RNAi)* slows down furrow ingression and causes symmetric furrow closure but does not affect midzone microtubules.

(A) Images of time-lapse videos of control and *ani-1(RNAi)* EMS cells. Numbers correspond to time in seconds after anaphase onset. Scale bar, 5 µm. Schematic on the bottom illustrates successful furrow ingression after *ani-1(RNAi)*. **(B)** NMY-2::GFP fluorescence intensity measured along a line scan that covers both sides of the cleavage furrow at 70% ingression in a control and *ani-1(RNAi)* EMS cell, as illustrated on the right. **(C)** Mean contractile ring diameter over time in *ani-1(RNAi)* EMS cells at 22°C or 26°C and corresponding controls (mean ± 95% CI). Ring diameter is normalized to ring diameter before ingression, time zero corresponds to anaphase onset, and *n* is the number of cells

analyzed. **(D)** Images of tubulin (GFP::TBB-2) in control and *ani-1(RNAi)* EMS cells. Scale bars, 5 µm. This figure corresponds to figure S4 in Santos and Silva et al., 2023.

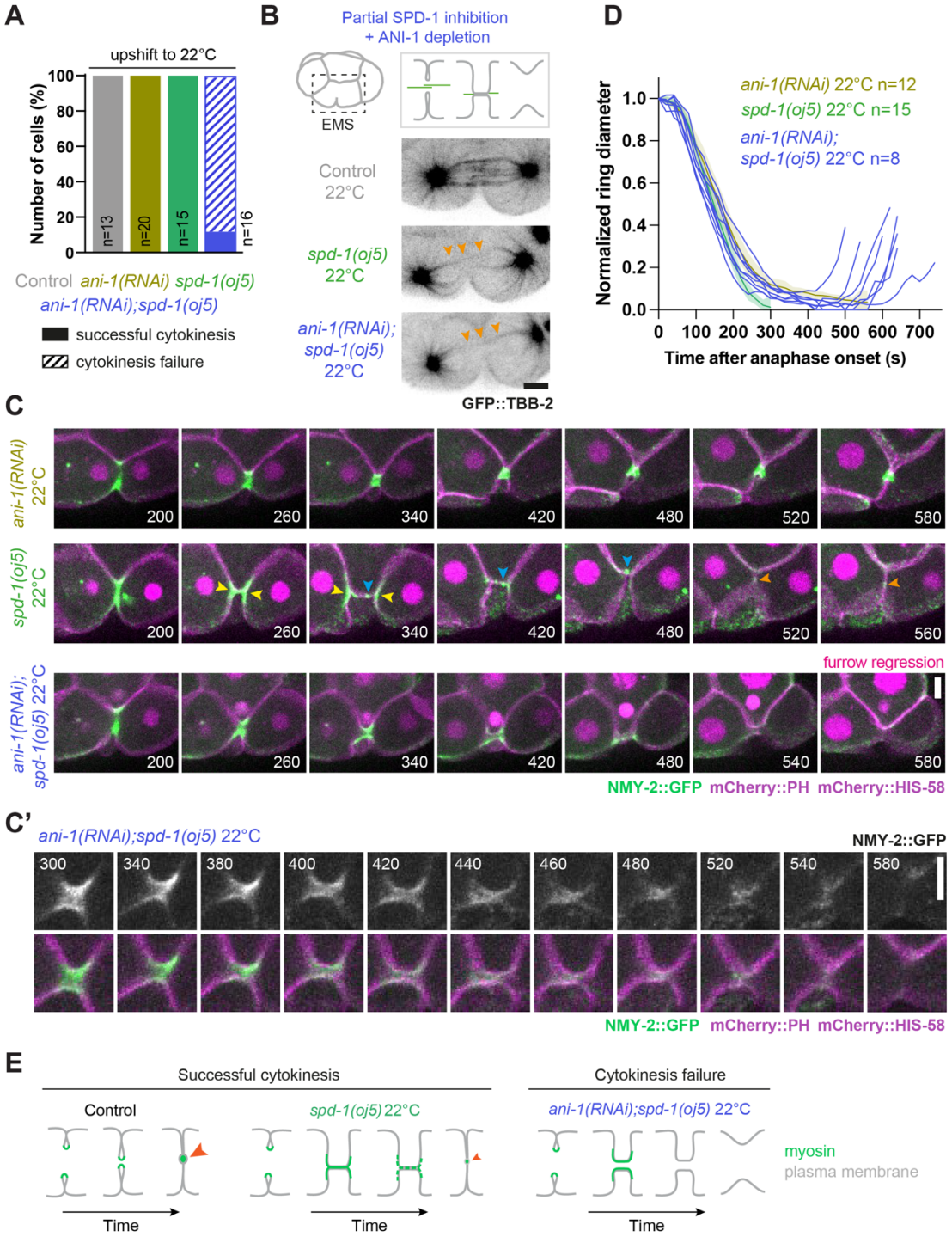

Figure 26- ANI-1 depletion in *spd-1(oj5)* embryos at 22°C leads to myosin loss and furrow regression during late furrowing.

(A) Percentage of EMS cells that succeed/fail cytokinesis for each condition. *n* is the number of cells analyzed. **(B)** Images of tubulin (GFP::TBB-2) in EMS cells filmed under no

compression. Orange arrowheads point at residual microtubules traversing the midzone. Schematic on top illustrates that the presence of residual bundled microtubules at the midzone is similar in *spd-1(oj5)* at 22°C and *ani-1(RNAi);spd-1(oj5)*. **(C)** Images of time-lapse videos of EMS cells showing that the intercellular bridge does not elongate as much and furrow regresses before membrane sealing in *ani-1(RNAi);spd-1(oj5)* at 22°C. Arrowheads as in Figure 23A. **(C')** Images of the intercellular bridge of an *ani-1(RNAi);spd-1(oj5)* EMS cell at 22°C showing that the myosin signal at the bridge disappears before furrow regression. **(D)** Individual curves of contractile ring diameter over time after anaphase onset in *ani-1(RNAi);spd-1(oj5)* EMS cells at 22 °C. Average curves (mean ± 95% CI) are shown for *ani-1(RNAi)* and *spd-1(oj5)* at 22°C. Ring diameter is normalized to ring diameter before ingression, time zero corresponds to anaphase onset, and *n* is the number of cells analyzed. **(E)** Schematic illustrating that furrow ingression does not complete and furrow regression ensues after myosin loss from the intercellular bridge in *ani-1(RNAi)*;*spd-1(oj5)* at 22°C. Orange arrowheads point at midbody or mini-midbody. Scale bars, 5 µm. This figure corresponds to figure 5 in Santos and Silva et al., 2023.

17. Co-inhibition of ANI-1 and SPD-1 results in progressive myosin loss from the constricting contractile ring

To understand why co-inhibition of ANI-1 and SPD-1 aggravates cytokinesis defects relative to the single inhibitions, we examined myosin localization. In contrast to single inhibitions, depletion of ANI-1 in *spd-1(oj5)* cells at 22°C or 26°C caused myosin to progressively disappear from the contractile ring until it was barely detectable just prior to furrow regression (Fig. 26C, C', E, 27C-D). Furthermore, acute inactivation of myosin during the second half of furrow ingression in otherwise normal EMS cells, using the temperature sensitive mutant *nmy-2(ne3409)*, resulted in abrupt stalling of ingression followed by furrow regression (Fig. 28A, A'). These results suggest that ANI-1 depletion in *spd-1(oj5)* cells aggravates cytokinesis defects due to a failure to maintain myosin in the contractile ring.

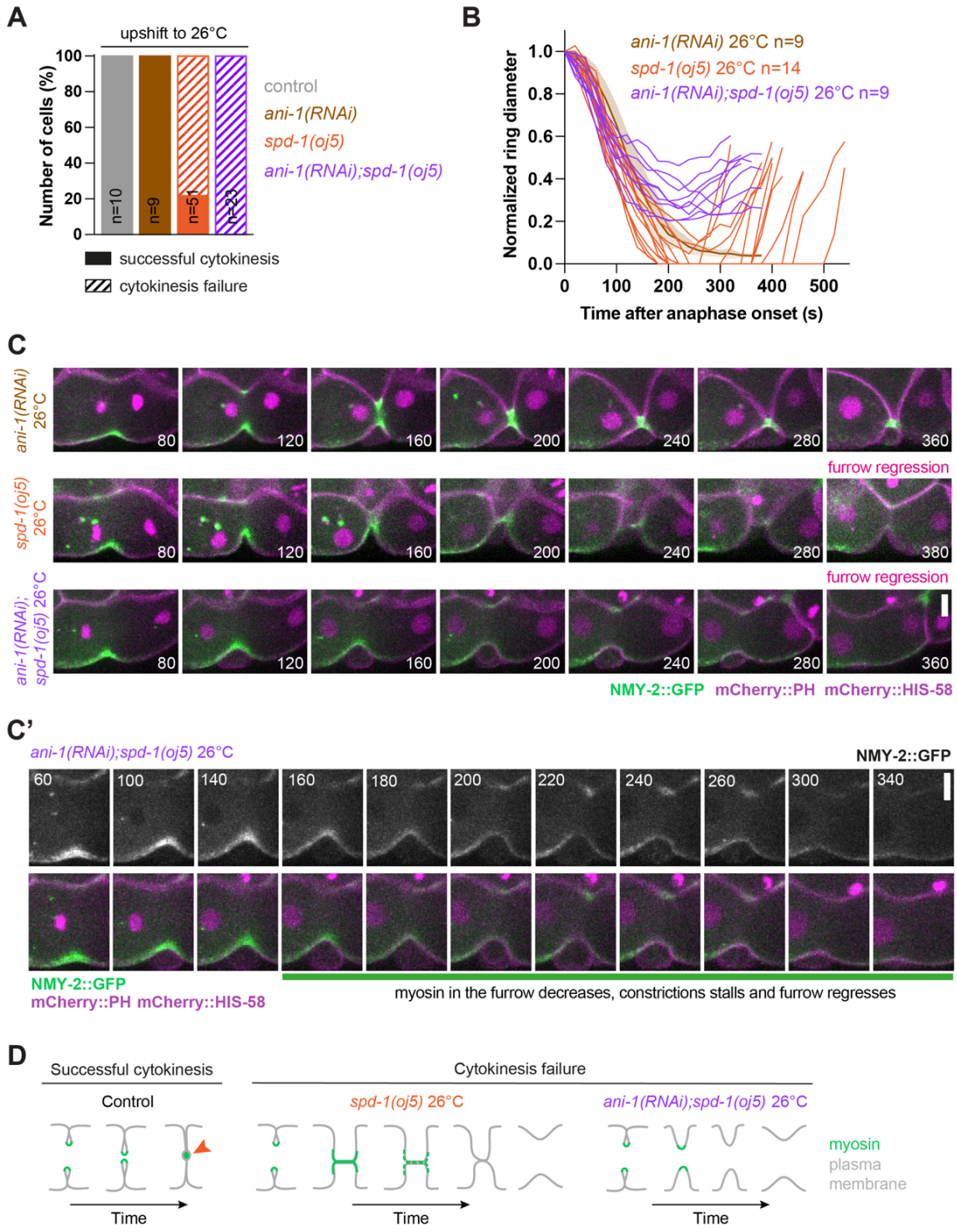

Figure 27- ANI-1 depletion in *spd-1(oj5)* embryos at 26°C leads to myosin loss and furrow regression at 70% furrow ingression.

(A) Percentage of EMS cells that succeed and fail cytokinesis for each condition. *n* is the number of cells analyzed. **(B)** Individual curves of contractile ring diameter over time after anaphase onset in *spd-1(oj5)* and *ani-1(RNAi);spd-1(oj5)* EMS cells at 26°C. Average curve (mean ± 95% CI) is shown for *ani-1(RNAi)* at 26°C. Ring diameter is normalized to ring diameter before ingression and *n* is the number of cells analyzed. **(C)** Images of time-lapse

videos of EMS cells showing that furrow regression occurs before an intercellular bridge forms in *ani-1(RNAi);spd-1(oj5)* at 26°C. **(C')** Images of the furrow region of an *ani-1(RNAi);spd-1(oj5)* EMS cell at 26°C showing that the myosin signal disappears, before furrow regression. **(D)** Schematic illustrating that furrow ingression fails at an early stage and furrow regression ensues after myosin loss from the furrow in *ani-1(RNAi)*;*spd-1(oj5)* at 26°C. Orange arrowhead points at the midbody. Scale bars, 5 µm. This figure corresponds to figure 6 in Santos and Silva et al., 2023.

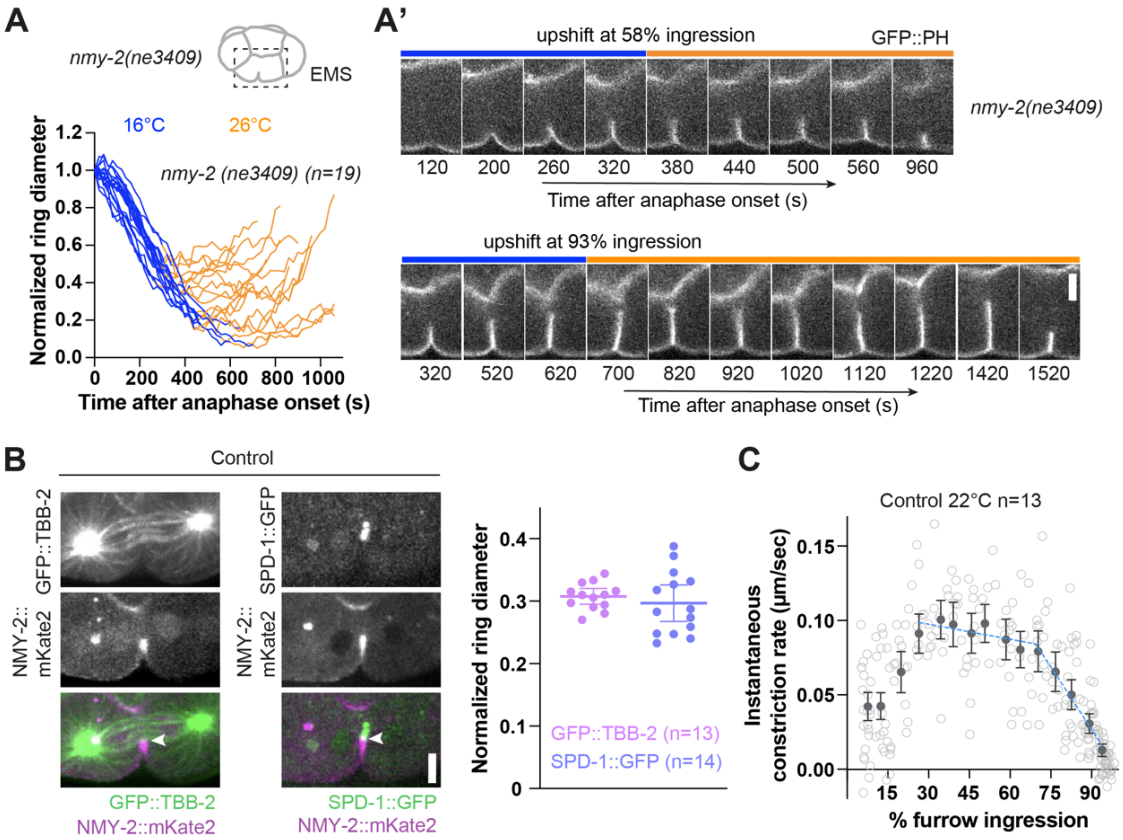

Figure 28- Myosin is required for continuous furrow ingression and ring regression after co-inhibition of SPD-1 and ANI-1 occurs at the stage when the contractile ring encounters midzone microtubules in control embryos.

(A) Individual curves of contractile ring diameter over time after anaphase onset in *nmy-2(ne3409)* EMS cells. Temperature was upshifted from 16°C (blue) to 26°C (orange) during the second half of furrow ingression. Ring diameter is normalized to ring diameter before ingression. **(A´)** Images of time-lapse videos of the furrow region of *nmy-2(ne3409)* EMS cells upshifted to restrictive temperature at 58% and 93% ingression. Numbers correspond to time in seconds after anaphase onset. Scale bar, 5 µm. **(B)** Percentage of furrow ingression (mean % ± 95% CI) when the ring labeled with NMY-2::GFP touches the central spindle labeled with GFP::TBB-2 or SPD-1::GFP (white arrow). Images on the left show the time point when measurements were determined. Scale bar, 5 µm. **(C)** Instantaneous

constriction rate (mean ± 95% CI) against percentage of furrow ingression in control EMS cells. Blue dashed line segments are linear regressions used to determine the point when the contractile ring starts to constrict slower, which is indicated by the vertical gray line. This figure was adapted from figure 7 in Santos and Silva et al., 2023.

18. Ring regression after co-inhibition of SPD-1 and ANI-1 occurs at the stage when the contractile ring encounters midzone microtubules in control embryos

We found that 70% ingression, which is when furrowing stops on average in *ani-1(RNAi);spd-1(oj5)* cells at 26°C, corresponds to the point when the contractile ring approaches midzone microtubules in control embryos: the diameter of the contractile ring when it first approached the central spindle, measured in embryos co-expressing NMY-2::mKate2 and a microtubule marker (GFP::TBB-2), was 5.5±0.2 µm, which corresponds to 69±1% ingression (n=13). Similar values were obtained when measuring the diameter of the contractile ring in embryos co-expressing SPD-1::GFP and NMY-2:.mKate2 (5.5±0.5 µm corresponding to 70±3% ingression) (Fig. 28B). Analysis of instantaneous contractile ring constriction rate showed that 72% ingression also corresponds to the stage when furrow ingression abruptly starts to slow down in control embryos (Fig. 28C).

These observations suggest that the central spindle slows the advance of the contractile ring. Together with the finding that co-inhibition of SPD-1 and ANI-1 lead to ring regression at a point when the cleavage furrow would normally encounter the spindle midzone, our results suggest that anillin in the contractile ring and the central spindle (through SPD-1 or other central spindle components) act jointly to induce changes in the contractile ring at this time point. These changes involve the maintenance of myosin in the contractile ring, thereby ensuring the continuation and completion of furrow ingression (Fig. 29).

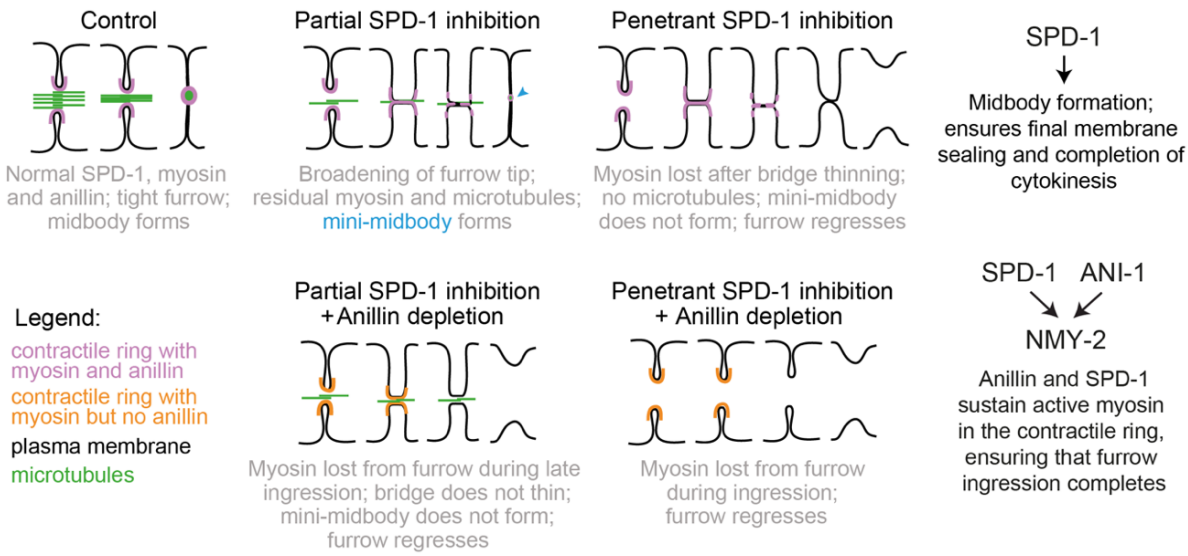

Figure 29- SPD-1 and ANI-1 cooperate to keep myosin active during ring constriction. Summary of results. *n* is the number of examples analyzed in *(A)*, *(B),* and *(C)*. This figure corresponds to panel D) from figure 7 in Santos and Silva et al., 2023.

CHAPTER V

EXPLORING THE REQUIREMENTS FOR BRIDGE FORMATION UPON SPD-1 DISRUPTION

Exploring the requirements for bridge formation upon SPD-1 disruption

19. SPD-1 perturbation impacts embryonic viability

Since SPD-1 disruption resulted in successful cytokinesis after the formation of the elongated bridge between the two daughters of the EMS cell, we tested whether the occurrence of these impacted embryo development.

We evaluated embryonic viability, which is a readout for defects caused by SPD-1 inhibition or depletion during embryogenesis (Fig. 30A). SPD-1 perturbation resulted in a significant decrease in embryonic viability (0.2±1 % in *spd-1(oj5)* at 26°C and 66±21% in *spd-1(RNAi)*) when compared with corresponding controls (90±7% in *spd-1(oj5)* at 16°C and 100% in non-depleted embryos) (Fig. 30B). The fact that SPD-1 depletion by RNAi also resulted in some embryonic viability indicates that failure in later embryonic cytokineses may happen.

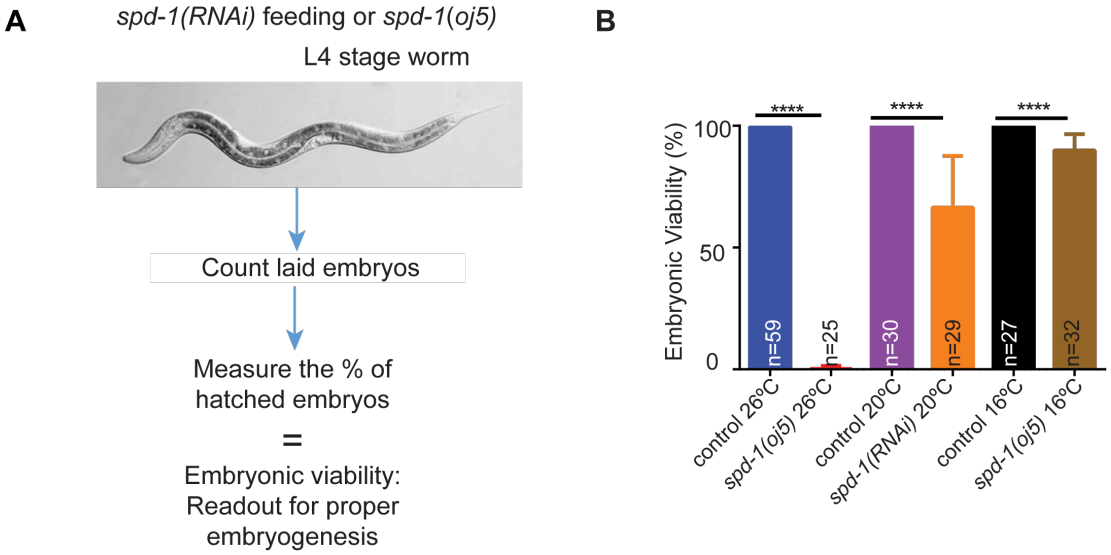

Figure 30- SPD-1 perturbation affects embryo viability.

(A) Embryonic viability test design. **(B)** Graph showing the percentage of viable embryos for each condition. *n* is the number of worms analyzed. **** P < 0.00001.

20. SPD-1-CYK-4 interaction is dispensable for CYK-4 accumulation at the midzone and for central spindle elongation in the EMS cell

It was previously described that the SPD-1 N-terminal region directly binds to the CYK-4 C-terminal region (Lee et al. 2015). The SPD-1 mutation in the *oj5* allele is within the CYK-4 binding region and has been shown to weaken the SPD-1-CYK-4 interaction

(Lee et al. 2015). Thus, the bridges observed after SPD-1 inhibition could be a result of the loss of this interaction.

CYK-4 mutants that lack the SPD-1 binding region or in which 3 essential residues for this interaction were mutated (CYK-4(Δtail) and CYK-4(EAE), respectively) were reported to exhibit disrupted central spindles in *C. elegans* 1-cell embryos (Lee et al. 2015). In agreement with a disrupted midzone, the centrosome-to-centrosome distance was reported to abruptly increase at anaphase onset much more than in controls (Lee et al., 2015). Consequently, the SPD-1-CYK-4 interaction was described to function as a brake for spindle pole separation (Lee et al., 2015). Bearing this in mind, we wondered whether the elongated intercellular bridges in EMS cells could also be a consequence of defective SPD-1-CYK-4 interaction. To test this, we aimed at checking whether EMS cells from embryos expressing CYK-4(Δtail)::GFP or CYK-4(EAE)::GFP also formed elongated intercellular bridges.

We started by confirming Lee et al., 2015 results, by imaging 1-cell embryos co-expressing mCherry::tubulin and CYK-4(WT)::GFP, CYK-4(Δtail)::GFP, or CYK-4(EAE)::GFP. CYK-4(WT)::GFP starts to accumulate at the midzone at anaphase onset and its levels progressively increase until the midbody forms. By contrast, in *cyk-4(Δtail)::gfp* and *cyk-4(EAE)::gfp* embryos, CYK-4 accumulation at the midzone is severely decreased, and the signal is dispersed; no signal is detected in midbodies (Fig. 31A). We also confirmed that in both mutants the two centrosomes snap apart and the pole-to-pole distance drastically increases at anaphase onset when compared with controls (Fig. 31B). Interestingly, 36% (5/14) and 50% (7/14) of *cyk-4(EAE)::gfp* and *cyk-4(Δtail)::gfp* 1-cell embryos, respectively, fail cytokinesis after full furrow ingression.

Next, we checked whether similar differences occur in the EMS cell. Intriguingly, we observed that although initially slightly less compacted, CYK-4(Δtail)::GFP and CYK-4(EAE)::GFP can accumulate at the midzone and midbody in *cyk-4(Δtail)* or *cyk-4(EAE)* EMS cells, indicating the midzone has not been disrupted. In addition, central spindle microtubules are still observed in the midbodies, although signal seems to be decreased (Fig. 31C). Supporting these observations is the fact that pole-to-pole distance profiles are similar to those of controls (Fig. 31D). No bridges were observed in *cyk-4(Δtail)::gfp* or *cyk-4(EAE)::gfp* EMS cells and all completed cytokinesis (n=8 and n=9, respectively).

These results indicate that it is not the disrupted interaction between SPD-1 and CYK-4 that is triggering the formation of the intercellular bridges in the EMS cell. However, these results revealed the interesting possibility that the mechanisms necessary for central spindle microtubule bundling and spindle organization are different in the P0 and EMS cells.

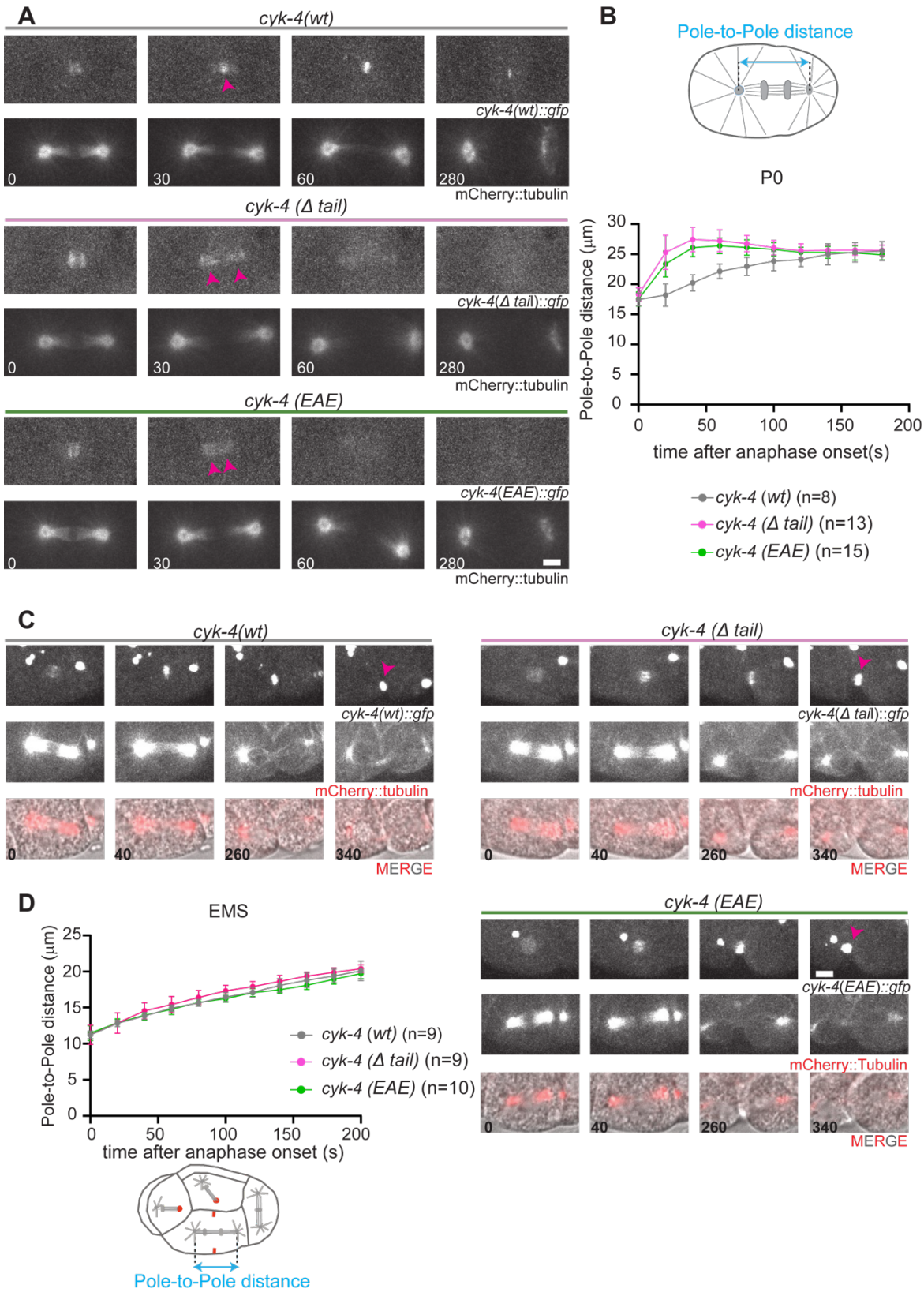

Figure 31- SPD-1-CYK-4 interaction is not essential for spindle midzone formation in the EMS cell and loss of this interaction does not result in intercellular bridge formation.

(A) Images of time-lapse videos of *C. elegans* 1-cell embryos co-expressing mCherry::tubulin and CYK-4::GFP versions. **(B)** Pole-to-pole distance in the 1-cell embryo plotted against time after anaphase onset. Schematic on top illustrates how pole-to-pole distance was measured in the 1-cell embryo. The plasma membrane, microtubules, centrosomes, and DNA are represented in grey. **(C)** Images of time-lapse videos of EMS cells co-expressing mCherry::tubulin and CYK-4::GFP versions. Corresponding DIC images are overlaid with mCherry::tubulin on the bottom row. **(D)** Pole-to-pole distance in the EMS cell plotted against time after anaphase onset. Schematic of 4-cell embryo illustrating how pole-to-pole distance was measured in the EMS cell. The plasma membrane, microtubules, centrosomes, and DNA are represented in grey. The contractile ring is represented in red. Pink arrowheads point out to the presence of GFP signal in the spindle in (A) and midbodies in (C). Numbers on stills in (A) and (C) correspond to time in seconds after anaphase onset. Scale bars, 5 μm. Error bars in (B) and (D), 95% CI. *n* is the number of embryos analyzed in (B) and (D).

21. SPD-1 disruption leads to the abrupt separation of DNA masses in the EMS cell

SPD-1 depletion leads to the unbundling of central spindle microtubules in the 1-cell embryo (Verbrugghe et al. 2004) and in the EMS cell of the 4-cell embryos. Due to the existence of cortical forces pulling the poles apart, the distance between the two centrosomes should abruptly increase at anaphase after SPD-1 inhibition (Lee et al. 2015; Verbrugghe et al. 2004). Since we observed that the mechanisms of central spindle organization may differ in the EMS cell, we checked whether the distance between the two masses of chromatin also abruptly increased after SPD-1 inhibition in this cell. Measuring the distance between two masses of chromatids that are moving towards opposing poles is equivalent to measuring the distance between the two (Fig. 32A). Our analysis demonstrated that the distance between DNA masses abruptly increases at anaphase onset in *spd-1(RNAi)* EMS cells, similar to what happens in the P0 (Fig. 32B,C). Similar results were obtained in *spd-1*(*oj5*) at 26°C in EMS and P0 cells (Fig. 32B,C). We conclude that SPD-1 depletion and partial/full inactivation led to similar profiles of DNA-DNA distance (Fig. 33A) and that the cytokinesis failure observed upon SPD-1 full inactivation is unlikely a consequence of the abrupt increase in the distance between the two spindle poles.

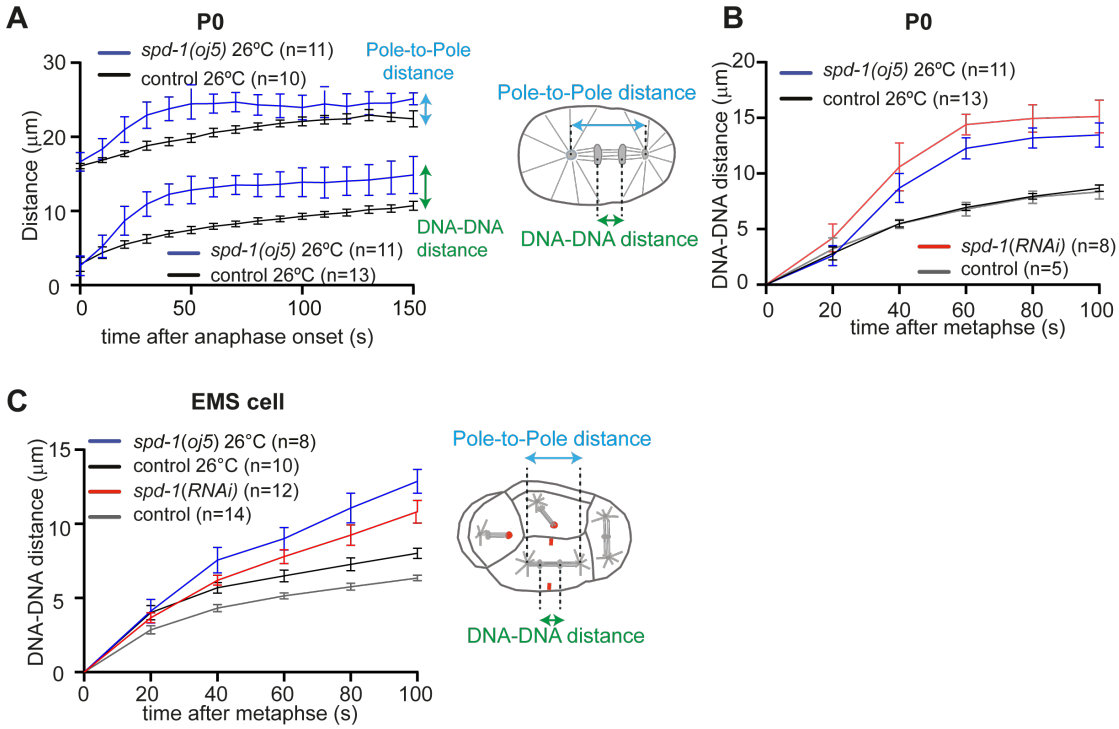

Figure 32- SPD-1 perturbation results in abrupt chromosome/centrosome separation in P0 and EMS cells.

(A) DNA-DNA distance (lower curves) and Pole-to-Pole distance (higher curves) plotted against time after anaphase onset in P0. The schematic on the right illustrates how pole-to-pole and DNA-DNA distances were measured. The plasma membrane, microtubules, centrosomes, and DNA are represented in grey, the contractile ring is in red. **(B, C)** DNA-DNA distance in P0 (B) and EMS cell (C) plotted against time after metaphase in seconds (s) for *spd-1(RNAi)*, *spd-1(oj5)* at 26ºC, and corresponding controls. The schematic on the right illustrates how pole-to-pole and DNA-DNA distances were measured in the EMS cell (colours as in schematic in panel A). *n* is the number of embryos analyzed. Error bars, 95% CI.

22. The abrupt separation of DNA masses is unlikely to be responsible for intercellular bridge formation after SPD-1 inhibition

Next, we tried to understand whether elongated intercellular bridge formation could be associated with the abrupt separation of DNA masses after anaphase onset.

To further assess the impact of the abrupt poles separation on bridge formation, we checked whether intercellular bridges also formed after depletion of EFA-6, whose loss of function has been described to affect the distance between DNA masses or centrosomes in a way similar to that of *spd-1(RNAi)*. EFA-6 was described to be a negative regulator of dynein-based cortical pulling force, and *C. elegans* 1-cell embryos that lack this protein present accelerated spindle elongation. First, we confirmed that the DNA-DNA profile in the

1-cell embryo after *efa-6(RNAi)* was similar to the previously described and similar to that we observed after SPD-1 inhibition (Fig. 33A left panel) (Lee et al. 2015). Second, we looked at the DNA-DNA profile in the EMS cell. In contrast to *spd-1(RNAi)*, EFA-6 depletion did not affect centrosome-centrosome distance in the EMS cell (Fig. 33A right panel). We could not use EFA-6 depletion to test whether exaggerated spindle elongation could per se cause bridge formation. These observations reinforced the idea that the mechanisms that govern central spindle organization in P0 may differ from those in the EMS cell.

Next, we checked whether reducing cortical pulling forces that pull the poles apart prevents spindle snapping and bridge formation. GPR1/2 together with Gα proteins and LIN-5 form a complex that anchors cortical dynein to the plasma membrane. Cortical dynein is responsible for exerting pulling forces on the astral microtubules. Depletion of GPR-1/2 has previously been shown to slow the separation of centrosomes during anaphase in the *C. elegans* zygote (Pecreaux et al. 2006; Srinivasan et al. 2003; Nguyen-Ngoc, Afshar, and Gonczy 2007; Gotta et al. 2003). Therefore, we depleted GPR-1/2 in the EMS cell to check whether the same happens. Depletion of GPR1/2 in the EMS led to a decrease in DNA-DNA separation when compared to that in control embryos (Fig. 33B and C). When GPR-1/2 depletion was combined with SPD-1 partial inactivation, the distance between the DNA masses was restored to control levels in the EMS cell (Fig. 33B and C). However, depletion of GPR-1/2 in the EMS cell of *spd-1(oj5)* embryos resulted in contractile ring tilting, which made it challenging to determine whether an intercellular bridge still formed or not. Additionally, 11 out of 15 cells failed cytokinesis after full ingression of the furrow, which complicated the interpretation even further. Thus, we turned our attention to the P2 cell, which like EMS cells divides parallel relative to the imaging plane, and forms intercellular bridges before completing cytokinesis in 90% of *spd-1(oj5)* embryos at 22 °C (9/10). *gpr-1/2(RNAi)* also led to a decrease in DNA-DNA separation in this cell and restored DNA-DNA distance profile in *spd-1(oj5)* at 22ºC. *gpr-1/2(RNAi);spd-1(oj5)* P2 cells continued to form intercellular bridges (88% (7/8) of P2 cells exhibited intercellular bridges). Interestingly, cytokinesis failure was not observed in this cell (Fig. 33D and E).

Altogether, these results suggest that intercellular bridges observed after SPD-1 inhibition are not a result of abrupt spindle poles separation.

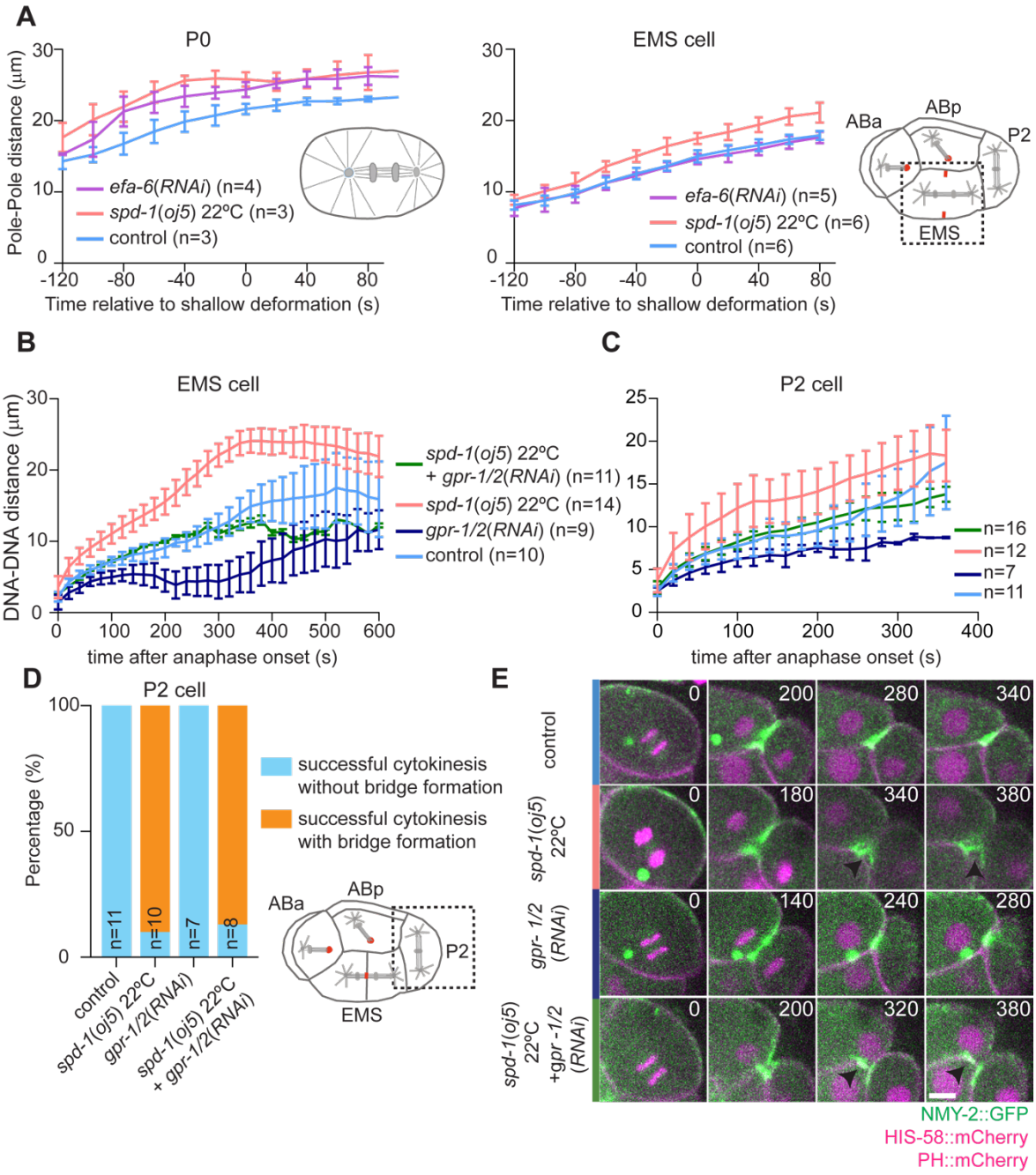

Figure 33- Bridges observed after SPD-1 inhibition are unlikely to be a consequence of abrupt spindle pole and DNA masses separation.

(A) Pole-to-pole distance plotted against time relative to shallow deformation in the P0 or EMS cell. Schematic on the right of each graph illustrates dividing P0 and EMS cell. The plasma membrane, microtubules, centrosomes, and DNA are represented in grey, the contractile ring is in red. **(B, C)** DNA-to-DNA distance in the EMS cell (B) or P2 cell (C) plotted against time after anaphase onset. **(D)** Percentage of P2 cells that completed cytokinesis after forming or not forming an intercellular bridge. Schematic on the right of each graph illustrates dividing P2 cell. The plasma membrane, microtubules, centrosomes, and DNA are represented in grey, the contractile ring is in red. **(E)** Images of time-lapse

videos of *spd-1(oj5)*, *gpr-1/2(RNAi)* and *gpr-1/2(RNAi);spd-1(oj5)* P2 cells co-expressing NMY-2::GFP to label the contractile ring, HIS-58::mCherry to label chromosomes, and PH::mCherry to label the plasma membrane (filmed at 22ºC). Black arrows point to intercellular bridges. Numbers on stills correspond to time is in seconds after anaphase onset. Scale bars, 5 µm. *n* is the number of embryos analyzed and error bars correspond to 95% CI in panels A-C.

CHAPTER VI

DISCUSSION AND CONCLUSIONS

Discussion and conclusions

The impact of central spindle microtubules during the second half of the cytokinetic ring constriction remains far from being completely elucidated.

In this thesis, we explored the changes that the contractile ring suffers when it approaches the bundled central spindle microtubules, primarily in the 4-cell *C. elegans* embryo. We observed that the ring suffers topological and molecular changes that include the increasing concentration of some contractile and central spindle proteins during the last phases of ring constriction. We also observed that the central spindle bundler SPD-1 influences anillin turnover in the contractile ring, and that the current list of PRC1/SPD-1 interactors is likely to include contractile ring, midzone, and abscission-related proteins. Results gathered from SPD-1 inhibition revealed that SPD-1 is required for successful cytokinesis and to prevent contractile ring broadening during the last phases of cytokinesis. In addition, our findings revealed that SPD-1 and ANI-1 cooperate to maintain myosin at the cleavage furrow to ensure cytokinesis completion. All of these conclusions will be further elaborated and discussed in the next sections.

23. SPD-1 contributes to molecular changes in the contractile ring during the second half of constriction

Midbody ring is the term given to the contractile ring when it stops constricting and has already compacted the central spindle. It has been previously described in *D. melanogaster* S2 cells that contractile ring to midbody ring transition involves molecular changes (Amine et al., 2013; Kechad, Jananji, and Ruella, 2012). We gathered evidence that the contractile ring starts changing at topological and molecular level when constriction is still under way. It was previously shown that contractile ring constriction slows down when this encounters the central spindle microtubules in *C. elegans* early embryonic cells (Carvalho, Desai and Oegema, 2009). We confirmed the same happens in the EMS cell (at approximately 72% of ingression). Moreover, our protein distribution analysis showed that ANI-1, CYK-4, UNC-59, and NMY-2 start to increase their levels at 69-85% of ingression and ring acquires a circular, rather than a more triangular shape at ~82% of ingression. In addition, we observed that ANI-1 turnover decreases during the second half of contractile ring constriction when SPD-1 is depleted by RNAi.

The fact that several changes occur in the contractile ring when it approaches the central spindle microtubules indicates that these microtubules and/or molecules that localize in the central spindle contribute to these changes.

24. SPD-1 putative interaction with contractile ring, midzone, and abscission proteins

Given that changes in the contractile ring were found to occur when this approaches the central spindle microtubules, we looked at the impact of depleting SPD-1 in contractile ring behaviour (section 27-29) and SPD-1 interacting partners (this section). In the context of a yeast two-hybrid screen we found that SPD-1 interacts with contractile ring ANI-1 and CYK-1 N-terminus, midzone CYK-4, PLK-1 and CLS-2, and the abscission protein TSG-101, but not with contractile ring UNC-59, UNC-61, NMY-2, MLC-4, and CYK-7 nor midzone ZEN-4, AIR-2, BIR-1, and CSC-1 (Fig. 15).

Some of these interactions, such as $PRC1^{SPD-1}$- $MgcRacGAP^{CYK-4}$, $PRC1^{SPD-1}$-$PLK1^{PLK-1}$, and $PRC1^{SPD-1}$-$CLASP^{CLS-2}$ have already been described in mouse, *C. elegans*, HeLa cells or *Xenopus* eggs, validating our screen (Ban et al., 2004; Hu et al., 2012a; Lee et al., 2015; Jing Liu et al., 2009; Neef et al., 2007; Patel et al., 2012).

An interaction between SPD-1 and TSG-101 has not been previously characterized. If confirmed, this interaction would have to be temporally regulated as TSG-101 pattern of localization and midbody accumulation is different from that of SPD-1. TSG-101 starts by accumulating at the midzone during the last phases of cytokinesis, and its levels progressively increase until they reach a plateau until abscission ends (König et al., 2017) *(*section 10). In contrast to depletion of TSG101 in HeLa cells, which leads to cell arrest at the midbody stage and cytokinesis failure (Carlton & Martin-Serrano, 2007; Garrus et al., 2001; Lu et al., 2003; Morita et al., 2007), the role of TSG-101 in the *C. elegans* embryo is not essential as its depletion delays midbody release but does not prevent abscission (Green et al., 2013). Thus, the cytokinesis failure observed in SPD-1 inactivated cells at 26ºC (Fig. 17) should not due to the absence of TSG-101.

Our yeast-two-hybrid results also revealed that SPD-1 can directly interact with the N-terminus of the formin CYK-1. If confirmed, more investigation will be necessary to understand the meaning of this interaction. One hypothesis is that SPD-1 anchors the central spindle to the contractile ring via CYK-1. To test this, we could in the future inactivate CYK-1 using an existing *cyk-1* temperature sensitive mutant during the last stages of cytokinesis and check if broadening of the contractile ring also occurs.

The interaction between SPD-1 and ANI-1 that we also detected is for now difficult to explain, since we saw a synergistic effect between the two proteins. If the interaction between the two proteins really exists in the context of cytokinesis then the phenotype of depleting one of them should be the same of depleting the other.

25. Midbodies in *C. elegans* EMS cells organize similarly to those in HeLa cells

Midbody structure has been widely characterized in HeLa cells and it consists of an extended structure that distances the sister cells apart. It is composed of three different regions: the midbody ring, the midbody core, and the midbody flanking arms (Elia et al., 2011; Hu et al., 2012b). In *C. elegans* embryos, dividing cells remain juxtaposed and the midbody cannot adopt an elongated configuration. Our analysis in the EMS cell however revealed that the distribution of midbody components is similar to that in HeLa cells.

Our data indicate that myosin and anillin persist at the tips of the cleavage furrow until constriction stops, and they adopt a more peripheral configuration than the identified midbody core proteins, which indicates that they localize at the midbody ring, in agreement with what was previously published in HeLa cells (Hu et al., 2012b; Kechad, Jananji, and Ruella, 2012; Wang, 2019). In HeLa cells, anillin and myosin are also observed next to the two presumptive abscission sites, external to the midbody arms, where they are responsible for constricting and narrowing the central spindle microtubules allowing for abscission to take place (Hu et al., 2012b; Wang, 2019). In contrast, we found no evidence that secondary ingression sites exist in the EMS cell midbody. Interestingly, we observed that the levels of ANI-1 and NMY-2, but not of CYK-1 nor actin, increase during the last steps of cytokinesis (Fig. 12). I could not find data in the literature reporting contractile ring protein levels during the last steps of cytokinesis in mammalian cells. The reason for the increase in anillin and myosin is still unclear, but inactivation of myosin at the very last stages of cleavage furrow ingression led to furrow regression, which indicates that myosin is required for the last steps of cytokinesis (also see section 17; Davies et al., 2014, 2018). However, ANI-1 depletion does not prevent embryonic cytokinesis (Maddox et al., 2005), indicating that the increase in ANI-1 levels is not critical for cytokinesis.

We show that the midbody core includes SPD-1, TSG-101, PLK-1, CYK-4, TBB-2, and AIR-2. SPD-1 localization at the midbody core was expected, as its human orthologue, PRC1, is known to localize at the midbody core in HeLa cells (Hu et al., 2012b). SPD-1 signal starts to fade 540± 61s after anaphase onset, contrasting with what happens to that of CYK-4 and AIR-2 that maintain their levels until the midbody is released. According to a recent publication in HeLa cells, midbody proteins can be divided into two distinct groups: 1) the transient midbody proteins, which accumulate but then slowly start to disappear, and 2) stable midbody proteins, whose levels do not vary during abscission (Halcrow et al., 2022). In that study, PRC1 and Aurora B were described to belong to the transient midbody group, supporting in part our results.

Aurora B and tubulin were found to localize at the midbody arms and midbody core. Our results revealed that AIR-2 signal extends from the midbody core to the adjacent regions (midbody arms) and, later, it fades from the midbody arms and accumulates only at the midbody core until the midbody is released. This partly contrasts with what was described in HeLa cells: Aurora B starts to accumulate at the midbody core after complete furrow ingression, and later is translocated to the midbody arms (Capalbo et al., 2019); as abscission completes, Aurora B is degraded from the midbody arms (Elia et al., 2012; Green, Paluch and Oegema, 2012; Gruneberg et al., 2004; Hu et al., 2012b) and does not accumulate at the midbody remnant (McNeely and Dwyer, 2020). In *C. elegans*, AIR-2 depletion prevents polar bodies extrusion, suggesting a role of AIR-2 during the last steps of cytokinesis (Schumacher et al., 1998).

The CYK-4 homologue in HeLa cells, MgcRacGAP, has been described to localize at the central spindle and in the midbody core as the central spindle compacts by the advance of the contractile ring (Elia et al., 2011). One study reported that MgcRacGAP translocates from the microtubules to the midbody ring in HeLa cells (Hu et al., 2012b), but we found no clear evidence for this in the EMS cell. We also observed a substantial increase in CYK-4 levels during the last stages of ring constriction. The relevance of this increase might be related to the described CYK-4/centralspindlin complex functions during the last phases of cytokinesis, including the recruitment of the abscission machinery and the anchoring of the plasma membrane to the midbody ring (Lekomtsev et al., 2012). In HeLa cells, centralspindlin recruits CEP55 to the midbody (Zhao et al., 2006), which, in turn, recruits its downstream effectors ALIX and TSG101. Although CEP55 is not conserved neither in *D. melanogaster* nor in *C. elegans*, it could still be possible that the *C. elegans* centralspindlin complex (namely, ZEN-4) directly interacts and recruits ALX-1 and TSG-101 to the midbody, allowing for successful cytokinesis, as described in *D. melanogaster* S2 and female germline stem cells (Lie-Jensen et al., 2019). Beyond recruiting abscission effectors, MgcRacGAP also anchors the midbody to the plasma membrane through its C1 domain, in HeLa kyoto cells (Lekomtsev et al., 2012): mutants that disrupt the MgcRacGAP C1 domain can recruit midbody proteins, but cause the detachment of the plasma membrane from the midbody, leading to furrow regression after midbody formation (Lekomtsev et al., 2012).

TSG-101 was proposed to localize in the midbody ring in *C. elegans* 1-cell embryos in the absence of central spindle microtubules (Green et al., 2013). Our yeast-two-hybrid results revealed that SPD-1 can interact with TSG-101, as was discussed in section 24, and this interaction may be responsible for TSG-101 localization at the midbody core.

In HeLa cells, PLK1 is known to prevent CEP-55 recruitment to the midbody, which together with ALX-1 are responsible for recruiting the ESCRT machinery to the midbody

(Bastos and Barr, 2010). Thus, PLK1 levels at the midbody must drop for abscission to take place in HeLa cells. According to this, our data in the EMS cell indicate that PLK-1 accumulates at the midbody core and its signal starts to decrease 537±87s after anaphase onset. Our data indicate that PLK-1, like SPD-1, belongs to the group of proteins that transiently localize to the midbody (Halcrow et al., 2022).

In sum, the midbody in the EMS shares organizational similarities to that in HeLa cells, however, some differences exist that might rely upon distinct evolutionary mechanisms.

26. Central spindle organization requirements are not exactly the same in the P0 and EMS cells

Midzone architecture has been mostly studied in unicellular contexts (Wadsworth, 2021). Our analysis in the *C. elegans* EMS cell revealed characteristics of the central spindle that are distinct from those in the P0 cell (zygote).

Both in the P0 and EMS cells, SPD-1 inhibition led to the abrupt separation of the two centrosomes, because of unbundling of the central spindle microtubules. In contrast, the impact of perturbing the CYK-4-SPD-1 interaction or EFA-6 is different between the two cells: expression of CYK-4(Δtail) or CYK-4(EAE) mutants or depletion of EFA-6 (Lee et al., 2015) lead to an affected pole-to-pole distance in P0 cells, but not in EMS cells. Moreover, the CYK-4-SPD-1 interaction is essential for midzone assembly and cytokinesis completion in P0 cells, but not in the EMS cell. As far as I am aware these differences had not been previously reported in the literature and they may be due to cell-intrinsic and/or cell-extrinsic mechanisms (Davies et al., 2018; Ozugergin et al., 2022). Indeed, a thorough study of single-cell transcripts in *C. elegans* embryos showed differences between cells (Tintori, et al., 2016). The fact that the EMS cell establishes contacts with neighboring cells may also be a factor.

Altogether, this indicates that the organization or properties of the central spindle/cytokinesis in the EMS cell is different from that in the 1-cell embryo but further studies will be needed to elucidate the mechanisms.

27. SPD-1 is required for robust cytokinesis in the *C. elegans* early embryo

Our analysis of the temperature-sensitive *spd-1(oj5)* allele using a device for fast and reliable temperature control clarifies that penetrant inactivation of SPD-1, i.e. *spd-1(oj5)* at 26°C, results in frequent cytokinesis failure in all cells of the *C. elegans* early embryo. The consistent cytokinesis success that we observed after RNAi-mediated depletion of

SPD-1 correlated with residual microtubule bundles traversing the furrow region, which indicates that RNAi is not sufficiently penetrant to reveal SPD-1's requirement for cytokinesis. This idea is further supported by the observations that the phenotype of *spd-1(RNAi)* resembled that of *spd-1(oj5)* at the semi-restrictive temperature (22°C). The EMS cell of the 4-cell embryo was the most sensitive to SPD-1 inhibition, which is in agreement with the study that initially characterized the *spd-1(oj5)* mutant (Verbrugghe and White, 2004). The reason why EMS is more sensitive to SPD-1 inhibition is not clear and contrasts with the finding that EMS is more resistant to cytokinesis failure than ABa and ABp following formin (CYK-1) inactivation or Latrunculin A treatment (Davies et al., 2018). Protection against cytokinesis failure after actin perturbation in the EMS cell was found to be mediated by extrinsic regulation through Wnt/Src signaling and direct contact with the neighboring P2 cell. Our observations indicate that Wnt signaling originating from the P2 cell is unaffected after SPD-1 inactivation because spindle positioning, division axis orientation, and the extent of EMS-P2 contact appeared normal (Walston and Hardin, 2006; Zhang et al., 2008; Sugioka and Bowerman, 2018). In addition, we observed the same sensitivity to SPD-1 inactivation when inactivation was acutely inflicted during furrow ingression, past the time when Wnt signaling is thought to be critical. It remains, however, possible that the Wnt signaling pathway does have a function during late cytokinesis and that this function is perturbed when the central spindle and the midbody cannot form after acute SPD-1 inactivation. In fact, Wnt and Src effectors have been localize to the midbody in tissue culture cells (Fumoto et al., 2012; Kikuchi et al., 2010; Kaplan et al., 2004; Kasahara et al., 2007; Yu et al., 2021). Alternatively, the increased sensitivity of EMS to SPD-1 inactivation may be related to intrinsic cell-lineage-specific characteristics. In this latter case EMS descendants should also display increased sensitivity to SPD-1 inactivation, which remains to be determined.

28. Residual SPD-1 activity is required to ensure membrane sealing at the end of cytokinesis

Embryonic cytokinesis typically occurs with a back-to-back configuration of the cleavage furrow, which results in tightly juxtaposed sister cells. Intercellular bridges that separate sister cells during the last stages of cleavage furrow ingression are therefore minimal in normal embryos. Our findings reveal that full or partial inhibition of SPD-1 results in long intercellular bridges that start to form at ~90% furrow ingression, which suggests that interactions between the tip of the furrow and the compacting spindle midzone are required to maintain a tight furrow during the last stages of cytokinesis. As elongated bridges form in several cells with distinct shapes, identities and number of cell-cell

interactions, it is unlikely that they arise from pulling forces acting on the EMS cell poles. Indeed, our experiments show that elongated bridges still form in SPD-1 partially inactivated embryos where the cortical pulling forces were decreased to avoid abrupt pole separation, by depletion of the cortical anchors GPR-1 and GPR-2. Elongated bridges could also form because of the defective interaction between SPD-1 and CYK-4, since the mutation present in *spd-1(oj5)* significantly decreases it (Lee et al., 2015). However, we showed that the inverse mutants of CYK-4 whose interaction with SPD-1 is significantly decreased (*cyk-4(Δtail)* or *cyk-4(EAE)*) did not form elongated bridges during the last stages of cytokinesis. Another possibility is that broadening of the contractile ring is caused by broadening of the RhoA active signal during late ring constriction. However, our experiments with *spd-1(oj5)* embryos expressing the RhoA biosensor that consists of the anillin C-terminus (AHPH::GFP) did not reveal any increase in signal (data not shown). An attractive possibility that we did not test is that SPD-1 inhibition compromises the adhesion between the two sides of the furrow. How midzone microtubules, SPD-1 or other midzone components would contribute will require further investigation. Of note, we find that partial inhibition of SPD-1 leads to elongation of the intercellular bridge but the increased distance between the sister cells is transient as these eventually juxtapose. This suggests that any defects in establishing cell-cell adhesions is only temporary in this condition.

In the SPD-1-inhibited EMS, we find contractile ring components are tightly localized to the tip of the ingressing furrow but become subsequently broadly distributed along the entire length of the intercellular bridge and beyond. If SPD-1 is penetrantly inhibited, bridge thinning is followed by myosin/anillin signal fragmentation until no signal is detectable, which precedes furrow regression. When SPD-1 is partially inhibited, which allows cytokinesis to complete, some myosin and anillin remain enriched at a mini-midbody within the intercellular bridge. Thus, our data suggest that the presence of a residual mini-midbody is critical to ensure complete sealing during abscission, which is a prerequisite for successful completion of cytokinesis. However, it has previously been reported that abscission does not require central spindle microtubules and that the midbody ring is sufficient to scaffold the abscission machinery in the *C. elegans* 1-cell embryo (P0) (König et al. 2017; Green et al. 2013). To test the requirement for microtubules, both Green et al. and Konig et al. used *spd-1(RNAi)*, which our results suggest may not completely prevent microtubule bundle formation at the midzone. Whether the contrasting conclusions regarding the requirement of a midbody for abscission reflect inherent differences between P0 and EMS will require further investigation. We show that the formation of an elongated intercellular bridge after SPD-1 inhibition is not EMS-specific but mini-midbody formation could only be examined in EMS, where the position and orientation of the bridge facilitated this type of analysis.

Electron tomographic reconstruction of late cytokinesis in the 1- and 4-cell embryo after full SPD-1 inactivation using *spd-1(oj5)* would be required to gain further insight into this issue.

29. Anillin and SPD-1-bundled midzone microtubules act redundantly to maintain myosin in the cleavage furrow during late cytokinesis

We previously showed that myosin motor activity is required for cytokinesis in the *C. elegans* 1-cell embryo (Osório et al. 2019). Using fast inactivation of a myosin temperature sensitive mutant, we now show that myosin is required for continuous furrow ingression: the moment myosin is inactivated, furrow ingression stalls and is followed by furrow regression. It is known that RhoA activation is required to recruit active myosin to the cell equator when furrowing initiates (Pollard and O'Shaughnessy 2019). Our data reveal that this initial myosin loading step is not sufficient to complete cytokinesis. ANI-1 and SPD-1 act redundantly in EMS to maintain myosin in the contractile ring during the second half of furrow ingression. While cytokinesis completes when SPD-1 is partially inactivated or when ANI-1 is depleted by RNAi, cytokinesis fails when the two perturbations are combined: furrow ingression advances to final stages (97% ingression) but myosin progressively disappears from the intercellular bridge, which loses the ability to keep thinning and elongating, and eventually the furrow regresses. When ANI-1 is depleted in the background of penetrant SPD-1 inactivation, myosin disappears from the contractile ring earlier (70% ingression). Our data therefore supports the idea that myosin-mediated contractility is required until the end of cytokinesis, and that anillin in the contractile ring and SPD-1-bundled midzone microtubules jointly ensure that myosin is maintained/activated at the tip of the furrow during late cytokinesis. As myosin levels at the cleavage furrow have been shown to be a good proxy for RhoA activation (Zhang and Glotzer 2015b), it is likely that myosin's disappearance from the furrow region reflects RhoA inactivation. Indeed, both ANI-1 and midzone microtubules participate in RhoA activation. Anillin stabilizes active RhoA at the membrane, increasing its residency time to engage with effectors (Budnar et al. 2019) and is required for stable RhoA signal (Reyes et al. 2014). The centralspindlin component CYK-4, which localizes to midzone microtubule bundles, is required for ECT-2-mediated RhoA activation at the cleavage furrow, and its inactivation leads to a substantial decrease in active RhoA and myosin levels in the contractile ring and to furrow regression (Burkard et al. 2009; Wolfe et al. 2009; Basant et al. 2015; Lewellyn et al. 2011; Canman et al. 2008; Tse et al. 2012; Gómez-Cavazos et al. 2020; D. Zhang and Glotzer 2015b). As both anillin and SPD-1 interact with CYK-4 (Lee et al. 2018; Ban et al. 2004; Fu et al. 2009; D'Avino et al. 2008; Gregory et al. 2008), it is conceivable that co-inhibition of ANI-1 and

SPD-1 directly perturbs CYK-4 activity (i.e. independently of SPD-1's role in central spindle formation), preventing it from activating RhoA during the second half of constriction. Unfortunately, it was not feasible to monitor RhoA activity using the biosensor that is available for *C. elegans*, because this sensor consists of a C-terminal ANI-1 fragment (Tse et al. 2012), and cannot be used to address RhoA behavior when the effects of anillin depletion are being investigated. Another possible explanation for myosin's disappearance from the furrow region is that the contractile ring loses attachment to the membrane, as both ANI-1 and CYK-4 contain elements that associate directly with the membrane at the cleavage furrow (Lekomtsev et al. 2012; Sun et al. 2015).

It has been proposed that the contractile ring transitions into a midbody ring through molecular changes that occur at a late stage when the contractile ring is almost fully closed (~1 µm in *D.melanogaster* S2 cells) (Kechad et al. 2012). Anillin is thought to be required to template midbody ring assembly and to ensure stable anchoring of the midbody ring to the plasma membrane (Kechad et al. 2012). Our results raise the possibility that anillin-dependent molecular changes already occur when the contractile ring comes into contact with the spindle midzone. Indeed, the constriction rate decreases at 72% ingression in control EMS cells when the furrow encounters the midzone, and ANI-1 depletion considerably prolongs the last phase of furrow ingression even when midzone microtubules are reduced and therefore represent less of an obstacle (Carvalho, Desai, and Oegema 2009). The fact that depletion of ANI-1 and complete removal of midzone microtubule bundling stalls constriction at the point when the constricting ring would normally encounter the spindle midzone indicates that contact between the two structures ensures continuation of ingression. Since the spindle midzone has different dimensions in tissue culture cells versus embryonic cells, the timing of contractile ring maturation during furrow ingression may vary between cell types.

CHAPTER VI

REFERENCES

References

Adams, Richard R., Helder Maiato, William C. Earnshaw, and Mar Carmena. 2001. "Essential Roles of Drosophila Inner Centromere Protein (INCENP) and Aurora B in Histone H3 Phosphorylation, Metaphase Chromosome Alignment, Kinetochore Disjunction, and Chromosome Segregation." *Journal of Cell Biology* 153 (4): 865–79. https://doi.org/10.1083/jcb.153.4.865.

Adams, Richard R., Alvaro A.M. Tavares, Adi Salzberg, Hugo J. Bellen, and David M. Glover. 1998. "Pavarotti Encodes a Kinesin-Like Protein Required To Organize the Central Spindle and Contractile Ring for Cytokinesis." *Genes and Development* 12 (10): 1483–94. https://doi.org/10.1101/gad.12.10.1483.

Adell, Manuel Alonso Y., Georg F. Vogel, Mehrshad Pakdel, Martin Müller, Herbert Lindner, Michael W. Hess, and David Teis. 2014. "Coordinated Binding of Vps4 to ESCRT-III Drives Membrane Neck Constriction during MVB Vesicle Formation." *Journal of Cell Biology* 205 (1): 33–49. https://doi.org/10.1083/jcb.201310114.

Adriaans, Ingrid E., Angika Basant, Bas Ponsioen, Michael Glotzer, and Susanne M.A. Lens. 2019. "PLK1 Plays Dual Roles in Centralspindlin Regulation during Cytokinesis." *Journal of Cell Biology* 218 (4): 1250–64. https://doi.org/10.1083/jcb.201805036.

Agromayor, Monica, Jez G. Carlton, John P. Phelan, Daniel R. Matthews, Leo M. Carlin, Simon Ameer-Beg, Katherine Bowers, and Juan Martin-Serrano. 2009. "Essential Role of HIST1 in Cytokinesis Monica." *Molecular Biology of the Cell* 20: 1374–87. https://doi.org/10.1091/mbc.E08.

Ainsztein, Alexandra M., Stefanie E. Kandels-Lewis, Alastair M. Mackay, and William C. Earnshaw. 1998. "INCENP Centromere and Spindle Targeting: Identification of Essential Conserved Motifs and Involvement of Heterochromatin Protein HP1." *Journal of Cell Biology* 143 (7): 1763–74. https://doi.org/10.1083/jcb.143.7.1763.

Aist, J. R., C. J. Bayles, W. Tao, and M. W. Berns. 1991. "Direct Experimental Evidence for the Existence, Structural Basis and Function of Astral Forces during Anaphase B in Vivo." *Journal of Cell Science* 100 (2): 279–88. https://doi.org/10.1242/jcs.100.2.279.

Amine, Nour El, Amel Kechad, Silvana Jananji, and Gilles R.X. Hickson. 2013. "Opposing Actions of Septins and Sticky on Anillin Promote the Transition from Contractile to Midbody Ring." *Journal of Cell Biology* 203 (3): 487–504. https://doi.org/10.1083/jcb.201305053.

Arnold, Torey R., Rachel E. Stephenson, and Ann L. Miller. 2017. "Rho GTPases and Actomyosin: Partners in Regulating Epithelial Cell-Cell Junction Structure and Function." *Experimental Cell Research* 358 (1): 20–30. https://doi.org/10.1016/j.yexcr.2017.03.053.

Bajorek, Monika, Heidi L. Schubert, John McCullough, Charles Langelier, Debra M. Eckert,

William May B. Stubblefield, Nathan T. Uter, David G. Myszka, Christopher P. Hill, and Wesley I. Sundquist. 2009. “Structural Basis for ESCRT-III Protein Autoinhibition.” *Nature Structural and Molecular Biology* 16 (7): 754–62. https://doi.org/10.1038/nsmb.1621.

Ban, Reiko, Yasuhiro Irino, Kiyoko Fukami, and Hirofumi Tanaka. 2004. “Human Mitotic Spindle-Associated Protein PRC1 Inhibits MgcRacGAP Activity toward Cdc42 during the Metaphase.” *Journal of Biological Chemistry* 279 (16): 16394–402. https://doi.org/10.1074/jbc.M313257200.

Barbosa, Daniel J., Vanessa Teixeira, Joana Duro, Ana X. Carvalho, and Reto Gassmann. 2021. “Dynein-Dynactin Segregate Meiotic Chromosomes in C. Elegans Spermatocytes.” *Development (Cambridge)* 148 (3). https://doi.org/10.1242/dev.197780.

Basant, Angika, and Michael Glotzer. 2018. “Spatiotemporal Regulation of RhoA during Cytokinesis.” *Current Biology* 28 (9): R570–80. https://doi.org/10.1016/j.cub.2018.03.045.

Basant, Angika, Sergey Lekomtsev, Yu Chung Tse, Donglei Zhang, Katrina M. Longhini, Mark Petronczki, and Michael Glotzer. 2015a. “Aurora B Kinase Promotes Cytokinesis by Inducing Centralspindlin Oligomers That Associate with the Plasma Membrane.” *Developmental Cell* 33 (2): 204–15. https://doi.org/10.1016/j.devcel.2015.03.015.

Bassi, Zuni I., Morgane Audusseau, Maria Giovanna Riparbelli, Giuliano Callaini, and Pier Paolo D’Avino. 2013. “Citron Kinase Controls a Molecular Network Required for Midbody Formation in Cytokinesis.” *Proceedings of the National Academy of Sciences of the United States of America* 110 (24): 9782–87. https://doi.org/10.1073/pnas.1301328110.

Bastos, Ricardo Nunes, and Francis A. Barr. 2010. “Plk1 Negatively Regulates Cep55 Recruitment to the Midbody to Ensure Orderly Abscission.” *Journal of Cell Biology* 191 (4): 751–60. https://doi.org/10.1083/jcb.201008108.

Bastos, Ricardo Nunes, Sapan R. Gandhi, Ryan D. Baron, Ulrike Gruneberg, Erich A. Nigg, and Francis A. Barr. 2013. “Aurora B Suppresses Microtubule Dynamics and Limits Central Spindle Size by Locally Activating KIF4A.” *Journal of Cell Biology* 202 (4): 605–21. https://doi.org/10.1083/jcb.201301094.

Bembenek, Joshua N., Koen J.C. Verbrugghe, Jayshree Khanikar, Györgyi Csankovszki, and Raymond C. Chan. 2013. “Condensin and the Spindle Midzone Prevent Cytokinesis Failure Induced by Chromatin Bridges in C. Elegans Embryos.” *Current Biology* 23 (11): 937–46. https://doi.org/10.1016/j.cub.2013.04.028.

Bement, William M., Hélène A. Benink, and George Von Dassow. 2005. “A Microtubule-Dependent Zone of Active RhoA during Cleavage Plane Specification.” *Journal of Cell*

Biology 170 (1): 91–101. https://doi.org/10.1083/jcb.200501131.

Berlin, Ana, Anne Paoletti, and Fred Chang. 2003. “Mid2p Stabilizes Septin Rings during Cytokinesis in Fission Yeast.” *Journal of Cell Biology* 160 (7): 1083–92. https://doi.org/10.1083/jcb.200212016.

Biron, D., P. Libros, D. Sagi, D. Mirelman, and E. Moses. 2004. “Biphasic Cytokinesis and Cooperative Single Cell Reproduction. In Forces, Growth and Form in Soft Condensed Matter: At the Interface between Physics and Biology.” *Berlin:Springer*, 217–234.

Blanchoin, Laurent, Rajaa Boujemaa-Paterski, Cécile Sykes, and Julie Plastino. 2014. “Actin Dynamics, Architecture, and Mechanics in Cell Motility.” *Physiological Reviews* 94 (1): 235–63. https://doi.org/10.1152/physrev.00018.2013.

Bonaccorsi, Silvia, Maria Grazia Giansanti, and Maurizio Gatti. 1998. “Spindle Self-Organization and Cytokinesis during Male Meiosis in Asterless Mutants of Drosophila Melanogaster.” *Journal of Cell Biology* 142 (3): 751–61. https://doi.org/10.1083/jcb.142.3.751.

Brennan, IM, U Peters, TM Kapoor, and AF. Straight. 2007. “Polo-like Kinase Controls Vertebrate Spindle Elongation and Cytokinesis.” *PloS One*.

Bringmann, Henrik, Carrie R. Cowan, Jun Kong, and Anthony A. Hyman. 2007. “LET-99, GOA-1/GPA-16, and GPR-1/2 Are Required for Aster-Positioned Cytokinesis.” *Current Biology* 17 (2): 185–91. https://doi.org/10.1016/j.cub.2006.11.070.

Bringmann, Henrik, and Anthony A. Hyman. 2005. “A Cytokinesis Furrow Is Positioned by Two Consecutive Signals.” *Nature* 436 (7051): 731–34. https://doi.org/10.1038/nature03823.

Brust-Mascher, I., G. Civelekoglu-Scholey, M. Kwon, A. Mogilner, and J. M. Scholey. 2004. “Model for Anaphase B: Role of Three Mitotic Motors in a Switch from Poleward Flux to Spindle Elongation.” *Proceedings of the National Academy of Sciences of the United States of America* 101 (45): 15938–43. https://doi.org/10.1073/pnas.0407044101.

Brust-Mascher, I., P. Sommi, D.K. Cheerambathur, and J.M. Scholey. 2009. “Kinesin-5-Dependent Poleward Flux and Spindle Length Control in Drosophila Embryo Mitosis.” *Mol. Biol. Cell* 20: 1749–1762. https://doi.org/10.1091/mbc.E08.

Budirahardja, Yemima, and Pierre Gönczy. 2008. “PLK-1 Asymmetry Contributes to Asynchronous Cell Division of C . Elegans Embryos.” *Development* 1313: 1303–13. https://doi.org/10.1242/dev.019075.

Budnar, Srikanth, Kabir B. Husain, Guillermo A. Gomez, Maedeh Naghibosadat, Amrita Varma, Suzie Verma, Nicholas A. Hamilton, Richard G. Morris, and Alpha S. Yap. 2019. “Anillin Promotes Cell Contractility by Cyclic Resetting of RhoA Residence Kinetics.” *Developmental Cell* 49 (6): 894-906.e12. https://doi.org/10.1016/j.devcel.2019.04.031.

Burkard, Mark E, John Maciejowski, Verónica Rodriguez-Bravo, Michael Repka, Drew M Lowery, Karl R. Clauser, Chai Zhang, et al. 2009. “Plk1 Self-Organization and Priming Phosphorylation of HsCYK-4 at The.” *PLoS Biology* 7 (5). https://doi.org/10.1371/journal.pbio.1000111.

Burkard, ME, CL Randall, S Larochelle, C Zhang, and et al. Shokat, KM. 2007. “Chemical Genetics Reveals the Requirement for Polo-like Kinase 1 Activity in Positioning RhoA and Triggering Cytokinesis in Human Cells.” *Proc. Natl. Acad. Sci. USA* 104: 4383–88.

Cande, W Zacheus, and Kent L McDonald. 1985. “In Vitro Reactivation of Anaphase Spindle Elongation Using Isolated Diatom Spindles.” *Nature* 316 (6024): 168–70. https://doi.org/10.1038/316168a0.

Canman, Julie C., Arshad Desai, Bruce Bowerman, and Karen Oegema. 2008. “Activity of Centralspindlin Is Essential for Cytokinesis.” *Science*, no. December: 1543–46. https://doi.org/10.1126/science.1163086.

Canman, Julie C, Lindsay Lewellyn, Kimberley Laband, Stephen J Smerdon, Bruce Bowerman, and Karen Oegema. 2009. “Inhibition of Rac by the GAP Activity of Centralspindlin Is Essential for Cytokinesis.” *Science* 322 (5907): 1543–46. https://doi.org/10.1126/science.1163086.Inhibition.

Capalbo, Luisa, Zuni I. Bassi, Marco Geymonat, Sofia Todesca, Liviu Copoiu, Anton J. Enright, Giuliano Callaini, et al. 2019. “The Midbody Interactome Reveals Unexpected Roles for PP1 Phosphatases in Cytokinesis.” *Nature Communications* 10 (1). https://doi.org/10.1038/s41467-019-12507-9.

Carlton, Jez G., Jeremy, Anna Caballe, Monica Agromayor, Magdalena Kloc, and Juan Martin-Serrano. 2012. “ESCRT-III Governs the Aurora B–Mediated Abscission Checkpoint Through CHMP4C.” *Science* 336: 220–25.

Carlton, Jez G., and Juan Martin-Serrano. 2007. “Parallels between Cytokinesis and Retroviral Budding: A Role for the ESCRT Machinery.” *Science* 316 (5833): 1908–12. https://doi.org/10.1126/science.1143422.

Carmena, Mar, Sandrine Ruchaud, and William C. Earnshaw. 2009. “Making the Auroras Glow: Regulation of Aurora A and B Kinase Function by Interacting Proteins.” *Current Opinion in Cell Biology* 21 (6): 796–805. https://doi.org/10.1016/j.ceb.2009.09.008.

Carmena, Mar, Michael Wheelock, Hironori Funabiki, and William C. Earnshaw. 2012. “The Chromosomal Passenger Complex (CPC): From Easy Rider to the Godfather of Mitosis.” *Nature Reviews Molecular Cell Biology* 13 (12): 789–803. https://doi.org/10.1038/nrm3474.

Carvalho, Ana, Mar Carmena, Clara Sambade, William C. Earnshaw, and Sally P. Wheatley. 2003. “Survivin Is Required for Stable Checkpoint Activation in Taxol-

Treated HeLa Cells." *Journal of Cell Science* 116 (14): 2987–98. https://doi.org/10.1242/jcs.00612.

Carvalho, Ana, Arshad Desai, and Karen Oegema. 2009. "Structural Memory in the Contractile Ring Makes the Duration of Cytokinesis Independent of Cell Size." *Cell* 137 (5): 926–37. https://doi.org/10.1016/j.cell.2009.03.021.

Carvalho, Ana, Sara K Olson, Edgar Gutierrez, Kelly Zhang, Lisa B Noble, Esther Zanin, Alex Groisman, and Karen Oegema. 2011. "Acute Drug Treatment in the Early C . Elegans Embryo." *PloS One* 6 (9). https://doi.org/10.1371/journal.pone.0024656.

Cassada, R. C., and R. L. Russell. 1975. "The Dauer Larva, a Post-Embryonic Developmental Variant of the Nematode Caenorhabditis Elegans." *In Developmental Biology* 46 (2): 326–342.

Chai, Yongping, Dong Tian, Yihong Yang, Guoxin Feng, Ze Cheng, Wei Li, and Guangshuo Ou. 2012. "Apoptotic Regulators Promote Cytokinetic Midbody Degradation in C. Elegans." *Journal of Cell Biology* 199 (7): 1047–55. https://doi.org/10.1083/jcb.201209050.

Chan, Fung Yi, Ana M. Silva, Joana Saramago, Joana Pereira-Sousa, Hailey E. Brighton, Marisa Pereira, Karen Oegema, Reto Gassmann, and Ana Xavier Carvalho. 2019. "The ARP2/3 Complex Prevents Excessive Formin Activity during Cytokinesis." *Molecular Biology of the Cell* 30 (1): 96–107. https://doi.org/10.1091/mbc.E18-07-0471.

Chang-Jie, J., and S. Sonobe. 1993. "Identification and Preliminary Characterization of a 65 KDa Higher-Plant Microtubule-Associated Protein." *Journal of Cell Science* 105 (4): 891–901.

Cheerambathur, Dhanya K., Gul Civelekoglu-Scholey, Ingrid Brust-Mascher, Patrizia Sommi, Alex Mogilner, and Jonathan M. Scholey. 2007. "Quantitative Analysis of an Anaphase B Switch: Predicted Role for a Microtubule Catastrophe Gradient." *Journal of Cell Biology* 177 (6): 995–1004. https://doi.org/10.1083/jcb.200611113.

Chen, A., P. D. Arora, C. A. McCulloch, and A. Wilde. 2017. "Cytokinesis Requires Localized β-Actin Filament Production by an Actin Isoform Specific Nucleator." *Nature Communications* 8 (1). https://doi.org/10.1038/s41467-017-01231-x.

Chen, Chun-Ting, Andreas W. Ettinger, Wieland B. Huttner, and Stephen J. Doxsey. 2013. "Resurrecting Remnants: The Lives of Post-Mitotic Midbodies." *Trends in Cell Biology* 23 (3): 118–28. https://doi.org/10.1016/j.tcb.2012.10.012.

Chen, Wei, Margit Foss, Kuo Fu Tseng, and Dahong Zhang. 2008. "Redundant Mechanisms Recruit Actin into the Contractile Ring in Silkworm Spermatocytes." *PLoS Biology* 6 (9): 1927–41. https://doi.org/10.1371/journal.pbio.0060209.

Chircop, Megan. 2014. "Rho GTPases as Regulators of Mitosis and Cytokinesis in

Mammalian Cells." *Small GTPases* 5 (JUL). https://doi.org/10.4161/sgtp.29770.

Christ, Liliane, Camilla Raiborg, Eva M Wenzel, Coen Campsteijn, and Harald Stenmark. 2017. "Cellular Functions and Molecular Mechanisms of the ESCRT Membrane-Scission Machinery." *Trends in Biochemical Sciences* 42 (1): 42–56. https://doi.org/10.1016/j.tibs.2016.08.016.

Christ, Liliane, Eva M. Wenzel, Knut Liestøl, Camilla Raiborg, Coen Campsteijn, and Harald Stenmark. 2016. "ALIX and ESCRT-I/II Function as Parallel ESCRT-III Recruiters in Cytokinetic Abscission." *Journal of Cell Biology* 212 (5): 499–513. https://doi.org/10.1083/jcb.201507009.

Collins, Elizabeth, Barbara J. Mann, and Patricia Wadsworth. 2014. "Eg5 Restricts Anaphase B Spindle Elongation in Mammalian Cells." *Cytoskeleton* 71 (2): 136–44. https://doi.org/10.1002/cm.21158.

Conte, Darryl, Lesley T. MacNei, Albertha J.M. Walhout, and Craig C. Mello. 2015. *RNA Interference in Caenorhabditis Elegans*. *Current Protocols in Molecular Biology*. Vol. 2015. https://doi.org/10.1002/0471142727.mb2603s109.

Corsi, A. K., B. Wightman, and M. Chalfie. 2015. "A Transparent Window into Biology: A Primer on Caenorhabditis Elegans." *Genetics* 200 (2): 387–407.

Courthéoux, Thibault, David Reboutier, Thibaut Vazeille, Jean-Yves Cremet, Christelle Benaud, Isabelle Vernos, and Claude Prigent. 2019. "Microtubule Nucleation during Central Spindle Assembly Requires NEDD1 Phosphorylation on Serine 405 by Aurora A." *Journal of Cell Science* 132 (10): jcs231118. https://doi.org/10.1242/jcs.231118.

Cowan, Carrie R., and Anthony A. Hyman. 2004. "Asymmetric Cell Division in C. Elegans: Cortical Polarity and Spindle Positioning." *Annual Review of Cell and Developmental Biology* 20: 427–53. https://doi.org/10.1146/annurev.cellbio.19.111301.113823.

D'Avino, Pier Paolo. 2009. "How to Scaffold the Contractile Ring for a Safe Cytokinesis - Lessons from Anillin-Related Proteins." *Journal of Cell Science* 122 (8): 1071–79. https://doi.org/10.1242/jcs.034785.

D'Avino, Pier Paolo, Tetsuya Takeda, Luisa Capalbo, Wei Zhang, Kathryn S. Lilley, Ernest D. Laue, and David M. Glover. 2008. "Interaction between Anillin and RacGAP50C Connects the Actomyosin Contractile Ring with Spindle Microtubules at the Cell Division Site." *Journal of Cell Science* 121 (8): 1151–58. https://doi.org/10.1242/jcs.026716.

Dambournet, Daphné, Mickael MacHicoane, Laurent Chesneau, Martin Sachse, Murielle Rocancourt, Ahmed El Marjou, Etienne Formstecher, Rémi Salomon, Bruno Goud, and Arnaud Echard. 2011. "Rab35 GTPase and OCRL Phosphatase Remodel Lipids and F-Actin for Successful Cytokinesis." *Nature Cell Biology* 13 (8): 981–88. https://doi.org/10.1038/ncb2279.

Daniel, Emeline, Marion Daud, Irina Kolotuev, Kristi Charish, Vanessa Auld, and Roland Le Borgne. 2018. “Coordination of Septate Junctions Assembly and Completion of Cytokinesis in Proliferative Epithelial Article Coordination of Septate Junctions Assembly and Completion of Cytokinesis in Proliferative Epithelial Tissues,” 1380–91. https://doi.org/10.1016/j.cub.2018.03.034.

Dassow, George Von, Koen J.C. Verbrugghe, Ann L. Miller, Jenny R. Sider, and William M. Bement. 2009. “Action at a Distance during Cytokinesis.” *Journal of Cell Biology* 187 (6): 831–45. https://doi.org/10.1083/jcb.200907090.

Davies, Tim, S. Sundaramoorthy, S. N. Jordan, M. Shirasu-Hiza, J. Dumont, and J. C. Canman. 2017. *Using Fast-Acting Temperature-Sensitive Mutants to Study Cell Division in Caenorhabditis Elegans*. *Methods in Cell Biology*. Vol. 137. Elsevier Ltd. https://doi.org/10.1016/bs.mcb.2016.05.004.

Davies, Tim, Shawn N. Jordan, Vandana Chand, Jennifer A. Sees, Kimberley Laband, Ana X. Carvalho, Mimi Shirasu-Hiza, David R. Kovar, Julien Dumont, and Julie C. Canman. 2014. “High-Resolution Temporal Analysis Reveals a Functional Timeline for the Molecular Regulation of Cytokinesis.” *Developmental Cell* 30 (2): 209–23. https://doi.org/10.1016/j.devcel.2014.05.009.

Davies, Tim, Han X. Kim, Natalia Romano Spica, Benjamin J. Lesea-Pringle, Julien Dumont, Mimi Shirasu-Hiza, and Julie C. Canman. 2018. “Cell-Intrinsic and -Extrinsic Mechanisms Promote Cell-Type-Specific Cytokinetic Diversity.” *ELife* 7: 1–30. https://doi.org/10.7554/eLife.36204.

Dechant, Reinhard, and Michael Glotzer. 2003. “Centrosome Separation and Central Spindle Assembly Act in Redundant Pathways That Regulate Microtubule Density and Trigger Cleavage Furrow Formation.” *Developmental Cell* 4 (3): 333–44. https://doi.org/10.1016/S1534-5807(03)00057-1.

Desai, Arshad, and Timothy J. Mitchison. 1997. “Microtubule Polymerization Dynamics.” *Annual Review of Cell and Developmental Biology* 13: 83–117. https://doi.org/10.1146/annurev.cellbio.13.1.83.

Dickinson, Daniel J., Francoise Schwager, Lionel Pintard, Monica Gotta, and Bob Goldstein. 2017. “A Single-Cell Biochemistry Approach Reveals PAR Complex Dynamics during Cell Polarization.” *Developmental Cell* 42 (4): 416-434.e11. https://doi.org/10.1016/j.devcel.2017.07.024.

Ding, Wei Yung, Hui Ting Ong, Yusuke Hara, Jantana Wongsantichon, Yusuke Toyama, Robert C. Robinson, François Nédélec, and Ronen Zaidel-Bar. 2017. “Plastin Increases Cortical Connectivity to Facilitate Robust Polarization and Timely Cytokinesis.” *Journal of Cell Biology* 216 (5): 1371–86. https://doi.org/10.1083/jcb.201603070.

Duellberg, Christian, Franck J. Fourniol, Sebastian P. Maurer, Johanna Roostalu, and Thomas Surrey. 2013. “End-Binding Proteins and Ase1/PRC1 Define Local Functionality of Structurally Distinct Parts of the Microtubule Cytoskeleton.” *Trends in Cell Biology* 23 (2): 54–63. https://doi.org/10.1016/j.tcb.2012.10.003.

Dumont, Julien, Karen Oegema, and Arshad Desai. 2010. “A Kinetochore-Independent Mechanism Drives Anaphase Chromosome Separation during Acentrosomal Meiosis.” *Nature Cell Biology* 12 (9): 894–901. https://doi.org/10.1038/ncb2093.

Echard, Arnaud, Gilles r.x. Hickson, Edan Foley, and Patrick H. O’Farrell. 2004. “Terminal Cytokinesis Events Uncovered after an RNAi Screen.” *Current Biology* 14 (18): 1685–93. https://doi.org/10.1016/j.cub.2004.08.063.Terminal.

Eggert, Ulrike S, Timothy J Mitchison, and Christine M Field. 2006. “Animal Cytokinesis: From Parts List to Mechanisms.” *Annu Rev Biochem* 75: 543–66. https://doi.org/10.1146/annurev.biochem.74.082803.133425.

Elia, Natalie, Gur Fabrikant, Michael M. Kozlov, and Jennifer Lippincott-Schwartz. 2012. “Computational Model of Cytokinetic Abscission Driven by ESCRT-III Polymerization and Remodeling.” *Biophysical Journal* 102 (10): 2309–20. https://doi.org/10.1016/j.bpj.2012.04.007.

Elia, Natalie, Rachid Sougrat, Tighe A Spurlin, James H Hurley, and Jennifer Lippincott-schwartz. 2011. “Dynamics of Endosomal Sorting Complex Required for Transport (ESCRT) Machinery during Cytokinesis and Its Role in Abscission.” https://doi.org/10.1073/pnas.1102714108/-/DCSupplemental.www.pnas.org/cgi/doi/10.1073/pnas.1102714108.

Encalada, S. E., P. R. Martin, J. B. Phillips, R. Lyczak, D. R. Hamill, K. A. Swan, and B. Bowerman. 2000. “DNA Replication Defects Delay Cell Division and Disrupt Cell Polarity in Early Caenorhabditis Elegans Embryos.” *Developmental Biology* 228 (2): 225-238. https://doi.org/http://dx.doi.org/10.1006/dbio.2000.9965.

Fermino, Carline, Ying Zhang, Jennifer Stadnicki, Jennifer L Ross, and Patricia Wadsworth. 2023. “Lateral and Longitudinal Compaction of PRC1 Overlap Zones Drive Stabilization of Interzonal Microtubules.” *BioRxiv*. https://doi.org/https://doi.org/10.1101/2023.01.30.526324 ; this.

Field, Christine M., and Bruce M. Alberts. 1995. “Anillin, a Contractile Ring Protein That Cycles from the Nucleus to the Cell Cortex.” *Journal of Cell Biology* 131 (1): 165–78. https://doi.org/10.1083/jcb.131.1.165.

Field, Christine M., Margaret Coughlin, Steve Doberstein, Thomas Marty, and William Sullivan. 2005. “Characterization of Anillin Mutants Reveals Essential Roles in Septin Localization and Plasma Membrane Integrity.” *Development* 132 (12): 2849–60. https://doi.org/10.1242/dev.01843.

Fielenbach, N., and A. Antebi. 2008. “C. Elegans Dauer Formation and the Molecular Basis of Plasticity.” *Genes & Development, 22(16), 2149–2165.* 22 (16): 2149–65.

Fink, Gero, Isabel Schuchardt, Julien Colombelli, Ernst Stelzer, and Gero Steinberg. 2006. “Dynein-Mediated Pulling Forces Drive Rapid Mitotic Spindle Elongation in Ustilago Maydis.” *EMBO Journal* 25 (20): 4897–4908. https://doi.org/10.1038/sj.emboj.7601354.

Fire, A., S. Xu, M. K. Montgomery, S. A. Kostas, S. E. Driver, and C. C. Mello. 1998. “Potent and Specific Genetic Interference by Double-Stranded RNA in Caenorhabditis Elegans.” *Nature* 391 (6669): 806–11.

Foe, Victoria E., and George Von Dassow. 2008. “Stable and Dynamic Microtubules Coordinately Shape the Myosin Activation Zone during Cytokinetic Furrow Formation.” *Journal of Cell Biology* 183 (3): 457–70. https://doi.org/10.1083/jcb.200807128.

Fu, Chuanhai, Jonathan J. Ward, Isabelle Loiodice, Guilhem Velve-Casquillas, Francois J. Nedelec, and Phong T. Tran. 2009. “Phospho-Regulated Interaction between Kinesin-6 Klp9p and Microtubule Bundler Ase1p Promotes Spindle Elongation.” *Developmental Cell* 17 (2): 257–67. https://doi.org/10.1016/j.devcel.2009.06.012.

Fu, Chuanhai, Feng Yan, Fang Wu, Quan Wu, Joseph Whittaker, Haiying Hu, Renming Hu, and Xuebiao Yao. 2007. “Mitotic Phosphorylation of PRC1 at Thr470 Is Required for PRC1 Oligomerization and Proper Central Spindle Organization.” *Cell Research* 17 (5): 449–57. https://doi.org/10.1038/cr.2007.32.

Fujii, Takashi, Atsuko H. Iwane, Toshio Yanagida, and Keiichi Namba. 2010. “Direct Visualization of Secondary Structures of F-Actin by Electron Cryomicroscopy.” *Nature* 467 (7316): 724–28. https://doi.org/10.1038/nature09372.

Fujiwara, Ikuko, Shuichi Takeda, Toshiro Oda, Hajime Honda, Akihiro Narita, and Yuichiro Maéda. 2018. “Polymerization and Depolymerization of Actin with Nucleotide States at Filament Ends.” *Biophysical Reviews* 10 (6): 1513–19. https://doi.org/10.1007/s12551-018-0483-7.

Fumoto, K., K. Kikuchi, H. Gon, and A. Kikuchi. 2012. “Wnt5a Signaling Controls Cytokinesis by Positioning ESCRT-III to the Proper Site at the Midbody.” *J Cell Sci* 125: 4822-32.

Gai, Marta, Paola Camera, Alessandro Dema, Federico Bianchi, Gaia Berto, Elena Scarpa, Giulia Germena, and Ferdinando Di Cunto. 2011. “Citron Kinase Controls Abscission through RhoA and Anillin.” *Molecular Biology of the Cell* 22 (20): 3768–78. https://doi.org/10.1091/mbc.E10-12-0952.

Garno, Chelsea, Zoe H. Irons, Courtney M. Gamache, Quenelle McKim, Gabriela Reyes, Xufeng Wu, Charles B. Shuster, and John H. Henson. 2021. “Building the Cytokinetic Contractile Ring in an Early Embryo: Initiation as Clusters of Myosin II, Anillin and

Septin, and Visualization of a Septin Filament Network." *PLoS ONE* 16 (12 December): e0252845. https://doi.org/10.1371/journal.pone.0252845.

Gassmann, Reto, Ana Carvalho, Alexander J. Henzing, Sandrine Ruchaud, Damien F. Hudson, Reiko Honda, Erich A. Nigg, Dietlind L. Gerloff, and William C. Earnshaw. 2004. "Borealin: A Novel Chromosomal Passenger Required for Stability of the Bipolar Mitotic Spindle." *Journal of Cell Biology* 166 (2): 179–91. https://doi.org/10.1083/jcb.200404001.

Giansanti, M G, M Gatti, and S Bonaccorsi. 2001. "The Role of Centrosomes and Astral Microtubules during Asymmetric Division of Drosophila Neuroblasts." *Development* 128 (7): 1137–45. https://doi.org/10.1242/dev.128.7.1137.

Giurumescu, C. A., and A. D. Chisholm. 2011. "Cell Identification and Cell Lineage Analysis." *Methods in Cell Biology* 106: 325–41. https://doi.org/10.1016/B978-0-12-544172-8.00012-8.Cell.

Glotzer, Michael, and Angika Basant. 2017. "A GAP That Divides." *F1000Research* 6 (0): 1–10. https://doi.org/10.12688/f1000research.12064.1.

Goliand, Inna, Dikla Nachmias, Ofir Gershony, and Natalie Elia. 2014. "Inhibition of ESCRT-II-CHMP6 Interactions Impedes Cytokinetic Abscission and Leads to Cell Death." *Molecular Biology of the Cell* 25 (23): 3740–48. https://doi.org/10.1091/mbc.E14-08-1317.

Gómez-Cavazos, J. Sebastián, Kian Yong Lee, Pablo Lara-González, Yanchi Li, Arshad Desai, Andrew K. Shiau, and Karen Oegema. 2020. "A Non-Canonical BRCT-Phosphopeptide Recognition Mechanism Underlies RhoA Activation in Cytokinesis." *Current Biology* 30 (16): 3101-3115.e11. https://doi.org/10.1016/j.cub.2020.05.090.

Gotta, Monica, Yan Dong, Yuri K. Peterson, Stephen M. Lanier, and Julie Ahringer. 2003. "Asymmetrically Distributed C. Elegans Homologs of AGS3/PINSControl Spindle Position in TheEarly Embryo." *Curr Biol* 13: 1029–37. https://doi.org/10.1016/S.

Green, Rebecca A., Jonathan R. Mayers, Shaohe Wang, Lindsay Lewellyn, Arshad Desai, Anjon Audhya, and Karen Oegema. 2013. "The Midbody Ring Scaffolds the Abscission Machinery in the Absence of Midbody Microtubules." *Journal of Cell Biology* 203 (3): 505–20. https://doi.org/10.1083/jcb.201306036.

Green, Rebecca A., Ewa Paluch, and Karen Oegema. 2012. "Cytokinesis in Animal Cells." *Annual Review of Cell and Developmental Biology* 28: 29–58. https://doi.org/10.1146/annurev-cellbio-101011-155718.

Gregory, Stephen L., Saman Ebrahimi, Joanne Milverton, Whitney M. Jones, Amy Bejsovec, and Robert Saint. 2008. "Cell Division Requires a Direct Link between Microtubule-Bound RacGAP and Anillin in the Contractile Ring." *Current Biology* 18 (1): 25–29. https://doi.org/10.1016/j.cub.2007.11.050.

Grill, Stephan W., J. Howard, E. Schaffer, E.H. Stelzer, and A.A. Hyman. 2003. “The Distribution of Active Force Generators Controls Mitotic Spindle Position.” *Science* 301: 518–521.

Grill, Stephan W., and Anthony A. Hyman. 2005. “Spindle Positioning by Cortical Pulling Forces.” *Developmental Cell* 8 (4): 461–65. https://doi.org/10.1016/j.devcel.2005.03.014.

Grill, Stephan W, Pierre Gönczy, Ernst H K Stelzer, and Anthony A Hyman. 2001. “Polarity Controls Forces Governing Asymmetric Spindle Positioning in the Caenorhabditis Elegans Embryo.” *Nature* 409 (6820): 630–33. https://doi.org/10.1038/35054572.

Grishchuk, Ekaterina L, Maxim I Molodtsov, Fazly I Ataullakhanov, and J Richard McIntosh. 2005. “Force Production by Disassembling Microtubules.” *Nature* 438 (7066): 384–88. https://doi.org/10.1038/nature04132.

Gruneberg, Ulrike, Rüdiger Neef, Reiko Honda, Erich A. Nigg, and Francis A. Barr. 2004. “Relocation of Aurora B from Centromeres to the Central Spindle at the Metaphase to Anaphase Transition Requires MKlp2.” *Journal of Cell Biology* 166 (2): 167–72. https://doi.org/10.1083/jcb.200403084.

Gruneberg, Ulrike, Rüdiger Neef, Xiuling Li, Eunice H.Y. Chan, Ravindra B. Chalamalasetty, Erich A. Nigg, and Francis A. Barr. 2006. “KIF14 and Citron Kinase Act Together to Promote Efficient Cytokinesis.” *Journal of Cell Biology* 172 (3): 363–72. https://doi.org/10.1083/jcb.200511061.

Guertin, David A., Susanne Trautmann, and Dannel McCollum. 2002. “Cytokinesis in Eukaryotes.” *Microbiology and Molecular Biology Reviews* 66 (2): 155–78. https://doi.org/10.1128/mmbr.66.2.155-178.2002.

Guizetti, Julien, Lothar Schermelleh, Jana Mäntler, Sandra Maar, Ina Poser, Heinrich Leonhardt, and Thomas Müller-. 2011. “Cortical Constriction During Abscission Involves Helices of ESCRT-III – Dependent Filaments,” no. February.

Halcrow, Ella F. J., Riccardo Mazza, Anna Diversi, Anton Enright, and Pier Paolo D’Avino. 2022. “Midbody Proteins Display Distinct Dynamics during Cytokinesis.” *Cells* 11 (21): 3337. https://doi.org/10.3390/cells11213337.

Hara, Yuki, and Akatsuki Kimura. 2009. “Cell-Size-Dependent Spindle Elongation in the Caenorhabditis Elegans Early Embryo.” *Current Biology* 19 (18): 1549–54. https://doi.org/10.1016/j.cub.2009.07.050.

Harris, Andrew R., Pamela Jreij, and Daniel A. Fletcher. 2018. “Mechanotransduction by the Actin Cytoskeleton: Converting Mechanical Stimuli into Biochemical Signals.” *Annual Review of Biophysics* 47: 617–31. https://doi.org/10.1146/annurev-biophys-070816-033547.

Hartemink, Christopher A. 2005. “The Cross-Linking Mechanism of Filamin A in the Actin

Cytoskeleton." *Division of health sciences and technology in partial fulfillment of the requirements for the degree of doctor of philosophy in mechanical and medical engineering at the massachusetts institute of technology*.

Hartman, M. A., and J. A. Spudich. 2012. "The Myosin Superfamily at a Glance." *Journal of Cell Science* 125 (Pt7): 1627–32.

Hays, Thomas S., Dwayne Wise, and E. D. Salmon. 1982. "Traction Force on a Kinetochore at Metaphase Acts as a Linear Function of Kinetochore Fiber Length." *Journal of Cell Biology* 93 (2): 374–82. https://doi.org/10.1083/jcb.93.2.374.

Henson, John H., Casey E. Ditzler, Aphnie Germain, Patrick M. Irwin, Eric T. Vogt, Shucheng Yang, Xufeng Wu, and Charles B. Shuster. 2017. "The Ultrastructural Organization of Actin and Myosin II Filaments in the Contractile Ring: New Support for an Old Model of Cytokinesis." *Molecular Biology of the Cell* 28 (5): 613–23. https://doi.org/10.1091/mbc.E16-06-0466.

Herndon, L. A., C. A. Wolkow, M. Driscoll, and D. H. Hall. 2018. "Introduction to Aging in C. Elegans." *WormAtlas*.

Hickson, Gilles R.X., and Patrick H. O'Farrell. 2008. "Rho-Dependent Control of Anillin Behavior during Cytokinesis." *Journal of Cell Biology* 180 (2): 285–94. https://doi.org/10.1083/jcb.200709005.

Hirose, Koichi, Toshiyuki Kawashima, Itsuo Iwamoto, Tetsuya Nosaka, and Toshio Kitamura. 2001. "MgcRacGAP Is Involved in Cytokinesis through Associating with Mitotic Spindle and Midbody." *Journal of Biological Chemistry* 276 (8): 5821–28. https://doi.org/10.1074/jbc.M007252200.

Hirsch, Sophia M., Frances Edwards, Mimi Shirasu-Hiza, Julien Dumont, and Julie C. Canman. 2022. "Functional Midbody Assembly in the Absence of a Central Spindle." *Journal of Cell Biology* 221 (3). https://doi.org/10.1083/jcb.202011085.

Hochegger, Helfrid, Nadia Hégarat, and Jose B. Pereira-Leal. 2013. "Aurora at the Pole and Equator: Overlapping Functions of Aurora Kinases in the Mitotic Spindle." *Open Biology* 3 (MAR). https://doi.org/10.1098/rsob.120185.

Holmes, K. C., D. Popp, W. Gebhard, and W. Kabsch. 1990. "Atomic Model of the Actin Filament." *Nature* 347 (6288): 44–49.

Honda, Reiko, Roman Korner, and Erich A. Nigg. 2003. "Exploring the Functional Interactions between Aurora B, INCENP, and Survivin in Mitosis." *Molecular Biology of the Cell* 14 (august): 3325–41. https://doi.org/10.1091/mbc.E02.

Hu, Chi-kuo, Nurhan Özlü, Margaret Coughlin, Judith J Steen, Timothy J Mitchison, and Yu-li Wang. 2012a. "Plk1 Negatively Regulates PRC1 to Prevent Premature Midzone Formation before Cytokinesis." *MBoC*. https://doi.org/10.1091/mbc.E12-01-0058.

Hu, Chi-Kuo, Margaret Coughlin, Christine M. Field, and Timothy J. Mitchison. 2011. "KIF4

Regulates Midzone Length during Cytokinesis." *Current Biology* 21 (10): 815–24. https://doi.org/10.1016/j.cub.2011.04.019.

Hu, Chi-Kuo, Margaret Coughlin, and Timothy J. Mitchison. 2012b. "Midbody Assembly and Its Regulation during Cytokinesis." *Molecular Biology of the Cell* 23 (6): 1024–34. https://doi.org/10.1091/mbc.E11-08-0721.

Hugh, Huxley, and Jean Hanson. 1954. "Changes in the Cross-Striations of Muscle during Contraction and Stretch and Their Structural Interpretation." *Nature* 173 (4412): 973–76. https://doi.org/10.1038/173973a0.

Hurley, James H. 2011. "The ESCRT Complexes" 45 (6): 463–87. https://doi.org/10.3109/10409238.2010.502516.The.

Hyman, A.A. 1989. "Centrosome Movement in the Early Divisionsof Caenorhabditis Elegans: A Cortical Site Determining Centrosome Position." *The Journal of Cell Biology* 109 (September): 1185–93.

Hyung, Ho Lee, Natalie Elia, Rodolfo Ghirlando, Jennifer Lippincott-Schwartz, and James H. Hurley. 2008. "Midbody Targeting of the ESCRT Machinery by a Noncanonical Coiled Coil in CEP55." *Science* 322 (5901): 576–80. https://doi.org/10.1126/science.1162042.

Im, Young Jun, Thomas Wollert, Evzen Boura, and James H. Hurley. 2009. "Structure and Function of the ESCRT-II-III Interface in Multivesicular Body Biogenesis." *Developmental Cell* 17 (2): 234–43. https://doi.org/10.1016/j.devcel.2009.07.008.

Inoue, S., and E.D. Salmon. 1995. "Force Generation by Microtubule Assembly/Disassembly in Mitosis and Related Movements." *Mol. Biol. Cell* 6: 1619–1640. https://doi.org/10.1007/BF01599753.

Jagrić, Mihaela, Patrik Risteski, Jelena Martinčić, Ana Milas, and Iva M. Tolić. 2021. "Optogenetic Control of Prc1 Reveals Its Role in Chromosome Alignment on the Spindle by Overlap Length-Dependent Forces." *ELife* 10: 1–79. https://doi.org/10.7554/eLife.61170.

Jantsch-Plunger, Verena, Pierre Gönczy, Alper Romano, Heinke Schnabel, Danielle Hamill, Ralf Schnabel, Anthony A. Hyman, and Michael Glotzer. 2000. "CYK-4: A Rho Family GTPase Activating Protein (GAP) Required for Central Spindle Formation and Cytokinesis." *Journal of Cell Biology* 149 (7): 1391–1404. https://doi.org/10.1083/jcb.149.7.1391.

Jeyaprakash, A. Arockia, Ulf R. Klein, Doris Lindner, Judith Ebert, Erich A. Nigg, and Elena Conti. 2007. "Structure of a Survivin-Borealin-INCENP Core Complex Reveals How Chromosomal Passengers Travel Together." *Cell* 131 (2): 271–85. https://doi.org/10.1016/j.cell.2007.07.045.

Jiang, Wei, Gretchen Jimenez, Nicholas J. Wells, Thomas J. Hope, Geoffrey M. Wahl, Tony

Hunter, and Rikiro Fukunaga. 1998. “PRC1: A Human Mitotic Spindle-Associated CDK Substrate Protein Required for Cytokinesis.” *Molecular Cell* 2 (6): 877–85. https://doi.org/10.1016/s1097-2765(00)80302-0.

Jordan, Shawn N., and Julie C. Canman. 2012. “Rho GTPases in Animal Cell Cytokinesis: An Occupation by the One Percent.” *Cytoskeleton* 69 (11): 919–30. https://doi.org/10.1002/cm.21071.

Juang, Yue-Li, James Huang, Jan-Michael Peters, Margaret E. McLaughlin, Chin-Yin Tai, and David Pellman. 1997. “APC-Mediated Proteolysis of Ase1 and the Morphogenesis of the Mitotic Spindle.” *Science* 275 (February): 28–31. https://doi.org/10.7551/mitpress/8876.003.0036.

Kaletta, T., and M. O. Hengartner. 2006. “Finding Function in Novel Targets: C. Elegans as a Model Organism.” *Nature Reviews.* 5 (5): 387–398.

Kamath, R.S., A.G. Fraser, Y. Dong, G. Poulin, R. Durbin, M. Gotta, A. Kanapin, et al. 2003. “Systematic Functional Analysis of the Caenorhabditis Elegans Genome Using RNAi.” *Nature* 421: 231–37.

Kamijo, Keiju, Naoya Ohara, Mitsuhiro Abe, Takashi Uchimura, Hiroshi Hosoya, Jae-Seon Lee, and Toru Miki. 2006. “Dissecting the Role of Rho-Mediated Signaling in Contractile Ring Formation.” *Molecular Biology of the Cell* 17 (January): 43–55. https://doi.org/10.1091/mbc.E05.

Kanehira, Mitsugu, Toyomasa Katagiri, Arata Shimo, Ryo Takata, Taro Shuin, Tsuneharu Miki, Tomoaki Fujioka, and Yusuke Nakamura. 2007. “Oncogenic Role of MPHOSPH1, a Cancer-Testis Antigen Specific to Human Bladder Cancer.” *Cancer Research* 67 (7): 3276–85. https://doi.org/10.1158/0008-5472.CAN-06-3748.

Kaplan, Daniel D., Thomas E. Meigs, Patrick Kelly, and Patrick J. Casey. 2004. “Identification of a Role for β-Catenin in the Establishment of a Bipolar Mitotic Spindle.” *Journal of Biological Chemistry* 279 (12): 10829–32. https://doi.org/10.1074/jbc.C400035200.

Kasahara, Kousuke, Yuji Nakayama, Yoshimi Nakazato, Kikuko Ikeda, Takahisa Kuga, and Naoto Yamaguchi. 2007. “Src Signaling Regulates Completion of Abscission in Cytokinesis through ERK/MAPK Activation at the Midbody.” *Journal of Biological Chemistry* 282 (8): 5327–39. https://doi.org/10.1074/jbc.M608396200.

Keating, Heather H., and John G. White. 1998. “Centrosome Dynamics in Early Embryos of Caenorhabditis Elegans.” *Journal of Cell Science* 111 (20): 3027–33.

Kechad, Amel, Silvana Jananji, Yvonne Ruella, and Gilles R.X. Hickson. 2012. “Anillin Acts as a Bifunctional Linker Coordinating Midbody Ring Biogenesis during Cytokinesis.” *Current Biology*. https://doi.org/10.1016/j.cub.2011.11.062.

Kellogg, Elizabeth H., Stuart Howes, Shih-chieh Chieh Ti, Erney Ramírez-aportela, Tarun

M. Kapoor, Pablo Chacón, and Eva Nogales. 2016. “Near-Atomic Cryo-EM Structure of PRC1 Bound to the Microtubule.” *Proceedings of the National Academy of Sciences of the United States of America* 113 (34): 9430–39. https://doi.org/10.1073/pnas.1609903113.

Kemphues, K. J., J. R. Priess, D. G. Morton, and N. S. Cheng. 1988. “Identification of Genes Required for Cytoplasmic Localization in Early C. Elegans Embryos.” *Cell* 52 (3): 311-320.

Khodjakov, A., S. La Terra, and F. Chang. 2004. “Laser Microsurgery in Fission Yeast; Role of the Mitotic Spindle Midzone in Anaphase B.” *Curr Biol* 14: 1330–1340. https://doi.org/10.1016/j.

Kikuchi, Koji, Yohei Niikura, Katsumi Kitagawa, and Akira Kikuchi. 2010. “Dishevelled, a Wnt Signalling Component, Is Involved in Mitotic Progression in Cooperation with Plk1.” *EMBO Journal* 29 (20): 3470–83. https://doi.org/10.1038/emboj.2010.221.

Kim, D. H., and J. J. Rossi. 2008. “RNAi Mechanisms and Applications.” *In BioTechniques* 44 (5): 613–616. https://doi.org/10.2144/000112792.RNAi.

Kimble, J., and D. Hirsh. 1979. “The Postembryonic Cell Lineages of the Hermaphrodite and Male Gonads in Caenorhabditis Elegans.” *Dev. Biol.* 70: 396–417.

Klein, U. R., E. A. Nigg, and U. Gruneberg. 2006. “Centromere Targeting of the Chromosomal Passenger Complex Requires a Ternary Subcomplex of Borealin, Survivin, and the N-Terminal Domain of INCENP.” *Molecular Biology of the Cell* 17 (june): 2547–2558. https://doi.org/10.1091/mbc.E05.

König, Julia, E. B. Frankel, Anjon Audhya, and Thomas Müller-Reichert. 2017. “Membrane Remodeling during Embryonic Abscission in Caenorhabditis Elegans.” *Journal of Cell Biology* 216 (5): 1277–86. https://doi.org/10.1083/jcb.201607030.

Kozlowski, Cleopatra, Martin Srayko, and Francois Nedelec. 2007. “Cortical Microtubule Contacts Position the Spindle in C. Elegans Embryos.” *Cell* 129 (3): 499–510. https://doi.org/10.1016/j.cell.2007.03.027.

Kühn, Sonja, and Matthias Geyer. 2014. “Formins as Effector Proteins of Rho GTPases.” *Small GTPases* 5 (JUNE). https://doi.org/10.4161/sgtp.29513.

Kuo, Tse-chun, Chun-Ting Chen, Desiree Baron, Tamer T. Onder, Sabine Loewer, Sandra Almeida, Cara M. Weismann, et al. 2011. “Midbody Accumulation through Evasion of Autophagy Contributes to Cellular Reprogramming and Tumorigenicity.” *Nature Cell Biology* 13 (10): 1214–23. https://doi.org/10.1038/ncb2332.

Kurasawa, Yasuhiro, William C. Earnshaw, Yuko Mochizuki, Naoshi Dohmae, and Kazuo Todokoro. 2004. “Essential Roles of KIF4 and Its Binding Partner PRC1 in Organized Central Spindle Midzone Formation.” *The EMBO Journal* 23 (16): 3237–48. https://doi.org/10.1038/sj.emboj.7600347.

Laan, Liedewij, Nenad Pavin, Julien Husson, Guillaume Romet-Lemonne, Martijn Van Duijn, Magdalena Preciado López, Ronald D. Vale, Frank Jülicher, Samara L. Reck-Peterson, and Marileen Dogterom. 2012. “Cortical Dynein Controls Microtubule Dynamics to Generate Pulling Forces That Position Microtubule Asters.” *Cell* 148 (3): 502–14. https://doi.org/10.1016/j.cell.2012.01.007.

Lafaurie-Janvore, Julie, Paolo Maiuri, Irène Wang, Mathieu Pinot, Jean Baptiste Manneville, Timo Betz, Martial Balland, and Matthieu Piel. 2013. “ESCRT-III Assembly and Cytokinetic Abscission Are Induced by Tension Release in the Intercellular Bridge.” *Science* 340 (6127): 1625–29. https://doi.org/10.1126/science.1233866.

Landino, Jennifer, and Ryoma Ohi. 2016. “The Timing of Midzone Stabilization during Cytokinesis Depends on Myosin II Activity and an Interaction between INCENP and Actin.” *Current Biology* 26 (5): 698–706. https://doi.org/10.1016/j.cub.2016.01.018.

Laplante, Caroline, Julien Berro, Erdem Karatekin, Ariel Hernandez-Leyva, Rachel Lee, and Thomas D. Pollard. 2015. “Three Myosins Contribute Uniquely to the Assembly and Constriction of the Fission Yeast Cytokinetic Contractile Ring.” *Current Biology* 25 (15): 1955–65. https://doi.org/10.1016/j.cub.2015.06.018.

Laplante, Caroline, and Thomas D. Pollard. 2017. “Response to Zambon et Al.” *Current Biology* 27 (3): R101–2. https://doi.org/10.1016/j.cub.2016.12.025.

Lee, Kian-Yong, Behrooz Esmaeili, Ben Zealley, and Masanori Mishima. 2015. “Direct Interaction between Centralspindlin and PRC1 Reinforces Mechanical Resilience of the Central Spindle.” *Nature Communications* 6: 7290. https://doi.org/10.1038/ncomms8290.

Lee, Kian-Yong, Rebecca A. Green, Edgar Gutierrez, J. Sebastian Gomez-Cavazos, Irina Kolotuev, Shaohe Wang, Arshad Desai, Alex Groisman, and Karen Oegema. 2018. “CYK-4 Functions Independently of Its Centralspindlin Partner ZEN-4 to Cellularize Oocytes in Germline Syncytia.” *ELife* 7: 1–29. https://doi.org/10.7554/eLife.36919.001.

Leite, Joana, Daniel Sampaio Osorio, Ana Filipa Sobral, Ana Marta Silva, and Ana Xavier Carvalho. 2019. “Network Contractility during Cytokinesis—from Molecular to Global Views.” *Biomolecules* 9 (5): 1–28. https://doi.org/10.3390/biom9050194.

Lekomtsev, Sergey, Kuan Chung Su, Valerie E. Pye, Ken Blight, Sriramkumar Sundaramoorthy, Tohru Takaki, Lucy M. Collinson, Peter Cherepanov, Nullin Divecha, and Mark Petronczki. 2012. “Centralspindlin Links the Mitotic Spindle to the Plasma Membrane during Cytokinesis.” *Nature* 492 (7428): 276–79. https://doi.org/10.1038/nature11773.

Lens, Susanne M.A. Susanne, Jose A. Rodriguez, Gerben Vader, Simone W. Span, Giuseppe Giaccone, and and Rene H. Medema. 2006. “Uncoupling the Central Spindle-Associated Function of the Chromosomal Passenger Complex from Its Role

at Centromeres." *Molecular Biology of the Cell* 17 (April): 1897–1909. https://doi.org/10.1091/mbc.E05.

Lens, Susanne M A, Emile E Voest, and René H Medema. 2010. "Shared and Separate Functions of Polo-like Kinases and Aurora Kinases in Cancer." *Nature Reviews Cancer* 10 (12): 825–41. https://doi.org/10.1038/nrc2964.

Leslie, R. J., and J. D. Pickett Heaps. 1983. "Ultraviolet Microbeam Irradiations of Mitotic Diatoms: Investigation of Spindle Elongation." *Journal of Cell Biology* 96 (2): 548–61. https://doi.org/10.1083/jcb.96.2.548.

Lewellyn, Lindsay, Ana Carvalho, Arshad Desai, Amy S. Maddox, and Karen Oegema. 2011. "The Chromosomal Passenger Complex and Centralspindlin Independently Contribute to Contractile Ring Assembly." *Journal of Cell Biology* 193 (1): 155–69. https://doi.org/10.1083/jcb.201008138.

Lewellyn, Lindsay, Julien Dumont, Arshad Desai, and Karen Oegema. 2010. "Analyzing the Effects of Delaying Aster Separation on Furrow Formation during Cytokinesis in the Caenorhabditis Elegans Embryo." *Molecular Biology of the Cell* 21 (22): 4042–56. https://doi.org/10.1091/mbc.E09.

Li, Jing, Marlene Dallmayer, Thomas Kirchner, Julian Musa, and Thomas G.P. Grünewald. 2018. "PRC1: Linking Cytokinesis, Chromosomal Instability, and Cancer Evolution." *Trends in Cancer* 4 (1): 59–73. https://doi.org/10.1016/j.trecan.2017.11.002.

Lie-Jensen, Anette, Kristina Ivanauskiene, Lene Malerød, Ashish Jain, Kia Wee Tan, Jon K. Laerdahl, Knut Liestøl, Harald Stenmark, and Kaisa Haglund. 2019. "Centralspindlin Recruits ALIX to the Midbody during Cytokinetic Abscission in Drosophila via a Mechanism Analogous to Virus Budding." *Current Biology* 29 (20): 3538-3548.e7. https://doi.org/10.1016/j.cub.2019.09.025.

Lioutas, Antonios, and Isabelle Vernos. 2013. "Aurora A Kinase and Its Substrate TACC3 Are Required for Central Spindle Assembly." *EMBO Reports* 14 (9): 829–36. https://doi.org/10.1038/embor.2013.109.

Little, Jessica N., Katrina C. McNeely, Nadine Michel, Christopher J. Bott1, Kaela S. Lettieri, Madison R. Hecht, Sara A. Martin, and Noelle D. Dwyer. 2020. "Loss of Coiled-Coil Protein Cep55 Impairs Abscission Processes and Results in P53-Dependent Apoptosis in Developing Cortex." *BioRxiv*. https://doi.org/10.1017/CBO9781107415324.004.

Liu, Jing, Zhikai Wang, Kai Jiang, Liangyu Zhang, Lingli Zhao, Shasha Hua, Feng Yan, et al. 2009. "PRC1 Cooperates with CLASP1 to Organize Central Spindle Plasticity in Mitosis." *Journal of Biological Chemistry* 284 (34): 23059–71. https://doi.org/10.1074/jbc.M109.009670.

Liu, Jinghe, Gregory D. Fairn, Derek F. Ceccarelli, Frank Sicheri, and Andrew Wilde. 2012.

"Cleavage Furrow Organization Requires PIP 2-Mediated Recruitment of Anillin." *Current Biology* 22 (1): 64–69. https://doi.org/10.1016/j.cub.2011.11.040.

Loıodice, Isabelle, Jayme Staub, Thanuja Gangi Setty, Nam-Phuong T. Anne Paoletti Nguyen, and P. T. Tran. 2005. "Ase1p Organizes Antiparallel Microtubule Arrays during Interphase and Mitosis in Fission Yeast." *Mol Biol Cell* 16 (April): 1756–68. https://doi.org/10.1091/mbc.E04.

Lord, Matthew, Ellen Laves, and Thomas D. Pollard. 2005. "Cytokinesis Depends on the Motor Domains of Myosin-II in Fission Yeast but Not in Budding Yeast." *Molecular Biology of the Cell* 16 (November): 5346–55. https://doi.org/10.1091/mbc.E05.

Loria, Andy, Katrina M. Longhini, and Michael Glotzer. 2012. "The RhoGAP Domain of CYK-4 Has an Essential Role in RhoA Activation." *Current Biology* 22 (3): 213–19. https://doi.org/10.1016/j.cub.2011.12.019.

Lujan, Pablo, Teresa Rubio, Giulia Varsano, and Maja Köhn. 2017. "Keep It on the Edge: The Post-Mitotic Midbody as a Polarity Signal Unit." *Communicative & Integrative Biology* 10 (4): e1338990. https://doi.org/10.1080/19420889.2017.1338990.

Luján, Pablo, Giulia Varsano, Teresa Rubio, Marco L. Hennrich, Timo Sachsenheimer, Manuel Gálvez-Santisteban, Fernando Martín-Belmonte, Anne Claude Gavin, Britta Brügger, and Maja Köhn. 2016. "PRL-3 Disrupts Epithelial Architecture by Altering the Post-Mitotic Midbody Position." *Journal of Cell Science* 129 (21): 4130–42. https://doi.org/10.1242/jcs.190215.

Mabuchi, I, Y Hamaguchi, H Fujimoto, N Morii, M Mishima, and S Narumiya. 1993. "A Rho-like Protein Is Involved in the Organisation of the Contractile Ring in Dividing Sand Dollar Eggs." *Zygote (Cambridge, England)* 1 (4): 325–31. https://doi.org/10.1017/s0967199400001659.

Mackay, Douglas R., Masaki Makise, and Katharine S. Ullman. 2010. "Defects in Nuclear Pore Assembly Lead to Activation of an Aurora B-Mediated Abscission Checkpoint." *Journal of Cell Biology* 191 (5): 923–31. https://doi.org/10.1083/jcb.201007124.

Mackay, Douglas R., and Katharine S. Ullman. 2015. "ATR and a Chk1-Aurora B Pathway Coordinate Postmitotic Genome Surveillance with Cytokinetic Abscission." *Molecular Biology of the Cell* 26 (12): 2217–26. https://doi.org/10.1091/mbc.E14-11-1563.

Maddox, Amy Shaub, Bianca Habermann, Arshad Desai, and Karen Oegema. 2005. "Distinct Roles for Two C. Elegans Anillins in the Gonad and Early Embryo." *Development* 132 (12): 2837–48. https://doi.org/10.1242/dev.01828.

Maddox, Amy Shaub, Lindsay Lewellyn, Arshad Desai, and Karen Oegema. 2007. "Anillin and the Septins Promote Asymmetric Ingression of the Cytokinetic Furrow." *Developmental Cell* 12 (5): 827–35. https://doi.org/10.1016/j.devcel.2007.02.018.

Makyio, Hisayoshi, Minako Ohgi, Tomomi Takei, Senye Takahashi, Hiroyuki Takatsu, Yohei

Katoh, Ayako Hanai, et al. 2012. “Structural Basis for Arf6-MKLP1 Complex Formation on the Flemming Body Responsible for Cytokinesis.” *EMBO Journal* 31 (11): 2590–2603. https://doi.org/10.1038/emboj.2012.89.

Mangal, Sriyash, Jennifer Sacher, Taekyung Kim, Daniel Sampaio Osório, Fumio Motegi, Ana Xavier Carvalho, Karen Oegema, and Esther Zanin. 2018. “TPXL-1 Activates Aurora A to Clear Contractile Ring Components from the Polar Cortex during Cytokinesis.” *Journal of Cell Biology* 217 (3): 837–48. https://doi.org/10.1083/jcb.201706021.

Mani, Nandini, Shuo Jiang, Alex E Neary, Sithara S Wijeratne, and Radhika Subramanian. 2021. “Differential Regulation of Single Microtubules and Bundles by a Three-Protein Module.” *Nature Chemical Biology* 17 (9): 964–74. https://doi.org/10.1038/s41589-021-00800-y.

Mastronarde, D. N., K. L. McDonald, R. Ding, and J. R. McIntosh. 1993. “Interpolar Spindle Microtubules in PTK Cells.” *Journal of Cell Biology* 123 (6 I): 1475–89. https://doi.org/10.1083/jcb.123.6.1475.

Maton, Gilliane, Frances Edwards, Benjamin Lacroix, Marine Stefanutti, Kimberley Laband, Tiffany Lieury, Taekyung Kim, Julien Espeut, Julie C. Canman, and Julien Dumont. 2015. “Kinetochore Components Are Required for Central Spindle Assembly.” *Nature Cell Biology* 17 (5): 697–705. https://doi.org/10.1038/ncb3150.

Matsumura, Fumio. 2005. “Regulation of Myosin II during Cytokinesis in Higher Eukaryotes.” *Trends in Cell Biology* 15 (7): 371–77. https://doi.org/10.1016/j.tcb.2005.05.004.

Mcdonald, Kent, Jeremy D Pickett-heaps, J Richard Mcintosh, and David H Tippit. 1977. “ON THE MECHANISM IN OF SPINDLE ELONGATION From the Department of Molecular , Cellular , and Developmental Biology , University of Colorado , Boulder , Colorado 80302 ABSTRACT Central Spindles from Five Dividing Cells (One Metaphase , Three Anaphase , And” 74: 377–88.

McIntosh, J.R., P K Helper, and D G V A N Wie. 1969. “Model for Mitosis.” *Nature* 224 (5220): 659–63. https://doi.org/10.1038/224659a0.

McNally, Karen Perry, Michelle T. Panzica, Taekyung Kim, Daniel B. Cortes, and Francis J. McNally. 2016. “A Novel Chromosome Segregation Mechanism during Female Meiosis.” *Molecular Biology of the Cell* 27 (16): 2576–89. https://doi.org/10.1091/mbc.E16-05-0331.

McNeely, Katrina C., and Noelle D. Dwyer. 2020. “Cytokinesis and Postabscission Midbody Remnants Are Regulated during Mammalian Brain Development.” *Proceedings of the National Academy of Sciences* 117 (17): 201919658. https://doi.org/10.1073/pnas.1919658117.

Mendes Pinto, Inês, Boris Rubinstein, Andrei Kucharavy, Jay R. Unruh, and Rong Li. 2012. "Actin Depolymerization Drives Actomyosin Ring Contraction during Budding Yeast Cytokinesis." *Developmental Cell* 22 (6): 1247–60. https://doi.org/10.1016/j.devcel.2012.04.015.

Mendoza, Manuel, Caren Norden, Kathrin Durrer, Harald Rauter, Frank Uhlmann, and Yves Barral. 2009. "A Mechanism for Chromosome Segregation Sensing by the NoCut Checkpoint." *Nature Cell Biology* 11 (4): 477–83. https://doi.org/10.1038/ncb1855.

Meneely, Philip M, Caroline L Dahlberg, and Jacqueline K Rose. 2019. "Working with Worms : Caenorhabditis Elegans as a Model Organism," 1–35. https://doi.org/10.1002/cpet.35.

Mierzwa, Beata, and Daniel W. Gerlich. 2014. "Cytokinetic Abscission: Molecular Mechanisms and Temporal Control." *Developmental Cell* 31 (5): 525–38. https://doi.org/10.1016/j.devcel.2014.11.006.

Miller, Ann L., and William M. Bement. 2009. "Regulation of Cytokinesis by Rho GTPase Flux." *Nature Cell Biology* 11 (1): 71–77. https://doi.org/10.1038/ncb1814.

Mishima, Masanori, Susanne Kaitna, and Michael Glotzer. 2002. "Central Spindle Assembly and Cytokinesis Require a Kinesin-like Protein/RhoGAP Complex with Microtubule Bundling Activity." *Developmental Cell* 2 (1): 41–54. https://doi.org/10.1016/S1534-5807(01)00110-1.

Mishima, Masanori, Visnja Pavicic, Ulrike Grüneberg, Erich A. Nigg, and Michael Glotzer. 2004. "Cell Cycle Regulation of Central Spindle Assembly." *Nature* 430 (7002): 908–13. https://doi.org/10.1038/nature02767.

Mollinari, Cristiana, Jean-Philippe Kleman, Wei Jiang, Guy Schoehn, Tony Hunter, and Robert L Margolis. 2002. "PRC1 Is a Microtubule Binding and Bundling Protein Essential to Maintain the Mitotic Spindle Midzone." *The Journal of Cell Biology* 157 (7): 1175–86. https://doi.org/10.1083/jcb.200111052.

Mollinari, Cristiana, Jean-Philippe Kleman, Yasmina Saoudi, Sandra A. Jablonski, Julien Perard, Tim J. Yen, and Robert L Margolis. 2005. "Ablation of PRC1 by Small Interfering RNA Demonstrates That Cytokinetic Abscission Requires a Central Spindle Bundle in Mammalian Cells, Whereas Completion of Furrowing Does Not." *Molecular Biology of the Cell* 16 (8): 10-43–1055. https://doi.org/10.1091/mbc.E04.

Morais-De-Sá, Eurico, and Claudio Sunkel. 2013. "Adherens Junctions Determine the Apical Position of the Midbody during Follicular Epithelial Cell Division." *EMBO Reports* 14 (8): 696–703. https://doi.org/10.1038/embor.2013.85.

Morita, Eiji, Virginie Sandrin, Hyo Young Chung, Scott G. Morham, Steven P. Gygi, Christopher K. Rodesch, and Wesley I. Sundquist. 2007. "Human ESCRT and ALIX Proteins Interact with Proteins of the Midbody and Function in Cytokinesis." *EMBO*

Journal 26 (19): 4215–27. https://doi.org/10.1038/sj.emboj.7601850.

Mullins, J . Michael, and John J. Biesele. 1977. “Terminal Phase of Cytokinesis in D-98S Cells.” *Journal of Cell Biology* 73 (8): 672–84.

Murthy, Kausalya, and Patricia Wadsworth. 2008. “Dual Role for Microtubules in Regulating Cortical Contractility during Cytokinesis.” *J Cell Sci* 121 (Pt 14): 2350–59. https://doi.org/10.1242/jcs.027052.Dual.

Musacchio, Andrea, and Arshad Desai. 2017. “A Molecular View of Kinetochore Assembly and Function.” *Biology* 6 (1). https://doi.org/10.3390/biology6010005.

Nahaboo, Wallis, Melissa Zouak, Peter Askjaer, and Marie Delattre. 2015. “Chromatids Segregate without Centrosomes during Caenorhabditis Elegans Mitosis in a Ran- and CLASP-Dependent Manner.” *Molecular Biology of the Cell* 26 (11): 2020–29. https://doi.org/10.1091/mbc.E14-12-1577.

Nakajima, Yuko, Anthony Cormier, Randall G. Tyers, Adrianne Pigula, Yutian Peng, David G. Drubin, and Georjana Barnes. 2011. “Ipl1/Aurora-Dependent Phosphorylation of Sli15/INCENP Regulates CPC-Spindle Interaction to Ensure Proper Microtubule Dynamics.” *Journal of Cell Biology* 194 (1): 137–53. https://doi.org/10.1083/jcb.201009137.

Neef, Rüdiger, Ulrike Gruneberg, Robert Kopajtich, Xiuling Li, Erich a Nigg, Herman Sillje, and Francis A Barr. 2007. “Choice of Plk1 Docking Partners during Mitosis and Cytokinesis Is Controlled by the Activation State of Cdk1.” *Nature Cell Biology* 9 (4): 436–44. https://doi.org/10.1038/ncb1557.

Neumeier, Julia, and Gunter Meister. 2021. “SiRNA Specificity: RNAi Mechanisms and Strategies to Reduce Off-Target Effects.” *Frontiers in Plant Science* 11 (January): 1–7. https://doi.org/10.3389/fpls.2020.526455.

Nguyen-Ngoc, T., K. Afshar, and P. Gonczy. 2007. “Coupling of Cortical Dynein and G Alpha Proteins Mediates Spindle Positioning in Caenorhabditis Elegans.” *Nat. Cell Biol.* 9: 1294–1302.

Niiya, F., T. Tatsumoto, K. S. Lee, and T. Miki. 2006. “Phosphorylation of the Cytokinesis Regulator ECT2 at G2/M Phase Stimulates Association of the Mitotic Kinase Plk1 and Accumulation of GTP-Bound RhoA.” *Oncogene* 25 (6): 827–837.

Nishimura, Yukako, and Shigenobu Yonemura. 2006. “Centralspindlin Regulates ECT2 and RhoA Accumulation at the Equatorial Cortex during Cytokinesis.” *Journal of Cell Science* 119 (1): 104–14. https://doi.org/10.1242/jcs.02737.

Nislow, Corey, Vivian A Lombillo, Ryoko Kuriyama, and J Richard McIntosh. 1992. “A Plus-End-Directed Motor Enzyme That Moves Antiparallel Microtubules in Vitro Localizes to the Interzone of Mitotic Spindles.” *Nature* 359 (6395): 543–47. https://doi.org/10.1038/359543a0.

Norden, Caren, Manuel Mendoza, Jeroen Dobbelaere, Chitra V. Kotwaliwale, Sue Biggins, and Yves Barral. 2006. “The NoCut Pathway Links Completion of Cytokinesis to Spindle Midzone Function to Prevent Chromosome Breakage.” *Cell* 125 (1): 85–98. https://doi.org/10.1016/j.cell.2006.01.045.

O’Connell, Kevin F., Charles M. Leys, and John G. White. 1998. “A Genetic Screen for Temperature-Sensitive Cell-Division Mutants of Caenorhabditis Elegans.” *Genetics* 149 (3): 1303–21.

O’Rourke, Sean M., Clayton Carter, Luke Carter, Sara N. Christensen, Minh P. Jones, Bruce Nash, Meredith H. Price, et al. 2011. “A Survey of New Temperature-Sensitive, Embryonic-Lethal Mutations in C. Elegans: 24 Alleles of Thirteen Genes.” *PLoS ONE* 6 (3). https://doi.org/10.1371/journal.pone.0016644.

Oda, Toshiro, Mitsusada Iwasa, Tomoki Aihara, Yuichiro Maéda, and Akihiro Narita. 2009. “The Nature of the Globular- to Fibrous-Actin Transition.” *Nature* 457 (7228): 441–45. https://doi.org/10.1038/nature07685.

Oegema, Karen, and T. J. Mitchison. 1997. “Rappaport Rules: Cleavage Furrow Induction in Animal Cells.” *Proceedings of the National Academy of Sciences of the United States of America* 94 (10): 4817–20. https://doi.org/10.1073/pnas.94.10.4817.

Oegema, Karen, M. S. Savoian, T. J. Mitchison, and C. M. Field. 2000. “Functional Analysis of a Human Homologue of the Drosophila Actin Binding Protein Anillin Suggests a Role in Cytokinesis.” *Journal of Cell Biology* 150 (3): 539–51. https://doi.org/10.1083/jcb.150.3.539.

Oegema, Karen, and A. A. Hyman. 2006. “Cell Division.” In *WormBook:The Online Review of C. Elegans Biology*, 1–40. https://doi.org/10.1895/wormbook.1.72.1.

Ohashi, Akihiro, Momoko Ohori, and Kenichi Iwai. 2016. “Motor Activity of Centromere-Associated Protein-E Contributes to Its Localization at the Center of the Midbody to Regulate Cytokinetic Abscission.” *Oncotarget* 7 (48): 79964–80. https://doi.org/10.18632/oncotarget.13206.

Osório, Daniel S., Fung Yi Chan, Joana Saramago, Joana Leite, Ana M. Silva, Ana F. Sobral, Reto Gassmann, and Ana Xavier Carvalho. 2019. *Crosslinking Activity of Non-Muscle Myosin II Is Not Sufficient for Embryonic Cytokinesis in C. Elegans*. *Development (Cambridge, England)*. Vol. 146. https://doi.org/10.1242/dev.179150.

Ostergren, G. 1950. “Considerations on Some Elementary Features of Mitosis.” *Hereditas* 36: 1–19.

Ou, Guangshuo, Christian Gentili, and Pierre Gönczy. 2014. “Stereotyped Distribution of Midbody Remnants in Early C. Elegans Embryos Requires Cell Death Genes and Is Dispensable for Development.” *Cell Research* 24 (2): 251–53. https://doi.org/10.1038/cr.2013.140.

Özlü, Nurhan, Flavio Monigatti, Bernhard Y. Renard, Christine M. Field, Hanno Steen, Timothy J. Mitchison, and Judith J. Steen. 2010. “Binding Partner Switching on Microtubules and Aurora-B in the Mitosis to Cytokinesis Transition.” *Molecular and Cellular Proteomics* 9 (2): 336–50. https://doi.org/10.1074/mcp.M900308-MCP200.

Ozugergin, Imge, Karina Mastronardi, Chris Law, and Alisa Piekny. 2022. *Diverse Mechanisms Regulate Contractile Ring Assembly for Cytokinesis in the Two-Cell Caenorhabditis Elegans Embryo*. *Journal of Cell Science*. Vol. 135. https://doi.org/10.1242/jcs.258921.

Pacquelet, Anne, Perrine Uhart, Jean-Pierre Pierre Tassan, and Grégoire Michaux. 2015. “PAR-4 and Anillin Regulate Myosin to Coordinate Spindle and Furrow Position during Asymmetric Division.” *J Cell Biol* 210 (7). https://doi.org/10.1083/jcb.201503006.

Palani, Saravanan, Ting Gang Chew, Srinivasan Ramanujam, Anton Kamnev, Shrikant Harne, Bernardo Chapa-y-Lazo, Rebecca Hogg, et al. 2017. “Motor Activity Dependent and Independent Functions of Myosin II Contribute to Actomyosin Ring Assembly and Contraction in Schizosaccharomyces Pombe.” *Current Biology* 27 (5): 751–57. https://doi.org/10.1016/j.cub.2017.01.028.

Palozola, Katherine C., Hong Liu, Dario Nicetto, and Kenneth S. Zaret. 2017. “Low-Level, Global Transcription during Mitosis and Dynamic Gene Reactivation during Mitotic Exit.” *Cold Spring Harbor Symposia on Quantitative Biology* 82: 197–205. https://doi.org/10.1101/sqb.2017.82.034280.

Palozola, Katherine C, Greg Donahue, Hong Liu, Gregory R Grant, Justin S Becker, Allison Cote, Hongtao Yu, Arjun Raj, and Kenneth S Zaret. 2017. “Mitotic Transcription and Waves of Gene Reactivation during Mitotic Exit.” *Science* 358 (6359): 119–22. https://doi.org/10.1126/science.aal4671.

Patel, Kieren, Eva Nogales, and Rebecca Heald. 2012. “Multiple Domains of Human CLASP Contribute to Microtubule Dynamics and Organization In Vitro and in Xenopus Egg Extracts.” *Cytoskeleton* 165 (January): 155–65. https://doi.org/10.1002/cm.21005.

Pecreaux, Jacques, Jens Christian Röper, Karsten Kruse, Frank Jülicher, Anthony A. Hyman, Stephan W. Grill, and Jonathon Howard. 2006. “Spindle Oscillations during Asymmetric Cell Division Require a Threshold Number of Active Cortical Force Generators.” *Current Biology* 16 (21): 2111–22. https://doi.org/10.1016/j.cub.2006.09.030.

Pelham, R.J., and F. Chang. 2002. “Actin Dynamics in the Contractile Ring during Cytokinesis in Fission Yeast.” *Nature* 419: 82–86.

Pellman, David, Molly Bagget, Huei Tu, and Gerald R. Fink. 1995. “Two Microtubule-Associated Proteins Required for Anaphase Spindle Movement in Saccharomyces Cerevisiae.” *Journal of Cell Biology* 130 (6): 1373–85.

https://doi.org/10.1083/jcb.130.6.1373.

Pereira, Ana L., Antonio J. Pereira, Ana R.R. Maia, Ksenija Drabek, C. Laura Sayas, Polla J. Hergert, Mariana Lince-Faria, et al. 2006. “Mammalian CLASP1 and CLASP2 Cooperate to Ensure Mitotic Fidelity by Regulating Spindle and Kinetochore Function.” *Molecular Biology of the Cell* 18 (October): 4526–42. https://doi.org/10.1091/mbc.E06.

Pereira, Gislene, and Elmar Schiebel. 2003. “Separase Regulates INCENP-Aurora B Anaphase Spindle Function through Cdc14.” *Science (New York, N.Y.)* 302 (5653): 2120–24. https://doi.org/10.1126/science.1091936.

Peterman, Eric, Paulius Gibieža, Johnathon Schafer, Vytenis Arvydas Skeberdis, Algirdas Kaupinis, Mindaugas Valius, Xavier Heiligenstein, Ilse Hurbain, Graca Raposo, and Rytis Prekeris. 2019. “The Post-Abscission Midbody Is an Intracellular Signaling Organelle That Regulates Cell Proliferation.” *Nature Communications* 10 (1). https://doi.org/10.1038/s41467-019-10871-0.

Peterman, Erwin J.G., and Jonathan M. Scholey. 2009. “Mitotic Microtubule Crosslinkers: Insights from Mechanistic Studies.” *Current Biology* 19 (23): R1089–94. https://doi.org/10.1016/j.cub.2009.10.047.

Petronczki, M, M Glotzer, N Kraut, and JM Peters. 2007. “Polo-like Kinase 1 Triggers the Initiation of Cytokinesis in Human Cells by Promoting Recruitment of the RhoGEF Ect2 to the Central Spindle.” *Dev. Cell* 12: 713–25.

Petry, Sabine. 2016. “Mechanisms of Mitotic Spindle Assembly.” *Annu Rev Biochem.* 85: 659–83. https://doi.org/doi:10.1146/annurev-biochem-060815-014528.

Piekny, Alisa J., and Michael Glotzer. 2008. “Anillin Is a Scaffold Protein That Links RhoA, Actin, and Myosin during Cytokinesis.” *Current Biology* 18 (1): 30–36. https://doi.org/10.1016/j.cub.2007.11.068.

Piekny, Alisa J., and Amy Shaub Maddox. 2010. “The Myriad Roles of Anillin during Cytokinesis.” *Seminars in Cell and Developmental Biology* 21 (9): 881–91. https://doi.org/10.1016/j.semcdb.2010.08.002.

Pollard, Thomas D. 2004. “Ray Rappaport Chronology: Twenty-Five Years of Seminal Papers on Cytokinesis in the Journal of Experimental Zoology.” *Journal of Experimental Zoology. Part A, Comparative Experimental Biology* 301 (1): 9–14. https://doi.org/10.1002/jez.a.20000.

Pollard, Thomas D. 2017. “Nine Unanswered Questions about Cytokinesis.” *Journal of Cell Biology* 216 (10): 3007–16. https://doi.org/10.1083/jcb.201612068.

Pollard, Thomas D., and Ben O’Shaughnessy. 2019. “Molecular Mechanism of Cytokinesis.” *Annual Review of Biochemistry* 88: 661–89. https://doi.org/10.1146/annurev-biochem-062917-012530.

Pollard, Thomas D, Laurent Blanchoin, and R Dyche Mullins. 2000. “Molecular Mechanisms

Controlling Actin Filament Dynamics in Nonmuscle Cells." *Annual Review of Biophysics* 29: 545–76.

Portran, D., M. Zoccoler, J. Stoppin-MelletGaillard, V. Stoppin-Mellet, E. Neumann, I. Arnal, J. L. Martiel, and M. Vantard. 2013. "MAP65/Ase1 Promote Microtubule Flexibility." *Molecular Biology of the Cell* 24 (12): 1964–73. https://doi.org/10.1091/mbc.E13-03-0141.

Powers, J, O Bossinger, D Rose, S Strome, and W Saxton. 1998. "A Nematode Kinesin Required for Cleavage Furrow Advancement." *Curr Biol* 8: 1133–36. https://doi.org/10.1038/nature08365.Reconstructing.

Prokopenko, Sergei N., Anthony Brumby, Louise O'Keefe, Leanne Prior, Yuchun He, Robert Saint, and Hugo J. Bellen. 1999. "A Putative Exchange Factor for Rho1 GTPase Is Required for Initiation of Cytokinesis in Drosophila." *Genes and Development* 13 (17): 2301–14. https://doi.org/10.1101/gad.13.17.2301.

Raich, W. B., A. N. Moran, J. H. Rothman, and J. Hardin. 1998. "Cytokinesis and Midzone Microtubule Organization in Caenorhabditis Elegans Require the Kinesin-like Protein ZEN-4." *Molecular Biology of the Cell* 9 (8): 2037-2049.

Rappaport, R. 1961. "Experiments Concerning the Cleavage Stimulus in Sand Dollar Eggs." *The Journal of Experimental Zoology* 148 (October): 81–89. https://doi.org/10.1002/jez.1401480107.

Rappaport, R., and B.N. Rappaport. 1983. "Cytokinesis: Effects Ofblocks between the Mitotic Apparatus and the Surface on Furrow Establishment in Flattened Echinoderm Eggs." *J. Exp. Zool.* 227: 213–27.

Reboutier, David, Marie Bérengère Troadec, Jean Yves Cremet, Lucie Chauvin, Vincent Guen, Patrick Salaun, and Claude Prigent. 2013. "Aurora a Is Involved in Central Spindle Assembly through Phosphorylation of Ser 19 in P150Glued." *Journal of Cell Biology* 201 (1): 65–79. https://doi.org/10.1083/jcb.201210060.

Reyes, Ciara C., Meiyan Jin, Elaina B. Breznau, Rhogelyn Espino, Ricard Delgado-Gonzalo, Andrew B. Goryachev, and Ann L. Miller. 2014. "Anillin Regulates Cell-Cell Junction Integrity by Organizing Junctional Accumulation of Rho-GTP and Actomyosin." *Current Biology* 24 (11): 1263–70. https://doi.org/10.1016/j.cub.2014.04.021.

Rieder, Conly L, Alexey Khodjakov, Leocadia V Paliulis, and Tina M Fortier. 1997. "Mitosis in Vertebrate Somatic Cells with Two Spindles : Implications for the Metaphase / Anaphase Transition Checkpoint and Cleavage." *PNAS* 94: 5107–12.

Rincon, Sergio A., Adam Lamson, Robert Blackwell, Viktoriya Syrovatkina, Vincent Fraisier, Anne Paoletti, Meredith D. Betterton, and Phong T. Tran. 2017. "Kinesin-5-Independent Mitotic Spindle Assembly Requires the Antiparallel Microtubule

Crosslinker Ase1 in Fission Yeast." *Nature Communications* 8 (May). https://doi.org/10.1038/ncomms15286.

Rossman, Kent L, Channing J Der, and John Sondek. 2005. "GEF Means Go: Turning on RHO GTPases with Guanine Nucleotide-Exchange Factors." *Nature Reviews Molecular Cell Biology* 6 (2): 167–80. https://doi.org/10.1038/nrm1587.

Rozelle, Daniel K., Scott D. Hansen, and Kenneth B. Kaplan. 2011. "Chromosome Passenger Complexes Control Anaphase Duration and Spindle Elongation via a Kinesin-5 Brake." *Journal of Cell Biology* 193 (2): 285–94. https://doi.org/10.1083/jcb.201011002.

Salzmann, Viktoria, Cuie Chen, C Ason Chiang, Amita Tiyaboonchai, Michael Mayer, and Julie Brill. 2014. "Centrosome-Dependent Asymmetric Inheritance of the Midbody Ring in Drosophila Germline Stem Cell Division" 25: 267–75. https://doi.org/10.1091/mbc.E13-09-0541.

Sasaki, Naoya, Takashi Shimada, and Kazuo Sutoh. 1998. "Mutational Analysis of the Switch II Loop of Dictyostelium Myosin II." *Journal of Biological Chemistry* 273 (32): 20334–40. https://doi.org/10.1074/jbc.273.32.20334.

Saunders, Adam M., James Powers, Susan Strome, and William M. Saxton. 2007. "Kinesin-5 Acts as a Brake in Anaphase Spindle Elongation." *Current Biology* 17 (12): 453–54. https://doi.org/10.1016/j.cub.2007.05.001.

Saurin, Adrian T., Joanne Durgan, Angus J. Cameron, Amir Faisal, Michael S. Marber, and Peter J. Parker. 2008. "The Regulated Assembly of a PKCe Complex Controls the Completion of Cytokinesis." *Nature Cell Biology* 10 (8): 891–901. https://doi.org/10.1038/ncb1749.

Saxton, W. M., and J. R. McIntosh. 1987. "Interzone Microtubule Behavior in Late Anaphase and Telophase Spindles." *Journal of Cell Biology* 105 (2): 875–86. https://doi.org/10.1083/jcb.105.2.875.

Schiel, John A, and Rytis Prekeris. 2010. "Making the Final Cut — Mechanisms Mediating the Abscission Step of Cytokinesis," 1424–34. https://doi.org/10.1100/tsw.2010.129.

Schiel, John A, Glenn C Simon, Chelsey Zaharris, Julie Weisz, David Castle, Christine C Wu, and Rytis Prekeris. 2012. "FIP3-Endosome-Dependent Formation of the Secondary Ingression Mediates ESCRT-III Recruitment during Cytokinesis." *Nature Cell Biology* 14 (10): 1068–78. https://doi.org/10.1038/ncb2577.

Schindelin, J, I Arganda-Carreras, E Frise, V Kaynig, M Longair, T Pietzsch, S Preibisch, et al. 2012. "Fiji: An Open-Source Platform for Biological-Image Analysis." *Nature Methods* 9: 676–682.

Scholey, Jonathan M., Ingrid Brust-Mascher, and Alex Mogilner. 2003. "Cell Division." *Nature* 422 (6933): 746–52. https://doi.org/10.1038/nature01599.

Scholey, Jonathan M., Gul Civelekoglu-Scholey, and Ingrid Brust-Mascher. 2016. “Anaphase B.” *Biology* 5 (4): 1–30. https://doi.org/10.3390/biology5040051.

Schroeder, T. E. 1968. “Cytokinesis: Filaments in the Cleavage Furrow.” *Experimental Cell Research* 53 (1): 272–276.

Schroeder, T.E. 1972. “The Contractile Ring. II. Determining Its Brief Existence, Volumetric Changes, and Vital Role in Cleaving Arbacia Eggs.” *The Journal of Cell Biology* 53 (2): 419–434.

Schroeder, T.E. 1973. “Actin in Dividing Cells: Contractile Ring Filaments Bind Heavy Meromyosin.” *Proceedings of the National Academy of Sciences of the United States of America,* 70 (6): 1688–1692.

Schumacher, Jill M., Andy Golden, and Peter J. Donovan. 1998. “AIR-2: An Aurora/Ipl1-Related Protein Kinase Associated with Chromosomes and Midbody Microtubules Is Required for Polar Body Extrusion and Cytokinesis in Caenorhabditis Elegans Embryos.” *Journal of Cell Biology* 143 (6): 1635–46. https://doi.org/10.1083/jcb.143.6.1635.

Schuster, Susan, Pascal Miesen, and Ronald P. van Rij. 2019. “Antiviral RNAi in Insects and Mammals: Parallels and Differences.” *Viruses* 11 (5). https://doi.org/10.3390/v11050448.

Schuyler, Scott C., Jenny Y. Liu, and David Pellman. 2003. “The Molecular Function of Ase1p: Evidence for a MAP-Dependent Midzone-Specific Spindle Matrix.” *Journal of Cell Biology* 160 (4): 517–28. https://doi.org/10.1083/jcb.200210021.

She, Zhen Yu, Ya Lan Wei, Yang Lin, Yue Ling Li, and Ming Hui Lu. 2019. “Mechanisms of the Ase1/PRC1/MAP65 Family in Central Spindle Assembly.” *Biological Reviews* 94 (6): 2033–48. https://doi.org/10.1111/brv.12547.

Shekhar, Shashank, Julien Pernier, and Marie France Carlier. 2016. “Regulators of Actin Filament Barbed Ends at a Glance.” *Journal of Cell Science* 129 (6): 1085–91. https://doi.org/10.1242/jcs.179994.

Shimada, Takashi, Naoya Sasaki, Reiko Ohkura, and Kazuo Sutoh. 1997. “Alanine Scanning Mutagenesis of the Switch I Region in the ATPase Site of Dictyostelium Discoideum Myosin II.” *Biochemistry* 36 (46): 14037–43. https://doi.org/10.1021/bi971837i.

Shimamoto, Yuta, Scott Forth, and Tarun M. Kapoor. 2015. “Measuring Pushing and Braking Forces Generated by Ensembles of Kinesin-5 Crosslinking Two Microtubules.” *Developmental Cell* 34 (6): 669–81. https://doi.org/10.1016/j.devcel.2015.08.017.

Shimo, Arata, Toshihiko Nishidate, Tomohiko Ohta, Mamoru Fukuda, Yusuke Nakamura, and Toyomasa Katagiri. 2007. “Elevated Expression of Protein Regulator of Cytokinesis 1, Involved in the Growth of Breast Cancer Cells.” *Cancer Science* 98 (2):

174–81. https://doi.org/10.1111/j.1349-7006.2006.00381.x.

Silva, Ana M., Daniel S. Osório, Antonio J. Pereira, Helder Maiato, Inês Mendes Pinto, Boris Rubinstein, Reto Gassmann, Ivo Andreas Telley, and Ana Xavier Carvalho. 2016. "Robust Gap Repair in the Contractile Ring Ensures Timely Completion of Cytokinesis." *Journal of Cell Biology* 215 (6): 789–99. https://doi.org/10.1083/jcb.201605080.

Singh, Deepika, and Christian Pohl. 2014. "Coupling of Rotational Cortical Flow, Asymmetric Midbody Positioning, and Spindle Rotation Mediates Dorsoventral Axis Formation in C. Elegans." *Developmental Cell* 28 (3): 253–67. https://doi.org/10.1016/j.devcel.2014.01.002.

Sisson, J. C., C. Field, R. Ventura, A. Royou, and W. Sullivan. 2000. "Lava Lamp, a Novel Peripheral Golgi Protein, Is Required for Drosophila Melanogaster Cellularization." *Journal of Cell Biology* 151 (4): 905–17. https://doi.org/10.1083/jcb.151.4.905.

Sobral, Ana Filipa, Fung-Yi Chan, Michael J. Norman, Daniel S. Osório, Ana Beatriz Dias, Vanessa Ferreira, Daniel J. Barbosa, et al. 2021. "Plastin and Spectrin Cooperate to Stabilize the Actomyosin Cortex during Cytokinesis." *Current Biology* 31 (24): 5415-5428.e10. https://doi.org/10.1016/j.cub.2021.09.055.

Somers, W. Gregory, and Robert Saint. 2003. "A RhoGEF and Rho Family GTPase-Activating Protein Complex Links the Contractile Ring to Cortical Microtubules at the Onset of Cytokinesis." *Developmental Cell* 4 (1): 29–39. https://doi.org/10.1016/S1534-5807(02)00402-1.

Somma, Maria Patrizia, Barbara Fasulo, Giovanni Cenci, Enrico Cundari, and Maurizio Gatti. 2002. "Molecular Dissection of Cytokinesis by RNA Interference in Drosophila Cultured Cells." *Molecular Biology of the Cell* 13 (April): 1227–37. https://doi.org/10.1091/mbc.01.

Srinivasan, Dayalan G., Ridgely M. Fisk, Huihong Xu, and Sander Van den Heuvel. 2003. "A Complex of LIN-5 and GPR Proteins Regulates G Protein Signaling and Spindle Function in C. Elegans." *Genes and Development* 17 (10): 1225–39. https://doi.org/10.1101/gad.1081203.

Steigemann, Patrick, Claudia Wurzenberger, Michael H.A. A Schmitz, Michael Held, Julien Guizetti, Sandra Maar, and Daniel W. Gerlich. 2009. "Aurora B-Mediated Abscission Checkpoint Protects against Tetraploidization." *Cell* 136 (3): 473–84. https://doi.org/10.1016/j.cell.2008.12.020.

Stiernagle, T. 2006. "Maintenance of C. Elegans. WormBook: Tle." *The Online Review of C. Elegans Biology*, 1–11.

Štimac, Valentina, Isabella Koprivec, Martina Manenica, Juraj Simunić, and Iva M. Tolić. 2022. "Augmin Prevents Merotelic Attachments by Promoting Proper Arrangement of

Bridging and Kinetochore Fibers." *ELife* 11: 1–26. https://doi.org/10.7554/eLife.83287.

Stossel, Thomas P., Gabriel Fenteany, and John H. Hartwig. 2006. "Cell Surface Actin Remodeling." *Journal of Cell Science* 119 (16): 3261–64. https://doi.org/10.1242/jcs.02994.

Straub, F. B., and G. Feuer. 1950. "Adenosinetriphosphate the Functional Group of Actin." *In Biochimica et Biophysica Acta* 4: 455–470.

Subramanian, Radhika, Shih Chieh Ti, Lei Tan, Seth A. Darst, and Tarun M. Kapoor. 2013. "Marking and Measuring Single Microtubules by PRC1 and Kinesin-4." *Cell* 154 (2): 377. https://doi.org/10.1016/j.cell.2013.06.021.

Subramanian, Radhika, Elizabeth M. Wilson-Kubalek, Christopher P. Arthur, Matthew J. Bick, Elizabeth A. Campbell, Seth A. Darst, Ronald A. Milligan, and Tarun M. Kapoor. 2010. "Insights into Antiparallel Microtubule Crosslinking by PRC1, a Conserved Nonmotor Microtubule Binding Protein." *Cell* 142 (3): 433–43. https://doi.org/10.1016/j.cell.2010.07.012.

Sugioka, Kenji, and Bruce Bowerman. 2018. "Combinatorial Contact Cues Specify Cell Division Orientation by Directing Cortical Myosin Flows." *Developmental Cell* 46 (3): 257-270.e5. https://doi.org/10.1016/j.devcel.2018.06.020.

Sulston, J. E., and H. R. Horvitz. 1977. "Post-Embryonic Cell Lineages of the Nematode, Caenorhabditis Elegans." *Dev. Biol.* 56: 110–56.

Sulston, J. E., E. Schierenberg, J. G. White, and J. N. Thomson. 1983. "The Embryonic Cell Lineage of the Nematode Caenorhabditis Elegans." *Developmental Biology* 100 (1): 64–119.

Sun, Lingfei, Ruifang Guan, I. Ju Lee, Yajun Liu, Mengran Chen, Jiawei Wang, Jian Qiu Wu, and Zhucheng Chen. 2015. "Mechanistic Insights into the Anchorage of the Contractile Ring by Anillin and Mid1." *Developmental Cell* 33 (4): 413–26. https://doi.org/10.1016/j.devcel.2015.03.003.

Sun, Sheng, Le Sun, Xi Zhou, Chuanfen Wu, Ruoning Wang, Sue Hwa Lin, and Jian Kuang. 2016. "Phosphorylation-Dependent Activation of the ESCRT Function of ALIX in Cytokinetic Abscission and Retroviral Budding." *Developmental Cell* 36 (3): 331–43. https://doi.org/10.1016/j.devcel.2016.01.001.

Swider, Zachary T., Rachel K. Ng, Ramya Varadarajan, Carey J. Fagerstrom, and Nasser M. Rusan. 2019. "Fascetto Interacting Protein Ensures Proper Cytokinesis and Ploidy." *Molecular Biology of the Cell* 30 (8): 992–1007. https://doi.org/10.1091/mbc.E18-09-0573.

Szafer-Glusman, Edith, Margaret T. Fuller, and Maria Grazia Giansanti. 2011. "Role of Survivin in Cytokinesis Revealed by a Separation-of-Function Allele." *Molecular Biology of the Cell* 22 (20): 3779–90. https://doi.org/10.1091/mbc.E11-06-0569.

Tasto, Joseph J., Jennifer L. Morrell, and Kathleen L. Gould. 2003. “An Anillin Homologue, Mid2p, Acts during Fission Yeast Cytokinesis to Organize the Septin Ring and Promote Cell Separation.” *Journal of Cell Biology* 160 (7): 1093–1103. https://doi.org/10.1083/jcb.200211126.

Tatsumoto, Takashi, Xiaozhen Xie, Rayah Blumenthal, Isamu Okamoto, and Toru Miki. 1999. “G2 / M Phases , and Involved in Cytokinesis.” *Cell* 147 (5): 921–27.

Tcherkezian, Joseph, and Nathalie Lamarche-Vane. 2007. “Current Knowledge of the Large RhoGAP Family of Proteins.” *Biology of the Cell* 99 (2): 67–86. https://doi.org/10.1042/bc20060086.

Tedeschi, Antonio, Jorge Almagro, Matthew J. Renshaw, Hendrik A. Messal, Axel Behrens, and Mark Petronczki. 2020. “Cep55 Promotes Cytokinesis of Neural Progenitors but Is Dispensable for Most Mammalian Cell Divisions.” *Nature Communications* 11 (1): 1–16. https://doi.org/10.1038/s41467-020-15359-w.

Telley, Ivo A., Imre Gáspár, Anne Ephrussi, and Thomas Surrey. 2012. “Aster Migration Determines the Length Scale of Nuclear Separation in the Drosophila Syncytial Embryo.” *Journal of Cell Biology* 197 (7): 887–95. https://doi.org/10.1083/jcb.201204019.

Thieleke-Matos, C., D.S. Osório, A.X. Carvalho, E. Morais-de-Sá, D.S. Osório, A.X. Carvalho, and E. Morais-de-Sá. 2017. “Emerging Mechanisms and Roles for Asymmetric Cytokinesis.” In *International Review of Cell and Molecular Biology*, 332:297–345. https://doi.org/10.1016/bs.ircmb.2017.01.004.

Tikhonenko, Irina, Dilip K. Nag, Nora Martin, and Michael P. Koonce. 2008. “Kinesin-5 Is Not Essential for Mitotic Spindle Elongation in Dictyostelium.” *Cell Motility and the Cytoskeleton* 65 (11): 853–62. https://doi.org/10.1002/cm.20307.

Tintori, Sophia C., Erin Osborne Nishimura, Patrick Golden, Jason D. Lieb, and Bob Goldstein. 2016. “A Transcriptional Lineage of the Early C. Elegans Embryo.” *Developmental Cell* 38 (4): 430–44. https://doi.org/10.1016/j.devcel.2016.07.025.

Tolic-Norrelykke, I.M., L. Sacconi, G. Thon, and F.S. Pavone. 2004. “Positioning and Elongation of the Fission Yeast Spindle by Microtubule-Based Pushing.” *Curr. Biol.* 14: 1181–1186. https://doi.org/10.1016/j.

Touré, Aminata, Olivier Dorseuil, Laurence Morin, Paula Timmons, Bernard Jégou, Louise Reibel, and Gérard Gacon. 1998. “MgcRacGAP, a New Human GTPase-Activating Protein for Rac and Cdc42 Similar to Drosophila RotundRacGAP Gene Product, Is Expressed in Male Germ Cells.” *Journal of Biological Chemistry* 273 (11): 6019–23. https://doi.org/10.1074/jbc.273.11.6019.

Trupinić, Monika, Barbara Kokanović, Ivana Ponjavić, Ivan Barišić, Siniša Šegvić, Arian Ivec, and Iva M. Tolić. 2022. “The Chirality of the Mitotic Spindle Provides a Mechanical

Response to Forces and Depends on Microtubule Motors and Augmin." *Current Biology* 32 (11): 2480-2493.e6. https://doi.org/10.1016/j.cub.2022.04.035.

Tse, Yu Chung, Michael Werner, Katrina M. Longhini, Jean Claude Labbe, Bob Goldstein, and Michael Glotzer. 2012. "RhoA Activation during Polarization and Cytokinesis of the Early Caenorhabditis Elegans Embryo Is Differentially Dependent on NOP-1 and CYK-4." *Molecular Biology of the Cell* 23 (20): 4020–31. https://doi.org/10.1091/mbc.E12-04-0268.

Uehara, Ryota, and Gohta Goshima. 2010. "Functional Central Spindle Assembly Requires de Novo Microtubule Generation in the Interchromosomal Region during Anaphase." *Journal of Cell Biology* 191 (2): 259–67. https://doi.org/10.1083/jcb.201004150.

Uehara, Ryota, Ryu-suke Nozawa, Akiko Tomioka, Sabine Petry, Ronald D Vale, Chikashi Obuse, and Gohta Goshima. 2009. "The Augmin Complex Plays a Critical Role in Spindle Microtubule Generation for Mitotic Progression and Cytokinesis in Human Cells." *Proceedings of the National Academy of Sciences of the United States of America* 106 (17): 6998–7003. https://doi.org/10.1073/pnas.0901587106.

Vader, Gerben, Jos J.W. Kauw, René H. Medema, and Susanne M.A. Lens. 2006. "Survivin Mediates Targeting of the Chromosomal Passenger Complex to the Centromere and Midbody." *EMBO Reports* 7 (1): 85–92. https://doi.org/10.1038/sj.embor.7400562.

Verbrugghe, Koen J.C., and White, J.C. Koen. 2004. "SPD-1 Is Required for the Formation of the Spindle Midzone but Is Not Essential for the Completion of Cytokinesis in C. Elegans Embryos." *Current Biology* 14 (19): 1755–60. https://doi.org/10.1016/j.

Verbrugghe, Koen J.C., and John G. White. 2007. "Cortical Centralspindlin and Gα Have Parallel Role in Furrow Initiation in Ealry C. Elegans Embryos." *Journal of Cell Science* 120 (10): 1772–78. https://doi.org/10.1242/jcs.03447.

Vernì, Fiammetta, Maria Patrizia Somma, Kristin C. Gunsalus, Silvia Bonaccorsi, Giorgio Belloni, Michael L. Goldberg, Maurizio Gatti, et al. 2004. "Feo, the Drosophila Homolog of PRC1, Is Required for Central-Spindle Formation and Cytokinesis." *Current Biology* 14: 1569–75. https://doi.org/10.1016/j.

Vicente-Manzanares, M., X. Ma, R. S. Adelstein, and A. R. Horwitz. 2009. "Non-Muscle Myosin II Takes Centre Stage in Cell Adhesion and Migration." *Nature Reviews.* 10 (11): 778–90.

Vukušić, Kruno, Renata Buđa, Agneza Bosilj, Ana Milas, Nenad Pavin, and Iva M. Tolić. 2017. "Microtubule Sliding within the Bridging Fiber Pushes Kinetochore Fibers Apart to Segregate Chromosomes." *Developmental Cell* 43: 11–23. https://doi.org/10.1016/j.devcel.2017.09.010.

Waddle, James A., John A. Cooper, and Robert H. Waterston. 1994. "Transient Localized Accumulation of Actin in Caenorhabditis Elegans Blastomeres with Oriented

Asymmetric Divisions." *Development* 120 (8): 2317–28.

Wadsworth, Patricia. 2021. "The Multifunctional Spindle Midzone in Vertebrate Cells at a Glance." *Journal of Cell Science* 134 (10): 1–8. https://doi.org/10.1242/jcs.250001.

Walston, Timothy D., and Jeff Hardin. 2006. "Wnt-Dependent Spindle Polarization in the Early C. Elegans Embryo." *Seminars in Cell and Developmental Biology* 17 (2): 204–13. https://doi.org/10.1016/j.semcdb.2006.04.005.

Wang, Kangji. 2019. "Non-Muscle Myosin-II Is Required for the Generation of a Constriction Site for Subsequent Abscission Non-Muscle Myosin-II Is Required for the Generation of a Constriction Site for Subsequent Abscission." *ISCIENCE* 13: 69–81. https://doi.org/10.1016/j.isci.2019.02.010.

Watanabe, Sadanori, Katsuya Okawa, Takashi Miki, Satoko Sakamoto, Tomoko Morinaga, Kohei Segawa, Takatoshi Arakawa, Makoto Kinoshita, Toshimasa Ishizaki, and Shuh Narumiya. 2010. "Rho and Anillin-Dependent Control of MDia2 Localization and Function in Cytokinesis." *Molecular Biology of the Cell* 21 (18): 3193–3204. https://doi.org/10.1091/mbc.E10-04-0324.

Watanabe, Sadanori, Tihana De Zan, Toshimasa Ishizaki, and Shuh Narumiya. 2013. "Citron Kinase Mediates Transition from Constriction to Abscission through Its Coiled-Coil Domain." *Journal of Cell Science* 126 (8): 1773–84. https://doi.org/10.1242/jcs.116608.

Werner, M., E. Munro, and M. Glotzer. 2007. "Astral Signals Spatially Bias Cortical Myosin Recruitment to Break Symmetry and Promote Cytokinesis." *Current Biology* 17 (15): 1286–1297.

Wheatley, Sally P., and Yu Li Wang. 1996. "Midzone Microtubule Bundles Are Continuously Required for Cytokinesis in Cultured Epithelial Cells." *Journal of Cell Biology* 135 (4): 981–89. https://doi.org/10.1083/jcb.135.4.981.

White, Erin A., and Michael Glotzer. 2012. "Centralspindlin: At the Heart of Cytokinesis." *Cytoskeleton* 69 (11): 882–92. https://doi.org/10.1002/cm.21065.

Winey, M., C.L. Mamay, E.T. O'Toole, D.N. Mastronarde, Jr. Giddings, T.H., K.L. McDonald, and J.R. McIntosh. 1995. "Three-Dimensional Ultrastructural Analysis of the Saccharomyces Cerevisiae Mitotic Spindle." *J. Cell Biol* 129: 1601–15. https://doi.org/10.7868/s0869803118010010.

Wolfe, Benjamin A., Tohru Takaki, Mark Petronczki, and Michael Glotzer. 2009. "Polo-like Kinase 1 Directs Assembly of the HsCyk-4 RhoGAP/Ect2 RhoGEF Complex to Initiate Cleavage Furrow Formation." *PLoS Biology* 7 (5). https://doi.org/10.1371/journal.pbio.1000110.

Wollert, Thomas, Christian Wunder, Jennifer Lippincott-Schwartz, and James H. Hurley. 2009. "Membrane Scission by the ESCRT-III Complex." *Nature* 458 (7235): 172–77.

https://doi.org/10.1038/nature07836.

Yamashita, Akira, Masamitsu Sato, Akiko Fujita, Masayuki Yamamoto, and Takashi Toda. 2005. “The Roles of Fission Yeast Ase1 in Mitotic Cell Division, Meiotic Nuclear Oscillation, and Cytokinesis Checkpoint Signaling.” *Mol Biol Cell* 16 (March): 1378–95. https://doi.org/10.1091/mbc.E04.

Yonemura, Shigenobu, Kazuyo Hirao-Minakuchi, and Yukako Nishimura. 2004. “Rho Localization in Cells and Tissues.” *Experimental Cell Research* 295 (2): 300–314. https://doi.org/10.1016/j.yexcr.2004.01.005.

Yoshizaki, Hisayoshi, Yusuke Ohba, Kazuo Kurokawa, Reina E. Itoh, Takeshi Nakamura, Naoki Mochizuki, Kazuo Nagashima, and Michiyuki Matsuda. 2003. “Activity of Rho-Family GTPases during Cell Division as Visualized with FRET-Based Probes.” *Journal of Cell Biology* 162 (2): 223–32. https://doi.org/10.1083/jcb.200212049.

Yu, Che Hang, Stefanie Redemann, Hai Yin Wu, Robert Kiewisz, Tae Yeon Yoo, William Conway, Reza Farhadifar, Thomas Müller-Reichert, and Daniel Needleman. 2019. “Central-Spindle Microtubules Are Strongly Coupled to Chromosomes during Both Anaphase A and Anaphase B.” *Molecular Biology of the Cell* 30 (19): 2503–14. https://doi.org/10.1091/mbc.E19-01-0074.

Yu, Ji Eun, Sun-Ok Kim, Jeong-Ah Hwang, Jin Tae Hong, Joonsung Hwang, Nak-Kyun Soung, Hyunjoo Cha-Molstad, Yong Tae Kwon, Bo Yeon Kim, and Kyung Ho Lee. 2021. “Phosphorylation of B-catenin Ser60 by Polo-like Kinase 1 Drives the Completion of Cytokinesis.” *EMBO Reports* 22 (12): 1–21. https://doi.org/10.15252/embr.202051503.

Yüce, Özlem, Alisa Piekny, and Michael Glotzer. 2005. “An ECT2-Centralspindlin Complex Regulates the Localization and Function of RhoA.” *Journal of Cell Biology* 170 (4): 571–82. https://doi.org/10.1083/jcb.200501097.

Yue, Zuojun, Ana Carvalho, Zhenjie Xu, Xuemei Yuan, Stefano Cardinale, Susana Ribeiro, Fan Lai, et al. 2008. “Deconstructing Survivin: Comprehensive Genetic Analysis of Survivin Function by Conditional Knockout in a Vertebrate Cell Line.” *Journal of Cell Biology* 183 (2): 279–96. https://doi.org/10.1083/jcb.200806118.

Zhang, Donglei, and Michael Glotzer. 2015a. “Cytokinesis: Placing the Furrow in Context.” *Current Biology* 25 (24): R1183–85. https://doi.org/10.1016/j.cub.2015.10.042.

Zhang, Donglei, and Michael Glotzer. 2015b. “The RhoGAP Activity of CYK-4/MgcRacGAP Functions Non-Canonically by Promoting RhoA Activation during Cytokinesis.” *ELife* 4 (AUGUST2015): 1–25. https://doi.org/10.7554/eLife.08898.

Zhang, Haining, Ahna R. Skop, and John G. White. 2008. “Src and Wnt Signaling Regulate Dynactin Accumulation to the P2-EMS Cell Border in C. Elegans Embryos.” *Journal of Cell Science* 121 (2): 155–61. https://doi.org/10.1242/jcs.015966.

Zhao, Wei Meng, and Guowei Fang. 2005. “Anillin Is a Substrate of Anaphase-Promoting Complex/Cyclosome (APC/C) That Controls Spatial Contractility of Myosin during Late Cytokinesis.” *Journal of Biological Chemistry* 280 (39): 33516–24. https://doi.org/10.1074/jbc.M504657200.

Zhu, Changjun, and Wei Jiang. 2005. “Cell Cycle-Dependent Translocation of PRC1 on the Spindle by Kif4 Is Essential for Midzone Formation and Cytokinesis.” *Proceedings of the National Academy of Sciences of the United States of America* 102 (2): 343–48. https://doi.org/10.1073/pnas.0408438102.

Zhu, Changjun, Eric Lau, Robert Schwarzenbacher, Ella Bossy-Wetzel, and Wei Jiang. 2006. “Spatiotemporal Control of Spindle Midzone Formation by PRC1 in Human Cells.” *Proceedings of the National Academy of Sciences of the United States of America* 103 (16): 6196–6201. https://doi.org/10.1073/pnas.0506926103.